Electronic Engineering

VOL. 39 No. 477.

Tomorrow's graduate

HIGHER LEARNING in the education of electronics engineers is sometimes a mixture of *ad hoc* theories on what should be known and a little experience of what is really required. A trio of teachers at Southampton University, Messrs. Sims, Gambling and Venning have written what we consider to be a very fine reasoned outline of the knowledge that ought to be imparted to students embarking on an electronics career. Their article, 'The future education of electronic engineers' (in the September issue of '*Radio and Electronic Engineer*') first defines the most likely direction in which electronic engineering is going. Having made the correct fundamental assumption (correct because we agree with them!) they discuss in detail the requirements for a first-degree course at a university, with schemes for subsequent post-graduate work and retraining. We note with some pleasure that they have excluded some of the miasma of general engineering subjects which are irrelevant to the pursuit of electronic engineering.

Whilst we do not intend to spell out all that S., G. and V. have so clearly indicated, we shall declare only those fundamental assumptions to which we have already referred. The world of electronics in industry (and even beyond) is envisaged as a large collection of systems engineers supported by device engineers, particularly active-device engineers. The present ratio of systems to active-device people engaged in the U.K. in industry is about four to one, so that there are a lot of systems types and fewer active-device men. Device engineers have, of course, to know all about the physics and characteristics of their components whilst the systems men must know enough of fundamentals to be able to specify their requirements whenever a suitable standard entity is not to hand. These entities or devices, now largely in the form of discrete components, will no doubt give way almost wholly to the fairly simple micro-electronics already with us, which in their turn will give way to more elaborate structures. As the Southampton people say: 'many of the systems of today will become the devices of tomorrow'.

The result of these assumptions in future education of our engineers is that the course must cater for both systems and device end-results and must inevitably have a large materials-physics content. The authors see the basic triumvirate of first-year knowledge to be circuit theory, electromagnetic theory and materials physics. The last-named is not to be restricted to semiconductors but should have a broad foundation of materials technology. From this three-pronged basis the course is developed on to the final year where a graduate has some option given to him in the choice of special studies selected from the several branches of electronic engineering, e.g. microwaves, communications, control etc.

The Southampton trio have emphasized the importance of physics, especially of materials, stating that a large number of advances in engineering have sprung from developments in materials. We have always held somewhat heretic views on the place of electronics engineering in the scheme of things and we are more than ever confirmed in our belief that the subject matter is a branch of physics, albeit a very special one to which indeed the whole of science has a relevant contribution. The circuit designers who figure so largely in our pages may turn into physicists with a flair for materials technology and an aptitude for algebra.

We have taken points from the article by Sims *et al.* out of context for our own purpose; we recommend the whole article to our readers—those who are graduates, those who do not intend to be and those who do.

Approach to applied circuit synthesis

by **R. H. Dadd,** *Portsmouth College of Technology*

This article shows some simple methods by which an amplifier design may be constrained to meet a desired specification. Routine methods for the necessary feedback-network synthesis are given and an example shows the application of the method.

(Voir page 731 pour le résumé en français: Zusammenfassung in deutscher Sprache auf Seite 732)

The following discussion introduces a systemized network synthesis leading to gain/frequency characteristics meeting a given specification. It does not attempt to be an exhaustive review but aims at describing a simple method which will encourage undergraduates and others to approach the phenomenon of amplifier frequency response from a synthetic, rather than wholly analytic, viewpoint.

Amplifiers with predicted characteristics

An amplifier with feedback (Fig. 1) may be shown to have net gain A' given by

$$A' = \frac{A}{1 + A\beta} \quad \ldots\ldots\ldots\ldots\ldots\ldots (1)$$

By making the loop gain $A\beta$ large, A' reduces $1/\beta$, and thus the amplifier characteristic is determined solely by

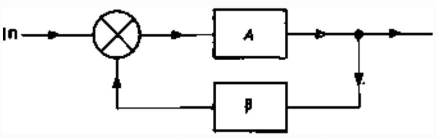

Fig. 1 Basic feedback configuration

the characteristic of β. Initially, therefore, a simple amplifier having the following characteristics must be available:

(i) a gain at least 10 times greater than the maximum required A';
(ii) good response within the bandwidth over which the response is to be predicted; this is a vague statement but for this simplified approach one may assume that a response flat within 3dB is adequate for most applications;
(iii) readily applied feedback in the correct phase.

If the basic amplifier does not meet these restrictions, it is still possible to obtain a predicted performance, but the approach has to be modified.

Calculation of feedback circuit

In order to calculate the necessary feedback circuit, the desired characteristic must be expressed mathematically. Frequently, this is already given as a specification of break frequencies and slopes of curves; however, in cases where the desired characteristic is expressed empirically as a certain curve, an analysis of the Bode diagram must be made. This requires the extraction of simple single-time-constant or complex-time-constant elements from the overall Bode diagram, and is described in many texts[1].

Suppose that the characteristic has been obtained as a ratio of two polynomials in $j\omega$ or s. (It is convenient to work in s, the Laplacian operator, to avoid pitfalls due to the squaring of $j\omega$). Thus we have:

$$A' = P(s)/Q(s) \quad \ldots\ldots\ldots\ldots\ldots (2)$$

where $P(s)$ and $Q(s)$ are polynomials in s

Thus $$\beta \simeq Q(s)/P(s) \quad \ldots\ldots\ldots\ldots\ldots\ldots (3)$$

The simple technique to be described uses an L-section to give the required value of β. Two basic configurations will be used, as in Fig. 2. In each, the resistive element is chosen so that the feedback factor depends almost entirely on Y or Z. Thus, in Fig. 2(a), the admittance Y is small and the conductance G large; in Fig. 2(b), the impedance Z is small and the resistance R large. The terms large and small here will depend on $A\beta$ being at least 10, as suggested earlier.

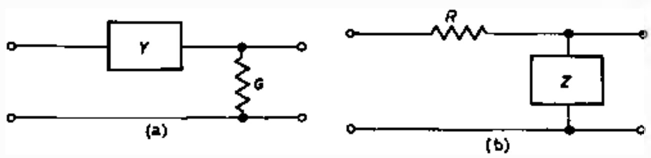

Fig. 2 L-section feedback circuits

If it is assumed that no complex poles or zeros are required in A' (i.e. no LC-type resonances), inductors may be excluded from the synthesis, provided that arrangement 2(a) is used for a response which falls with frequency and 2(b) is used for a response which rises with frequency. It must also be noted that Z and G may include the input conductance at the point where feedback is applied, and Y and R the source impedance of the point from which the feedback is obtained; although, for a simple approach, these may frequently be ignored and a performance obtained very close to that predicted. If a charateristic which is both rising and falling is required, it may be necessary for both series and shunt arms to be made up of reactive elements.

Neglecting the loading of the amplifier, for the circuit in Fig. 2(a),

$$\beta \simeq Y/G \quad \ldots\ldots\ldots\ldots\ldots\ldots (4)$$

and, for Fig. 2(b),

$$\beta \simeq Z/R \quad \ldots\ldots\ldots\ldots\ldots\ldots (5)$$

Since the desired β is known, an expression for Y or Z is therefore also established.

In order to simplify the technique, it is assumed that required slopes will not be greater than 6dB/octave. This means that the order of $Q(s)$ will differ from the order of $P(s)$ by not more than one power of s. If this is not so, inductors must be admitted to the synthesis, several stages must be cascaded, or an alternative feedback network must be used. These restrictions result in the following forms of Y and Z:

Y will always have a numerator of order either equal to or one higher than the denominator;
Z will always have the denominator of order either equal to or one higher than the numerator.

Thus, in determining the components of Z, it must first be inverted, and then the procedure is as for Y. To determine Y, algebraic division of the numerator by the denominator is carried out, stopping after the highest power of s is elminated. This gives a quotient of the form Cs and a remainder of the same order as the denominator of Y. This routine prevents the introduction of inductive terms later; i.e.

$$Y = L(s)/M(s) = C_1 s + \frac{\text{Rem1}}{M(s)} \quad \text{.............. (6)}$$

where Rem 1 is of the same order as $M(s)$.

Let $$Z' = \frac{M(s)}{\text{Rem1}} \quad \text{................. (7)}$$

Now divide $M(s)$ algebraically by Reml. This will give a constant R and a remainder of lower order than Rem1:

$$Z' = \frac{M(s)}{\text{Rem1}} = R_1 + \frac{\text{Rem2}}{\text{Rem1}} \quad \text{......... (8)}$$

Let $$Y'' = \frac{\text{Rem1}}{\text{Rem2}} \quad \text{................ (9)}$$

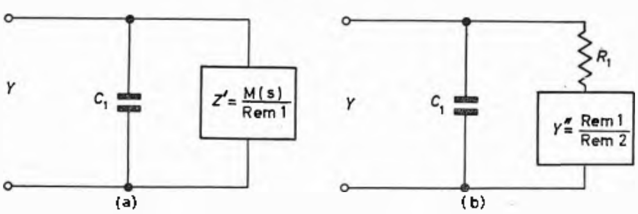

Fig. 3 First two stages in determination of Y
(a) after removal of the first shunt element
(b) after removal of the first shunt and first series elements

Y'' is now treated as Y. Fig. 3 shows the first two stages of the process; this is an application of Cauer's[2] method of repeated fractions and gives a routine method for quite complicated characteristics.

When the remaining admittance has been reduced to the form of a quadratic in s divided by a single power of s, the procedure outlined above may be followed or an alternative process used.

Thus

$$Y = \frac{K(1+sT_1)(1+sT_2)}{1+sT_3} = K\frac{(1+s(T_1+T_2)+s^2T_1T_2)}{1+sT_3} \quad \text{............ (10)}$$

A conductance G may be eliminated; i.e.

$$Y' = Y - G \quad \text{................ (11)}$$

Making $G = K$,

$$Y' = K\frac{s(T_1 + T_2 - T_3 + T_1T_2s)}{1 + T_3s} \quad \text{....... (12)}$$

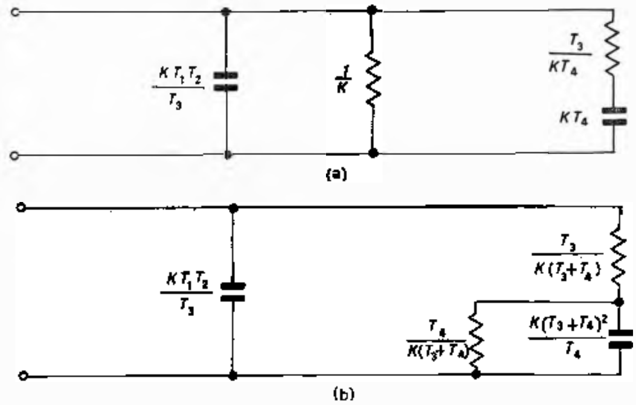

Fig. 4 Synthesis of equation (10)
(a) using alternative procedure
(b) using systematic procedure

A shunt capacitor may also be eliminated:

$$Y'' = Y' - C_1 s \quad \text{................ (13)}$$

If $C_1 = KT_1T_2/T_3$,

$$Y'' = \frac{KT_4 s}{1 + T_3 s} \quad \text{................ (14)}$$

where $$T_4 = T_1 + T_2 - T_3 - (T_1T_2/T_3) \quad \text{...... (15)}$$

therefore $$Z'' = \frac{1 + T_3 s}{KT_4 s} = T_3/KT_4 + 1/KT_4 s \quad \text{.... (16)}$$

i.e. a series resistor and capacitor. The whole arrangement is shown in Fig. 4(a). This procedure corresponds to continuing the division of $L(s)$ by $M(s)$ after the highest power of s is climinated, but does not introduce an inductor, owing to the low order of $L(s)$ and $M(s)$. If the systematic routine is followed, the configuration shown in Fig. 4(b) will be synthesized. The practical values may be chosen using a preferred-value resistor or capacitor for one of the components. There is some advantage in starting with a capacitor of preferred value, since resistors not in the preferred range may be cheaply made up using variable components.

Practical application

A suitable simple amplifier circuit is shown in Fig. 5. The feedback admittance Y is connected between A and B, while G and the input conductance at the emitter of the first transistor form the other part of the feedback circuit. If a rising characteristic is required, it may be possible to incorporate this conductance into the shunt impedance. If, however, this conductance is of an unsuit-

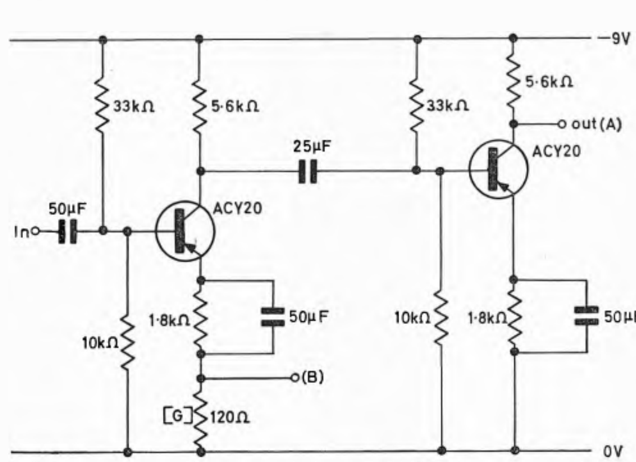

Fig. 5 Simple basic-amplifier stage

able value, an input emitter-follower stage with the bias supplied *via* a bootstrap circuit will give a sufficiently high input impedance to prevent unwanted shunting of the shunt-feedback impedance.

Fig. 6 shows a suitable input stage of this type; the output is taken from the collector so that, when followed by a 2-stage amplifier (as in Fig. 5), the output at A is in antiphase with the input. This allows the feedback circuit to be connected between A and the input terminal of the stage shown in Fig. 6. An alternative to this transistor input stage is to use a field-effect transistor which will inherently have a high-input impedance.

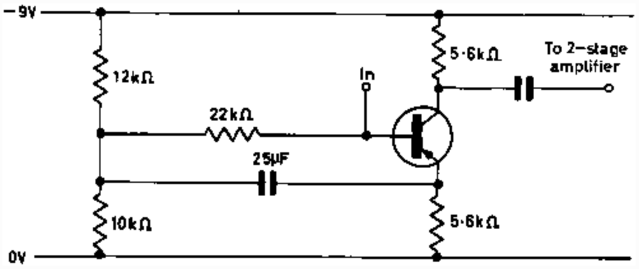

Fig. 6 Simple high-input-impedance stage

As a gain/frequency characteristic, the compensation necessary for a standard microgroove 33⅓ or 45rev/min gramophone record was taken. This has one high-pass and two low-pass time constants. Fig. 7 shows that the low-pass break frequencies are 50·049Hz and 2121·5Hz and the high-pass break frequency is at 500·49Hz. Thus the required characteristic is of the form:

$$A' = \frac{G(1 + sT_3)}{(1 + sT_1)(1 + sT_2)} \quad \text{(17)}$$

where T_1 corresponds to 50·049Hz,

T_2 corresponds to 2121·5Hz,

and T_3 corresponds to 500·49Hz.

Thus the feedback admittance is of the form

$$Y = \frac{K(1 + sT_1)(1 + sT_2)}{1 + sT_3}$$

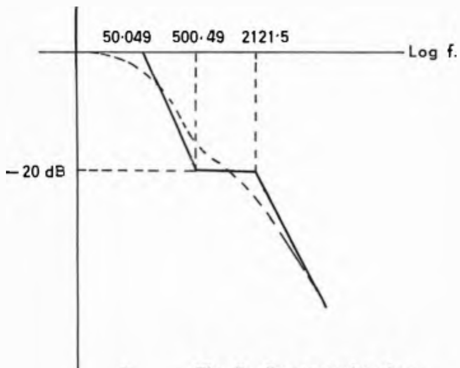

Fig. 7 Compensation for microgroove-record characteristic

Using the technique described above the circuit arrangement for the feedback admittance becomes as in Fig. 8; the calculations are given in the Appendix. Using these calculated values, a circuit was set up accurate to two significant figures. A constant current of 40μA was applied and the voltage across the admittance measured. This experimental plot proved indistinguishable from the predicted curves. The circuit was then made up using the nearest preferred-value components; these are shown in brackets in Fig. 8. This circuit was then connected between A and B in the simple amplifier in Fig. 5. The resultant response is shown in Fig. 9, where it is compared with the desired response initially specified and the response predicted from the nominal values of the components used.

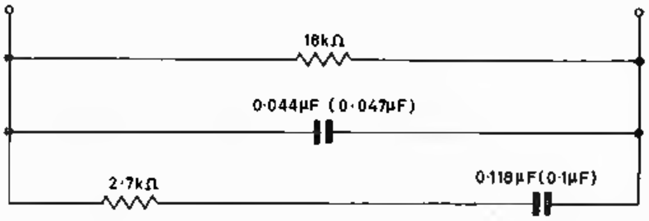

Fig. 8 Feedback circuit synthesized for recording compensation

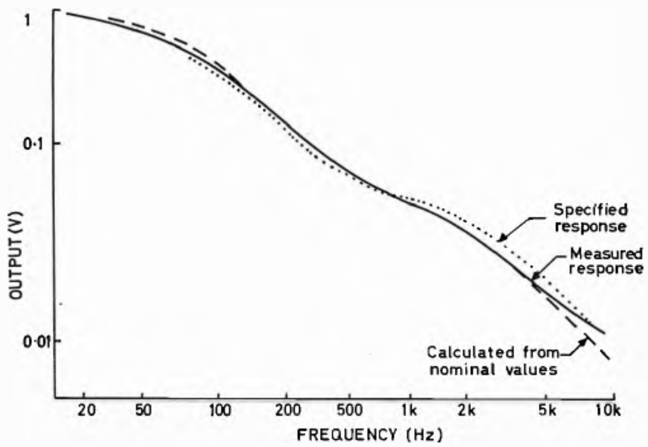

Fig. 9 Comparison between predicted and experimental characteristics (input 10mV)

Appendix

Feedback circuit for recording-characteristic compensation

Since $f_1 = 50{\cdot}049\text{Hz}$

therefore $T_1 = \dfrac{1}{2\pi \times 50{\cdot}049} = 3{\cdot}16 \times 10^{-3}\text{s}$

Similarly $T_2 = 7{\cdot}9 \times 10^{-5}\text{s}$

$T_3 = 3{\cdot}16 \times 10^{-4}\text{s}$

so that $T_1T_2/T_3 = 7{\cdot}9 \times 10^{-4}$

Now $T_4 = T_1 + T_2 - T_3 - (T_1T_2/T_3)$

$= 2{\cdot}13 \times 10^{-3}$

therefore $T_3/T_4 = 0{\cdot}15$

The shunt resistor was taken as the starting point, and the circuit components were calculated for various values of this resistor. A resistance of 18kΩ was found to give the required gain in the circuit used. Thus the component values are

shunt resistor $1/K = 18k\Omega$

shunt capacitor $\dfrac{KT_1T_2}{T_3} = \dfrac{7{\cdot}9 \times 10^{-4}}{18 \times 10^3} = 0{\cdot}044\mu\text{F}$

series resistor $(1/K)(T_3/T_4) = 0{\cdot}15 \times 18 = 2{\cdot}7\text{k}\Omega$

series capacitor $KT_4 = \dfrac{2{\cdot}13 \times 10^{-3}}{18 \times 10^3} = 0{\cdot}118\mu\text{F}$

These values are shown in Fig. 8.

REFERENCES

1 Bruns and Saunders: *Feedback control systems,* 299

2 Cauer, W.: *Arch. Elektrotech.* *17,* 355 (1927)

Multivibrator with very small mark/space ratio

by **S. Tesic,** *University of Belgrade, Yugoslavia*

A free-running multivibrator suitable for the generation of very unsymmetrical waveforms is described. The duration of both quasistable states can be controlled separately, thus allowing a very small mark/space ratio, of the order of 10^{-4} to 10^{-5}, to be obtained. In such a mode of operation, the circuit, based on the use of complementary transistors, is very economical in total power consumption.

(Voir page 731 pour le résumé en français: Zusammenfassung in deutscher Sprache auf Seite 732)

In order to obtain a small mark/space ratio (i.e. a low duty cycle) with a free-running multivibrator, it is necessary to make a very large difference in the time constants determining the quasistable states of the circuit; it is known that a conventional multivibrator is not suitable for such a mode of operation. Emitter-coupled multivibrators are better suited to generating unsymmetrical waveforms[1,2]; the mark/space ratio achieved by these circuits is of the order of 10^{-2} to 10^{-3}.

A better solution to this problem can be obtained using complementary transistors; several bistable and monostable circuits of this type have been published[3,4,5]. It seems, however, that astable multivibrators of this type have not been dealt with, although there is a free-running symmetrical-configuration circuit employed in a pulse generator in Reference 6.

The free-running multivibrator under consideration is of unsymmetrical configuration; i.e. it has one timing capacitor only. Moreover, this circuit has the capability of continuously controlling both quasistable states separately. By means of a potentiometer, the time between the pulses can be varied by about 1000 times, thus allowing a space/mark ratio of greater than 10 000 to be obtained.

If it is arranged that the pulses correspond to the conduction states of the transistors, the power consumption will be lower when the duty cycle is small. Thus the circuit described can be very economical, which may be of great interest in some applications.

Description of the circuit

The circuit configuration is shown in Fig. 1. As the batteries V_{cc} and V_{bb} are switched on, the transistor VT_1 starts to conduct immediately, its base potential being close to the cutoff potential. The collector of VT_1 brings transistor VT_2 into conduction also. Because of its collector current, a positive pulse is generated across the resistor R_{c2}. Since the voltage across the timing capacitor C cannot be changed instantaneously, the positive pulse will be carried to the base of VT_1, causing a regenerative process to start, which brings both transistors to saturation. The collector current of the saturated transistor VT_2 is determined by the external circuit components: therefore a constant voltage approximately equal to the supply voltage exists at R_{c2}.

Owing to the charging of the timing capacitor in the conducting period, the base voltage of VT_1 decreases, causing a reduction in the base current of VT_2. When this current reaches that at which VT_2 comes out of saturation, its collector current starts to decrease. The negative voltage drop across R_{c2} will cause a regenerative process again, reverting both transistors to cutoff. In the nonconducting period, C discharges, bringing the base potential of VT_1 towards the battery voltage V_{bb}. When this potential reaches the base-cutoff potential, VT_1 starts to conduct, re-establishing the conducting states of both transistors.

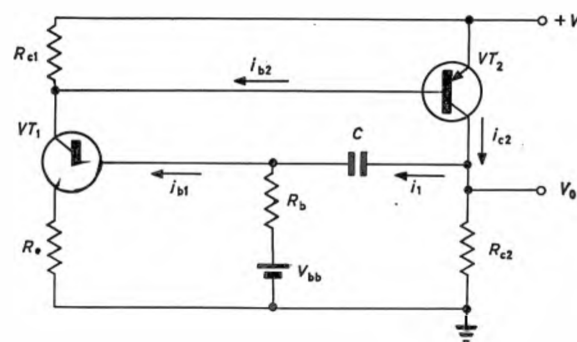

Fig. 1 Multivibrator circuit

The lowest battery voltage V_{bb} must be sufficient to keep the base of VT_1 in the vicinity of its cutoff potential. If the resistance R_b is large, it can be returned to the supply voltage V_{cc}. The resistors R_e and R_{c1} can be omitted from the circuit, making R_e zero and R_{c1} infinite; R_e improves the pulse shape and R_{c1} contributes to cutoff stability of VT_2.

The resistance R_{c2} can be determined from the condition of the circuit oscillation. On the assumption that both transistors are in the active state and that R_{c1}, R_b and C are large, $R_{c2} \simeq R_e/\beta_2$. Since the value of R_{c2} can be very small, it is specified with regard to the transistor dissipation or the collector current in the case of a low duty cycle of operation.

Calculation of the quasistable periods

The conducting period of the transistors may be determined from Fig. 2, in which r_o represents the resistance of the transistor VT_2 in saturation and R_{i1} the input resistance of VT_1, which is in saturation only at the beginning of this period. For the above network,

$$V_{bb} + R_b i_1 - (R_{i1} + R_b)\, i_{b1} = 0 \quad \ldots\ldots\ldots\ldots\ (1)$$

$$V_{cc} + R_{c2} i_1 - (r_0 + R_{c2})\, i_{c2} = 0 \quad \ldots\ldots\ldots\ldots\ (2)$$

$$V_{bb} + (R_b + R_{c2})\, i_1 - R_b i_{b1} - R_{c2} i_{c2} + q/C = 0 \quad \ldots\ (3)$$

From equation (1), the base current of VT_1 can be obtained in the form

$$i_{b1} = \frac{V_{bb}}{R_{i1} + R_b} + \frac{R_b}{R_{i1} + R_b}\, i_1 \quad \ldots\ldots\ldots\ (4)$$

Equation (2) gives the collector current of VT_2:

$$i_{c2} \simeq V_{cc}/R_{c2} + i_1, \text{ since } r_0 \ll R_{c2} \quad \ldots\ldots\ (5)$$

Using equations (4) and (5), equation (3) may now be rewritten in the form

$$(R_c' + R_i')\, dq/dt + q/C = V_{cc} - \frac{R_{i1}}{R_{i1} + R_b}\; V_{bb} \quad \ldots\ (6)$$

where $R_c' = \dfrac{r_0 R_{c2}}{r_0 + R_{c2}}$ and $R_i' = \dfrac{R_{i1} R_b}{R_{i1} + R_b}$

If the reverse currents of the transistors are very small, the initial capacitor voltage is

$$V_1 = (R_{c2}/R_b)\, V_{bb} - (1 + R_{c2}/R_b)\, V_{b01} \quad \ldots\ldots\ (7)$$

where V_{b01} represents the base-cutoff potential of VT_1. On the assumption that $R_{c2} \ll R_i'$, from equations (6) and (7) the following expression for the charging current of the capacitance C is derived:

$$i_1 = \left(\frac{V_{cc} + V_{b01}}{R_i'} - V_{bb}/R_b\right) \exp(-t/\tau_1) \quad \ldots\ldots\ (8)$$

where $\tau_1 = C(R_c' + R_i') \simeq CR_i'$.

The base current of VT_2 may be found as follows:

$$i_{b2} = \frac{\beta_1 R_{c1}}{R_{i2} + R_{c1}}\, i_{b1} \simeq \beta_1 i_{b1} \quad \ldots\ldots\ldots\ (9)$$

if $R_{c1} \gg R_{i2}$, where R_{i2} represents the input resistance of VT_2.

The conducting period will end as soon as the base current of VT_2 cannot keep it in saturation; i.e.

$$i_{b2}(T_1) = (1/\beta_2)\, i_{c2}(T_1) \quad \ldots\ldots\ldots\ (10)$$

with $R_{i1} \simeq \beta_1 R_e$ and $\beta_1\beta_2 \gg 1 + R_{i1}/R_b$, the conducting period T_1 results from equations (4), (5), (8), (9) and (10):

$$T_1 = \tau_1 \ln \frac{\dfrac{V_{cc} + V_{b01}}{R_e} - \dfrac{\beta_1 V_{bb}}{R_b + \beta_1 R_e}}{\dfrac{V_{cc}}{\beta_2 R_{c2}} - \dfrac{\beta_1 V_{bb}}{R_b + \beta_1 R_e}} \quad \ldots\ (11)$$

Since the numerator of the expression in the logarithm is certainly positive, from the condition that the denominator must be greater than zero, it follows that

$$R_b > \beta_1(\beta_2 R_{c2}\, V_{bb}/V_{cc} - R_e) \quad \ldots\ldots\ (12)$$

and
$$R_e < \beta_2 R_{c2}\, V_{bb}/V_{cc} \quad \ldots\ldots\ldots\ (13)$$

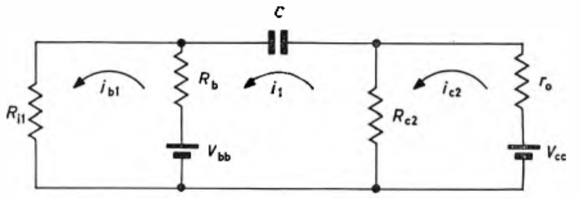

Fig. 2 Calculation of T_1

If the resistance R_b is very large, the above expression for the conducting period can be simplified to

$$T_1 \simeq \beta_1 R_e C \ln\left[\frac{\beta_2 R_{c2}}{R_e}\,(1 + V_{b01}/V_{cc})\right] \quad \ldots\ (14)$$

This expression shows that the effect of the supply voltage on the conducting period T_1 is very small.

From the given formulas it is seen that the resistors R_e and R_{c2} are convenient for controlling the pulsewidth. There is a value of R_e at which the pulsewidth passes through a maximum. With R_e approaching this value, the most constant pulsewidth may be achieved by changing R_b in the largest region. It should be mentioned that smaller values for R_e and R_{c2} allow generation of short rise and fall times, respectively.

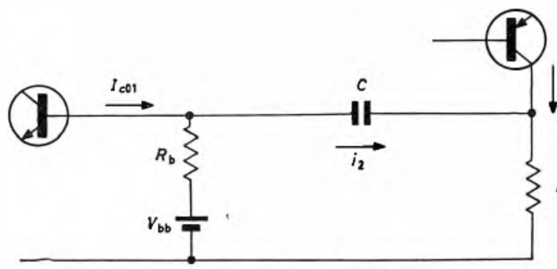

Fig. 3 Calculation of T_2

The circuit in Fig. 3 may be used to determine the nonconducting period T_2 of the transistors. For this circuit, the following equation is valid:

$$(R_b + R_{c2})\, dq/dt + q/C = -C(V_{bb} + R_b I_{c01} - R_{c2} I_{c02}) \quad \ldots\ldots\ldots\ (15)$$

At the beginning of the nonconducting period, the voltage across the timing capacitor is

$$V_2 \simeq V_{cc} - V_{b1}(T_1) \quad \ldots\ldots\ldots\ (16)$$

where $V_{b1}(T_1)$ is the base voltage of VT_1 at the end of T_1. Neglecting the reverse currents of both transistors, from equations (15) and (16), the current flowing through the timing capacitor may be found in the form

$$i_2 = \frac{V_{cc} + V_{bb} - V_{b1}(T_1)}{R_b + R_{c2}} \exp(-t/\tau_2) \quad \ldots\ldots\ (17)$$

where $\tau_2 = C(R_b + R_{c2})$.

The base voltage of VT_1 is

$$V_{b1}' = V_{bb} - R_b(i_2 - I_{c01}) \quad \ldots\ldots\ldots\ (18)$$

At the moment when this voltage reaches the base-cutoff potential of VT_1, it starts to conduct. Thus, using earlier simplifications, from equations (17) and (18), the expression for the nonconducting period may be derived as

$$T_2 = \tau_2 \ln \frac{V_{cc} + V_{bb} - V_{b1}(T_1)}{V_{bb} - V_{b01}} \quad \ldots\ldots\ (19)$$

The base voltage of VT_1 in the conducting period T_1 may be found from equations (4) and (8):

$$V_{b1} = \frac{R_{i1}}{R_{i1}+R_b} V_{bb} + \left(V_{cc} + V_{b01} - \frac{R_{i1}}{R_{i1}+R_b} V_{bb}\right) \exp\left(-t/\tau_1\right) \ldots\ldots (20)$$

The largest value of this voltage is approximately equal to the supply voltage V_{cc}. Since the base voltage decreases fairly rapidly towards the minimum, determined by the constant term in equation (20), this term can be substituted in equation (19) when estimating the duration of T_2:

$$T_2 < CR_b \ln \frac{V_{cc} + \dfrac{R_b}{R_b + \beta_1 R_e}}{V_{bb} - V_{b01}} \ldots\ldots\ldots (21)$$

From this expression it is seen that the resistor R_b and the voltage V_{bb} are convenient for controlling the space between pulses. If $R_b \gg \beta_1 R_e$, this time period will be independent of changes in R_e.

Experimental results

The described multivibrator has been tested experimentally on a circuit having the following components: VT_1 = BSX29 (p-n-p); VT_2 = BSY17 (n-p-n); $V_{cc} = 6$V; $V_{bb} = 2$V; $R_{c1} = 47\text{k}\Omega$; $R_{c2} = 180\Omega$; $R_e = 470\Omega$ (adjusted for constant T_1); $R_b = 1\text{M}\Omega$ (potentiometer); $C = 1$nF. The inverted waveforms obtained from the above circuit are shown in Fig. 4.

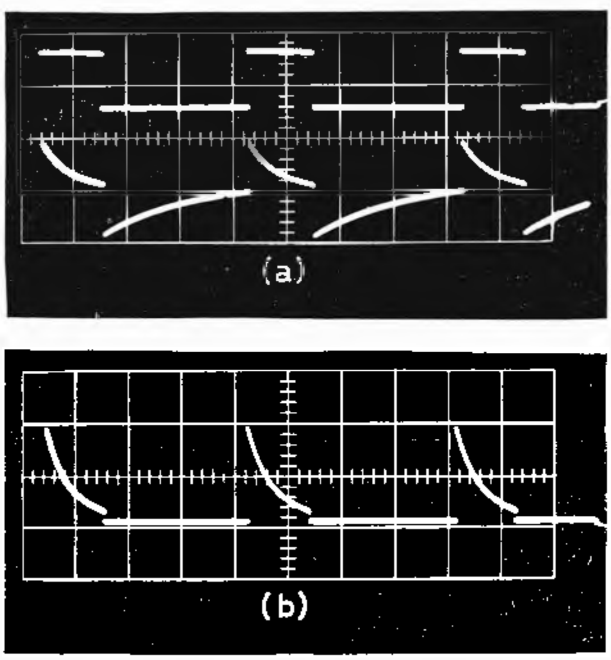

Fig. 4 (a) Voltage waveforms at the collector of VT_2 and the base of VT_1 (50μs/division; 5V/division)

(b) Current waveform at the base of VT_2 (50μs/division; 5mA/division)

For producing complementary output pulses, the resistance $R_{e2} = 180\Omega$ is put in the emitter of VT_2. Fig. 5 shows output waveforms for this case. The circuit in Fig. 6 is suitable for obtaining a very small mark/space ratio. The diode voltage limiter enables the generation of fairly short pulses, depending on the voltage V_D. The change in the potentiometer resistance has no effect on the pulsewidth. If $V_D = 2$V, this circuit produces rect-

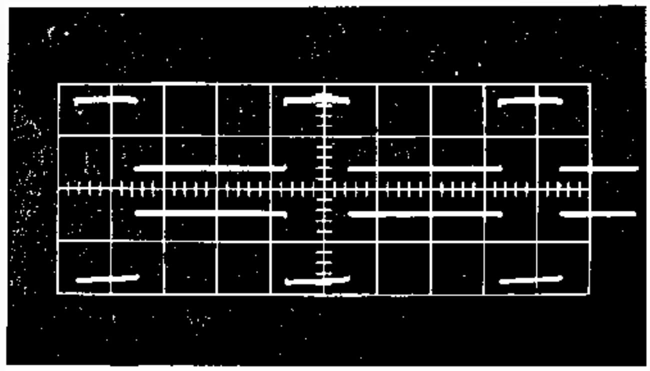

Fig. 5 Complementary output voltages (50μs/division; 2V/division)

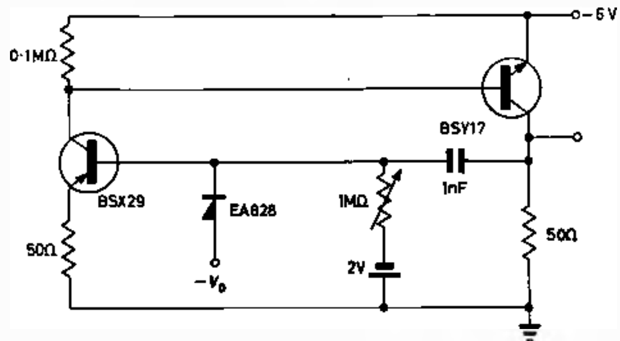

Fig. 6 Practical circuit with a low duty cycle

angular pulses of about 150ns duration. The rise and fall times (measured on an oscilloscope having a risetime of 10ns), are about 20ns and 30ns, respectively.

By means of the potentiometer, T_2 can be changed from less than 2μs to about 1600μs. Compared with T_1 of about 150ns, the maximum ratio T_2/T_1 extends to about 10000; the ratio can be considerably increased. With the following components changed in the above circuit: $V_{bb} = V_{cc} = 6$V, $V_D = 0{\cdot}5$V, $R_b = 2\text{M}\Omega$ and $C = 50$nF, the ratio T_2/T_1 is greater than 100 000, with a pulsewidth of about 250ns.

The problem of jitter has not been considered in detail. According to oscilloscope observations, the ratio $\Delta T_2/T_2$ is not greater than 0·1% in the tested circuits. However, it is to be expected that the temperature effect on the duration of T_2 may be high.

Conclusion

The free-running multivibrator described produces rectangular pulses having short transient times. The circuit is particularly suitable for the generation of waveforms with a very small mark/space ratio. In such a mode of operation, it has very low power consumption.

Acknowledgment

The author wishes to thank Prof. B. Rakovich and colleagues V. Cvekic and D. Jovanovic for their useful comments during the preparation of this article.

REFERENCES

1 Johnson, K. S.: Multivibrator with wide mark-to-space ratio, *Electronic Engng. 30* (Oct. 1958)
2 Tesic, S.: Pulses with variable mark-to-space ratio, *Electronics* (July 12, 1965)
3 Florida, C. D.: A new bistable element suitable for use in digital computers, *Electronic Engng. 30* (Feb. and March 1958)
4 Kleinberg, L. L.: Monostable circuits need power only when they work, *Electronics* (Aug. 24, 1964)
5 Rakovich, B.: A high-efficiency monostable circuit using complementary transistors, *Electronic Engng. 38* (June 1966)
6 *General Electric Company Transistor Manual (6th Edition)*, 172 (1962)

Sensitive thermistor thermometer

by **J. C. S. Richards**, Ph.D., M.I.E.E., *University of Aberdeen*

A closely specified thermistor is used in an a.c.-bridge circuit to make a direct-reading thermometer with a nearly linear scale. Without calibration, typical errors are less than ±0·5degC over a range of 20degC. An output signal of ±2·5V d.c. is available for a temperature change of ±0·05degC. The dissipation in the thermistor is always less than 30μW.

(Voir page 731 pour le résumé en français: Zusammenfassung in deutscher Sprache auf Seite 732)

There are many applications for an instrument which can detect very small changes in temperature and give an approximate indication of the actual temperature. Because of its small size, fast response and high sensitivity, the thermistor makes an excellent transducer for moderate temperatures (−50 to +150°C, say). Its chief disadvantages are its nonlinearity and its poor long-term stability. Information on the long-term stability of thermistors is scarce. If the temperature is reasonably constant and not too high (below 100°C, say), drifts in good specimens appear to be less than 0·001degC over several hours, and less than 0·01degC over weeks. At higher temperatures, or if the temperature is cycled over a wide range, the stability is poorer and there may be some hysteresis. In a general-purpose instrument, it is reasonable to provide a maximum sensitivity of 0·1degC f.s.d.; higher sensitivity is probably justified or required only in particular circumstances.

Until recently, a third disadvantage of the thermistor was in the large manufacturing tolerances in its resistance and temperature coefficient; these made it necessary to calibrate each individual instrument. However, close-tolerance thermistors are now available, and the present instrument uses the Gulton 33TD25, which has its resistance specified at 1degC intervals from −50 to +150°C, with a tolerance corresponding to ±0·2degC. The resistance is 3kΩ, and the temperature coefficient −4·4% per degC at 25°C. With such a thermistor, it it possible to design an instrument which requires virtually no calibration.

Linearization

The temperature coefficient of a thermistor is roughly proportional to the inverse square of the absolute temperature, but it is not difficult to obtain an electrical signal which varies sufficiently linearly with temperature over a moderate range. Suppose θ_L, θ_M and θ_H (degC) are the lowest, mean and highest temperatures in the range, and R_L, R_M and R_H are corresponding values of the thermistor resistance R_T. If a resistance R_S nearly equal to R_M is connected in series with R_T, the graph of the conductance $1/(R_s+R_T)$ *vs.* temperature is S-shaped over the range. If R_S is given by

$$R_S = (R_MR_H + R_MR_L - 2R_LR_H)/(R_H + R_L - 2R_M) \quad \ldots\ldots (1)$$

the S-shaped curve cuts the straight line joining the extreme points of the range in the middle. For ranges greater than 50degC, the S-shaped curve departs from the straight line by as much as 5degC for a range of 100degC. However, for a range of 50degC, the maximum nonlinearity is usually less than 1degC, and less than 0·2degC (the tolerance in the thermistor) for a range of 20degC. For these smaller ranges, it is reasonable to assume that

$$1/(R_S+R_T) = 1/(R_S+R_M) + b(\theta-\theta_M) \quad \ldots\ldots (2)$$

where θ(degC) is the temperature of the thermistor, and b is given by

$$b(\theta_H-\theta_L) = 1/(R_S+R_H) - 1/(R_S+R_L) \quad \ldots\ldots (3)$$

For the 33TD25 thermistor, b is of the order of μmho/degC. A suitable conductance bridge can be arranged to give a thermometer with a linear scale.

Bridge

The power dissipated in the thermistor must not cause it to become significantly hotter than its surroundings. This precaution is particularly important when the thermistor is immersed in a fluid, otherwise the temperature of the thermistor depends not only on the temperature of the fluid but also on its velocity. Satisfactory operation is usually possible if the maximum dissipation in the thermistor is less than 30μW, giving a temperature rise of less than 0·02degC in still air. This limits the e.m.f. across (R_S+R_T) to about 0·15V for a 33TD25 thermistor at temperatures less than 100°C.

For operation at such a low level, an a.c. bridge is much preferable to a d.c. one: the output can be easily amplified, there are no difficulties with thermal e.m.f.s and all the advantages of transformer ratio arms become available. A phase-sensitive detector is, of course, necessary to indicate the sense of the out-of-balance signal; it also serves to make the system insensitive to stray reactances and to mains or other interfering signals. A suitable bridge is shown in Fig. 1.

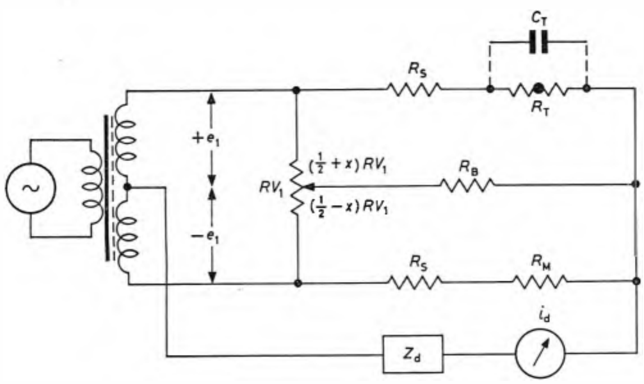

Fig. 1 Conductance bridge suitable for temperature measurement

If R_B is given by

$$R_B b(\theta_H - \theta_L) = 2 \quad \ldots\ldots\ldots\ldots\ldots \quad (4)$$

and $RV_1 \ll R_B$ and $|Z_d| \ll R_M$, then, to a good approximation, the detector current i_d is given by

$$i_d = e_1 b\,[(\theta - \theta_M) - x(\theta_H - \theta_L)]$$

Hence, if a linear potentiometer is used for RV_1, the balance setting x varies linearly from $+\frac{1}{2}$ to 0 to $-\frac{1}{2}$ as the temperature varies linearly from θ_H to θ_M to θ_L; if the temperature changes, the out-of-balance current is proportional to the change in temperature.

If the tolerances on R_S, R_M and R_B are $\pm 0{\cdot}5\%$, the total error in reading temperatures over a 20degC range is 1degC at most, and usually less than 0·5degC; on a 50degC range a tolerance of 1% in the resistances gives a total error of less than 2degC. Since R_S, R_M and R_B are not normally in the same environment as the thermistor, they must have very low temperature coefficients; when these are as low as 0·005% per degC, the output from the bridge is roughly the same, whether the temperature of the thermistor changes by 0·001degC, or that of the other bridge components by 1degC.

The most important reactive component in the circuit is the capacitance C_T associated with the leads to the thermistor. Provided that the phase-sensitive demodulator has a linear range of about three times that required to cope with the resistive unbalance signal alone, no serious errors should arise, even at the maximum sensitivity of 0·1degC f.s.d., provided that $100 R_T C_T \omega < 1$. A conveniently low value for the angular frequency ω is 3000rad/s, and with R_T as large as 10kΩ, C_T must be less than 300pF, corresponding to about 5 or 10m of coaxial cable. Where a longer lead must be used, C_T can be balanced over a limited temperature range by a capacitance in parallel with R_M.

Practical circuit

The circuit diagram of a complete thermometer is given in Fig. 2. The oscillator VT_3 provides 0·2V peak at a nominal 470Hz across each half of the transformer secondary. The unbalance signal from the bridge is amplified by two integrated-circuit operational amplifiers (Fairchild μA702). The oscillator output is squared by VT_1 and VT_2 and fed to the base of the shunt demodulator VT_4; its d.c. output signal is amplified by a third operational amplifier, for which RV_4 is a zero-setting control. At maximum sensitivity, an output of $\pm 2{\cdot}5$V d.c. is obtained for a temperature change of $\pm 0{\cdot}05$degC; the a.c. amplifier gain can be decreased by potentiometer RV_3,

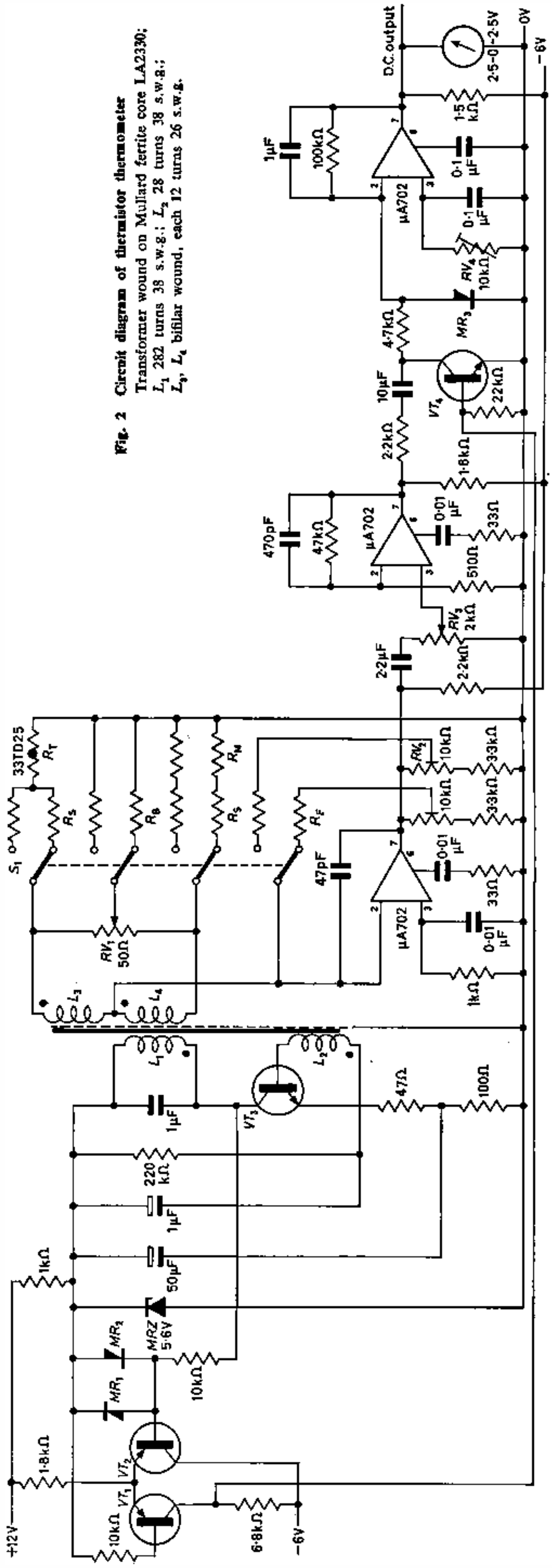

Fig. 2 Circuit diagram of thermistor thermometer
Transformer wound on Mullard ferrite core LA2330; L_1 282 turns 38 s.w.g.; L_2 28 turns 38 s.w.g.; L_3, L_4 bifilar wound, each 12 turns 26 s.w.g.

which is switched in a 1-2-5 sequence of steps, to give a minimum sensitivity of ±5degC f.s.d. A current of at least ±1mA is available to drive a recorder or control system.

Any desired ranges of temperature between 0 and 100°C may be incorporated and selected by the 4-pole switch S_1; two ranges only are shown in the diagram. For a particular range, R_S, R_M and R_B are determined with the aid of the manufacturer's data for the thermistor and equations (1), (3) and (4). To set the gain of the amplifier for each range, R_F is made roughly $0{\cdot}3/b$ ohms, and its associated preset RV_2 is adjusted using the bridge potentiometer RV_1 to give a known input signal. RV_1 is a 10-turn helical potentiometer, and its dial setting can be interpreted directly in terms of temperature change. For some of the more commonly used ranges, the values of the resistances are now given in kilohms in the order R_S, R_M, R_B, R_F: for 10 to 30°C, 2·7, 3·74, 25, 68; for 30 to 50°C, 1·1, 1·59, 11·5, 33; for 0-50°C, 2·4, 3, 9·7, 68; for 40-90°C, 0·47, 0·62, 2·3, 18.

Transistors VT_1, VT_2, VT_3 and diodes MR_1, MR_2, MR_3 are general-purpose silicon types; the transistors should have a current gain of more than 50. The demodulator transistor VT_4 may be either a bidirectional silicon type, or a less expensive unidirectional switching transistor (e.g. BFY51) selected to have an inverse current gain of more than 2 at 2mA. The power supplies (+12V, −6V at 50mA; internal impedance <0·1Ω) are decoupled to earth by 0·1μF capacitors at each operational amplifier.

On a typical instrument with a 20degCtemperature range, the error in absolute-temperature measurement is typically less than ±0·5degC, and the error in reading changes in temperature are less than 5%. The calibration of a completed instrument can be readily checked by replacing the thermistor with a suitable accurate resistance box; the calibration errors are then less than ±0·2degC, the tolerance in the thermistor.

Modifications

At temperatures greater than 100°C, the resistance of the specified thermistor is less than 200Ω. This is rather small for the circuit given, and either another thermistor must be used, or the transformer secondary e.m.f. and RV_1 must be reduced. On the other hand, at temperatures much below 0°C, the high resistance of the specified thermistor demands a larger secondary e.m.f. to maintain sensitivity, and greater care in keeping stray capacitance small.

In order to measure temperature gradients, R_M is replaced by a second thermistor of the same type. The system responds to the difference in temperature between the two thermistors without change of sensitivity, provided that the actual temperatures lie within the selected range.

An output of at least ±25μA d.c. is available directly from the demodulator, and for some applications the d.c. amplifier can be dispensed with. It is then also possible to do away with the negative supply line, since the squarer circuit (VT_1 and VT_2) can be modified in a fairly obvious way and its output capacitatively coupled to the base of VT_4; each of the operational amplifiers can be replaced by two-shunt feedback pair stages[1] in cascade. A judgment as to whether this modification results in a significantly cheaper instrument can only be made by detailed costing using current prices of components, labour etc.

Reference

1 Richards, J. C. S.: Simplified design of the feedback pair. *Electronic Engng.* 39, 97-99 (1967)

Low-voltage ring-of-two reference

by **P. Williams,** *Paisley College of Technology, Renfrewshire*

A circuit is described which has been discussed recently as a source of both constant current and constant voltage. A novel application is introduced which achieves a stability comparable with conventional reference circuits but requires a supply voltage lower than that of the lowest-voltage Zener diode. Its applications are indicated as those where the available supply is either too low or too variable for conventional designs.

(Voir page 731 pour le résumé en français: Zusammenfassung in deutscher Sprache auf Seite 732)

The majority of d.c. regulators with good stability against supply and temperature changes utilize a Zener diode with a breakdown voltage of 6V or higher. A supply voltage in excess of this is required, and the provision of a low stabilized direct voltage becomes inefficient. The problem is eased if the reference diode can be fed from a separate higher-voltage supply, with the output stages of the regulator receiving a voltage only slightly in excess of the required output (Fig. 1). For mains-operated equipment, efficiency may not be important, while the provision of separate supply rails for the Zener diode and the amplifier is a straightforward, though unwelcome, complication. Where battery power has to be used, cost and convenience make both solutions unattractive. There is thus a considerable advantage in having a circuit that can provide a stable voltage for use with d.c. regulators, but is able to operate from any available supply. The circuit shown in Fig 2 maintains its stability with a supply voltage down to about 1·1V and will tolerate voltages up to the V_{cb} breakdown for the transistors used. Over a 10:1 supply-voltage range, it is possible to hold the current to within 2 or 3%; and to this extent the performance is comparable with that of an earlier circuit using conventional Zener diodes[1]. For stability against temperature changes, the drift in forward voltage on a silicon diode is matched against that of the base-emitter junction of a germanium transistor. A resulting temperature coefficient of $\pm 0{\cdot}1\%$ per degC is reliably obtained under these conditions. Providing, as it does, more than one stable direct voltage, while drawing a constant current, the circuit may usefully be described as a ring-of-two reference, this conveying both function and form.

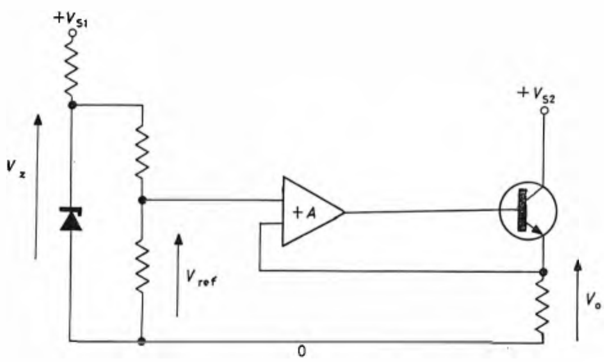

Fig. 1 For $V_{S1} > V_z$, low-current high-voltage reference supply
For $V_{S2} > V_0$, high-current low-voltage output supply

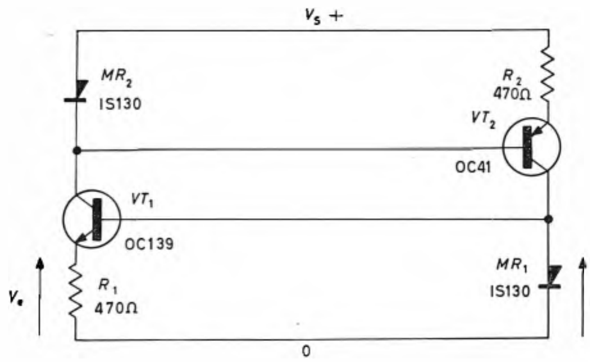

Fig. 2 Stable circuit with supply voltage down to 1·1V

Some earlier references to this circuit have covered its characteristics as both a source of stable direct voltages and the current dual of a Zener diode[1-3]. In all these cases, the Zener diodes have the task of stabilizing the currents, and hence the resistive voltage drops, in the circuit. It must be realized that they achieve this by virtue of a slope resistance that is much less than the V/I ratio at the operating point; i.e.

$$\delta V/\delta I \ll V/I$$

Alternatively, this may be expressed as

$$\delta V/V \ll \delta I/I$$

which describes the diode in a more usual way: for a given fractional change in current through the diode, the voltage across it will change by a much smaller fraction. The ratio

$$(V/I)\ /\ (\delta V/\delta I) = V\delta I/I\delta V$$

is then a suitable figure of merit for comparing Zener diodes of widely varying breakdown voltages and at differing currents. Any other component that shares this property of low slope resistance can replace Zener diodes in stabilizers with a variable measure of success. In particular, *p-n* junctions biased in the forward direction follow an exponential current/voltage law and, by differentiation, can be seen to meet the condition in principle. In the Appendix, it is shown that the above ratio may reach, perhaps, 15:1, a figure that is confirmed by the measurements plotted in Fig. 3. This is adequate

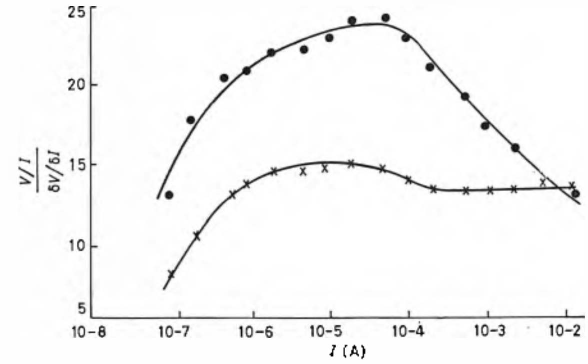

Fig. 3 Variation in figure of merit with output current
● V_{be} ME101 planar transistor
× IS921 diode

for simple stabilizers provided that the temperature drift can be compensated, though good Zener diodes may have a figure of merit one or more orders of magnitude greater. The present circuit overcomes the problem of supply-voltage variation by defining the current fed to each diode in terms of the voltage developed across the other.

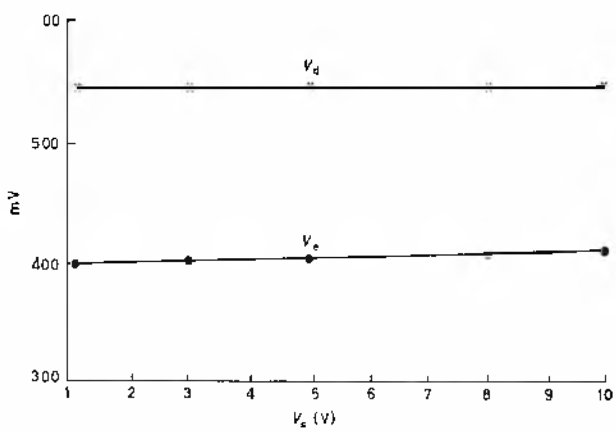

Fig. 4 Supply-voltage characteristics for the circuit in Fig. 2

The figure of merit to be considered is then the ratio of the collector dynamic resistance to the diode slope resistance, and this can be extremely high. The transistors operate almost in common base, with a relatively low resistance in the base circuit and a much larger one in the emitter; hence the transistor output resistance is of the order of r_c. Fig. 4 shows the variation in diode forward voltage and resistor voltage drop with supply voltage for the circuit in Fig. 2. As expected, there is an increase in current, and hence the resistor voltage V_e changes by more than the change in that across the diode, V_d. Since the change in supply voltage is in excess of 10:1, it can be said fairly that, under normal operating conditions, supply-induced changes will be negligible.

The major problem remains that of temperature drift, the low voltage levels making it important to achieve the best possible matching of diode and transistor drifts. It is simplest to assume that the desired characteristic of constant V_e can be achieved, and then deduce the relevant properties of the semiconductor components on the further assumption that the resistance temperature coefficient is negligible. These conditions imply that the transistor emitter currents, though not necessarily the collector currents, have to be stabilized. For high-gain transistors and at temperatures where leakage currents are moderately low, the collector currents will substantially equal the emitter currents, and will hence exhibit little change with temperature. Under these conditions, the total current will vary little, since it is equal to the sum of the collector currents.

Used as a 2-terminal element, the circuit behaves as a constant-current diode with a degree of temperature drift represented by the difference in emitter and collector currents. The relevant characteristics whose temperature drifts have to be matched are

(i) the V_{be} drift for constant emitter current in a germanium transistor

(ii) the forward voltage drift in a silicon diode carrying a current that decreases slightly with temperature fall: $I_{d2} = I_{c1} - I_{b2}$.

It will simplify the description if it is assumed that the circuit has perfect complementary symmetry of component values as well as of form:

$$I_{c1} = I_{c2} = I_c$$

$$I_{e1} = I_{e2} = I_e \text{ etc.}$$

To a first approximation, diode and emitter currents are equal to each other and to the transistor collector currents. Hence the required temperature drifts may be assumed from the figures more usually specified:

$$\left.\frac{\delta V_{be}}{\delta T}\right|_{I_c \text{ constant}} \text{ and } \left.\frac{\delta V_d}{\delta T}\right|_{I_d \text{ constant}}$$

From these it can be seen that the magnitude given by (i) will be a little low, since the current gain and leakage both rise with temperature, causing I_c to increase towards I_e; throughout it is assumed that the desired result of I_e constant is maintained. Similarly, the figure given by (ii) will also be low, since the base current is falling, and collector current rising, as temperature increases.

$$\left.\frac{\partial V_{be}}{\partial T}\right|_{I_c \text{ constant}} < \left.\frac{\partial V_{be}}{\partial T}\right|_{I_e \text{ constant}}$$

Here, due account must be taken of the negative sign of the derivatives;

$$\left.\frac{\partial V_d}{\partial T}\right|_{I_d \text{ constant}} < \left.\frac{\partial V_d}{\partial T}\right|_{I_e \text{ constant}}$$

Fortunately, most silicon diodes have temperature drifts that provide a moderately good match for the relevant transistor V_{be} drift in this circuit. The components originally chosen are shown in Fig. 2 and gave satisfactory operation for the temperature range 20-50°C without selection. Temperature stability of 0·1% per degC is possible for a wide range of diodes and transistors, but it appears unlikely that this can be improved to better than 0·04% without careful selection. Figs. 5 and 6 and Table 1 show the main characteristics of some alternative versions of this circuit. In comparing the performance of this with conventional stable direct-voltage sources, the major difference is the supply-voltage requirement. Where very high stability is required, there is no easy

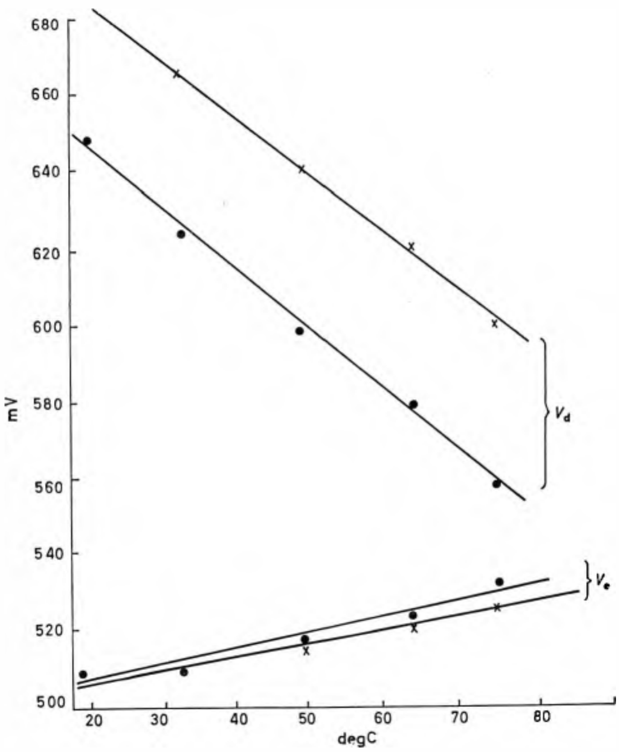

Fig. 5 Curves of V_e and V_d against temperature
× $R_1 = R_2 = 470\Omega$
● $R_1 = R_2 = 2{\cdot}2\text{k}\Omega$
MR_1, MR_2 base-emitter diodes of ME101 planar transistors

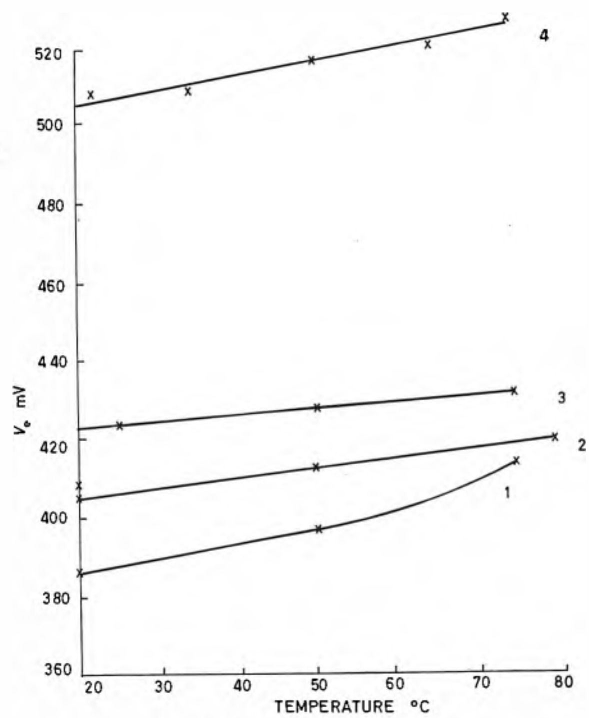

Fig. 6 Curve of V_e against temperature

alternative to a temperature-compensated reference diode operating from a stabilized current. The minimum supply voltage will then be high—normally in excess of 10-12 V—and the current consumption for the complete circuit is likely to be greater than 10mA. If an overall stability of 1% is adequate and the temperature range is not too great, a simple Zener-diode circuit may suffice; although, again, the supply voltage must be higher than the Zener breakdown voltage, fixing the minimum at about 4V for a 3·3V Zener diode and perhaps 9V for a 6V diode, with its lower temperature drift. Thus, for any supply below about 5V, the present circuit is one of the few viable alternatives; at still-lower supply voltages down to 1·1V, it may be the only simple circuit attaining overall stability of the order of 1%. Since this stability can be held for an extremely wide range of voltages, it permits the design of regulated battery supplies with lower end-of-life cell voltages. It is perfectly feasible to take a regulator delivering 0·9V ± 1% from a single dry cell, for cell voltages down to 1·1V.

TABLE 1

CURVE IN FIG. 6	1*	2	3	4†
VT_1	2N1308	0C139	2N1308	2N1308
VT_2	2N404	0C42	2N404	2N404
R_1	1k Ω	470 Ω	220 Ω	1k Ω
R_2	1k Ω	470 Ω	220 Ω	1k Ω
MR_1	IS130	IS130	IS130	ME101
MR_2	IS130	IS130	IS130	ME101

* High-leakage 2N1308: poor high-temperature stability
† Base-emitter diode of planar transistor used

If stability at low supply voltages were all this circuit could offer, its complexity relative to a simple Zener-diode circuit might limit its applications. In the applications envisaged, it would be used as the reference for a d.c. stabilizer, and other properties of the circuit could most usefully be employed. Since the circuit has total complementary symmetry of form and, as far as possible, of component values, it can be used without change for the regulation of positive and negative supplies. At low voltages, the error amplifier of any stabilizer will suffer from low loop gain, because of the small resistor values that must, of necessity, be used. Wherever possible, these resistors can be replaced by common-base transistors whose high output dynamic resistances provide ideal loads. Many standard regulators employ this technique, but there is always the difficulty of providing a suitable bias voltage for the bases of these transistors. It is not proposed to deal here with the detailed design of such circuits. In the ring-of-two, the voltages across the forward-biased diodes are precisely those which will produce the most constant current in a transistor biased from them, since their temperature drift has already been chosen to match that of a germanium transistor (Fig. 7).

This circuit, using six unselected components, provides four voltages of good stability against supply changes. One with respect to each supply line has a low temperature coefficient; one with respect to each supply line has a temperature coefficient reasonably matched to that of a germanium transistor. The supply voltage used is remarkably uncritical, being limited at the lower end to a value slightly less than the sum of the diode forward voltages, and at the upper end almost reaching the

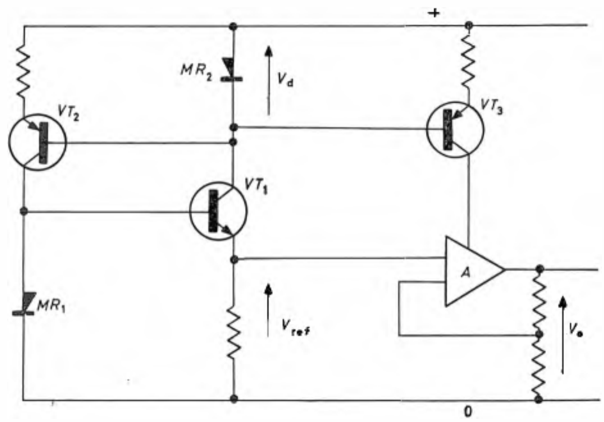

Fig. 7 Temperature drift of diode voltage V_d provides approximate compensation for that of the V_{be} of VT_3; the latter is then a constant-current source for the error amplifier, increasing gain

transistor V_{cb} breakdown. It could find application where moderate stability is acceptable but where the available supply is either too low or too variable for conventional designs.

APPENDIX

The forward-conduction characteristics of a semiconductor diode are given by an expression of the form:

$$I = I_0(e^{\lambda V} - 1)$$

where $\lambda = q/kT = 1/26\text{mV}$ at 25°C

For a silicon diode with a forward voltage drop of several hundred millivolts,

$$I \simeq I_0 e^{\lambda V}$$

$$dI/dV \simeq I_0 \lambda e^{\lambda V} = \lambda I$$

$$\text{Figure of merit } (V/I) / dV/dI) = (V/I)\lambda I = \lambda V$$

$$= V/26\text{mV} \quad \text{at room temperature.}$$

With typical values for V of 500-700mV for currents in the milliampere range, the figure of merit assumes values of 20-30. Thus, for a 5% change in current through a silicon diode under these conditions, the voltage would change by approximately $5/25 = 0{\cdot}2\%$.

The above is a much simplified analysis of the behaviour of such forward-biased diodes. At high currents (this term may mean a few milliamperes for small junctions), the slope resistance will not fall as rapidly as expected, and will reach a minimum value determined by the bulk resistance of the diode; thus the figure of merit will fall. Further, the basic equation ignores the recombination effects which would add an additional factor η to the equation, giving

$$I = I_0 \exp(qV/\eta kT)$$

This additional term is dependent on the current level and may be between 1 and 2, depending on the construction and operating level of the diode. The effect is to reduce the figure of merit from a maximum of, perhaps, 25 to 15 or less in some cases, while in others the full value is still obtained.

REFERENCES

1 WILLIAMS, P.: High-stability direct-voltage reference, *Electronics Letters* 3, 64-65 (1967)
2 WILLIAMS, P.: Constant-current circuit, *Wireless World*, 456 (Sept. 1966)
3 BAXANDALL, P. J.: Constant-current circuits, *ibid.*, 609 (Nov. 1966)
4 RUDGE, J. C.: Constant-current circuits, *ibid.*, 610 (Nov. 1966)
5 WILLIAMS, P.: Ring-of-two reference, *Wireless World*, 318-322 (July 1967)

Transistor parameters and their influence on amplifier risetime

by **D. Ivekovic,** *Institute 'Ruder Boskovic', Zagreb, Yugoslavia*

The influence of low-frequency current gain β_0, cutoff frequency f_t, collector-to-base capacitance C_c and base spreading resistance r_b on the common-emitter-transistor risetime is considered. A comparison of these parameters is given for several American and European transistor types. The limits of validity of the simplified transistor equivalent circuit for determining a single-pole gain transfer function are given, neglecting the collector-to-emitter capacitance. It is shown that, with the development of transistor technology, as the cutoff frequency is being raised, the influence of the Miller effect on the risetime is becoming more pronounced.

(Voir page 731 pour le résumé en français: Zusammenfassung in deutscher Sprache auf Seite 732)

When designing fast transistorized pulse amplifiers, it is necessary to know the transistor equivalent circuit. In determining the configuration of this, the gain transfer function determined by a single pole in the complex p-plane is required to simplify the risetime calculation when the transistors are connected in cascade for higher gain. The influence of the transistor output conditions on the risetime can usually be shown by the Miller effect, i.e. by increasing the transistor input capacitance. In this article, the error when accepting a single-pole transistor transfer function and expressing the simple Miller-effect mechanism will be evaluated.

The risetime is expressed in terms of transistor parameters by using Elmore's definition[1]. The transistor is assumed a linear active element; if the gain transfer function is of the form

$$A(p) = \frac{b_1 p + b_0}{a_2 p^2 + a_1 p + a_0}$$

the risetime of the response to a step function will be

$$T_R^2/2\pi = (a_1/a_0)^2 - (b_1/b_0)^2 - 2a_2/a_0 \quad \ldots\ldots \ (1)$$

Apart from the common-emitter current-gain/bandwidth product f_t, two normalized transistor parameters influencing the risetime are introduced.

Common-emitter equivalent circuit

The Giacoletto[2] equivalent circuit for a common-emitter transistor configuration is given in Fig. 1. The collector-current i_c source is driven by minority-carrier-recombination current i_b'. Between the external base contact b and the inherent base b', there is the base spreading resistance r_b. The ability of the base to accumulate a certain amount of charge due to the minority carriers is represented by the capacitance C_t:

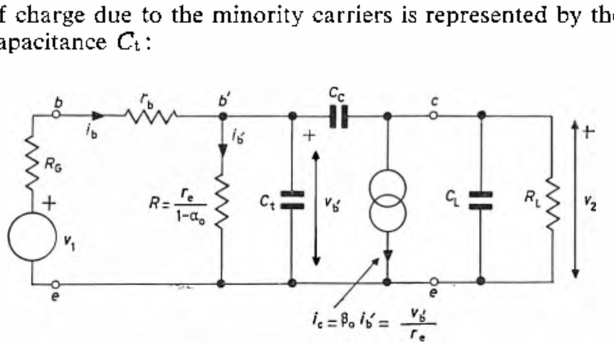

Fig. 1 Common-emitter Giacoletto equivalent circuit

$$C_t = \frac{1}{r_e \omega_t}$$

which is mostly contributed by the emitter-diffusion capacitance. The emitter resistance r_e depends on the temperature and on the steady collector current I_e. At room temperature,

$$r_e(\Omega) = \frac{27}{I_e(\mathrm{mA})}$$

Looking from the base, the emitter resistance is enlarged by the factor $1/(1-\alpha_0) \simeq \beta_0$, where α_0 is the common-base current gain and β_0 is the common-emitter current gain, both at low frequencies; $\omega_t = 2\pi f_t$ is the common-emitter current-gain/bandwidth product. There is a capacitance C_c between the collector c and the base b', contributed mostly by the collector-depletion-layer capacitance. R_G is the generator output impedance; the collector is loaded by the parallel combination of a load resistance R_L and a load capacitance C_L.

The voltage-gain transfer function for the circuit given in Fig. 1 is

$$A(p) = \frac{b_1 p + b_0}{a_2 p^2 + a_1 p + a_0}$$

When the generator output impedance R_G is zero, the transfer-function coefficients are

$$b_0 = 1/r_b r_e$$

$$b_1 = -(C_c/r_b)$$

$$a_0 = \frac{1}{r_e R_L} \frac{\beta_0 r_e + r_b}{\beta_0 r_b}$$

$$a_1 = C_c/r_e + \frac{C_t + C_c}{R_L} + \frac{C_c + C_L}{r_e} \frac{\beta_0 r_e + r_b}{\beta_0 r_b}$$

$$a_2 = C_c C_t + C_L C_t + C_L C_c$$

Since $b_0 > 0$ and $b_1 < 0$, a zero point occurs in the right half of the complex frequency plane. This zero is due to the direct flow of the signal from the base to the collector through the base-collector capacitance C_c. The gain is

$$A_0 = A(0) = b_0/a_0 = -R_L \frac{r_b + \beta_0 r_e}{\beta_0} \quad \ldots\ldots\ldots \ (2)$$

where $-\beta_0/(r_b + \beta_0 r_e)$ is the effective transconductance of the transistor.

According to equation (1), the risetime is

$$T_R^2/2\pi = \frac{A_0^2 r_b^2}{\omega_t^2 R_L^2}\left[(R_L/r_e)^2 \left(q_1 + \frac{q_1 + q_2}{q_3} \right)^2 + 2\, R_L/r_e\,(q_2^2 + q_2 + q_2^2/q_3) + (1+q_2)^2 - (q_2/q_3)^2 \right] \ldots \ (3)$$

where q_1, q_2 and q_3 are normalized parameters:

$$q_1 = C_L/C_t$$
$$q_2 = C_c/C_t$$
$$q_3 = \frac{\beta_0 r_b}{r_b + \beta_0 r_e}$$

Equation (3) is not suitable for evaluating the risetime and so some assumptions are made; i.e. some parameters in equation (3) are neglected in accordance with practical transistor values.

The influence of the direct signal from the base of the collector ($q_2^2/q_3^2 \ll 1$) can be neglected; the collector-emitter capacitance C_L and the collector-base capacitance C_c can be assumed much smaller than the base-emitter capacitance C_t ($q_1 \ll 1$, $q_2 \ll 1$); and the transistor mutual conductance can be assumed such that $q_3 \ll 1$, where q_3 represents the gain when $R_L = r_b$.

In accordance with the assumptions above, the normalized risetime is of the form

$$T = T_R\, f_t\, \sqrt{(2\pi)} = \mu_1 (1 + A_0\, \mu_2/\mu_1) \ \ldots\ldots \ (4)$$

where $$\mu_1 = q_3 = \frac{\beta_0 r_b}{r_b + \beta_0 r_e} \ \ldots\ldots\ldots\ldots\ldots \ (5)$$

and $$\mu_1 = r_b C_c \omega_t \ \ldots\ldots\ldots\ldots\ldots\ldots\ldots \ (6)$$

are normalized transistor parameters.

The factor μ_2/μ_1, when multiplied by the gain A_0, expresses the relative contribution of the Miller effect to the total risetime; so that the expression within parentheses gives the ratio between the transistor cutoff frequency f_t (usually used as a transistor figure of merit) and the effective inherent cutoff frequency. μ_1 gives the factor which, when multiplied by the effective inherent cutoff frequency, determines the ratio between f_t and the actual common-emitter voltage-gain cutoff frequency. Its physical explanation lies in the finite time needed to charge the base-emitter capacitance through the base spreading resistance. The normalized parameters μ_1 and μ_2 are influenced only by the transistor parameters and are invariants of the gain. The risetime is influenced by the gain only through the Miller effect; so that the initial slope of the time response to a step function increases with gain for the values of gain up to 10 or more.

The equivalent circuit in Fig. 1 can be simplified by omitting C_L and enlarging C_c by the factor $1 + A_0\ \mu_1/\mu_2$.

Comparison of several transistor types

A comparison of some American and European transistor types, with regard to μ_1 and μ_2, is given in Fig. 2. The material (Ge or Si) and the technology group (alloy, MADT or planar) is indicated. The f_t, β_0, C_c and r_b test collector voltage and current are chosen to give cutoff frequency f_t and low-frequency current gain β_0 as high as possible, and base spreading resistance r_b and collector-base capacitance C_c as low as possible. This will be fulfilled for a high-voltage low to medium-current working point, collector voltage being limited by the maximum allowed collector dissipation.

The sloping straight lines are the loci of the constant Miller-effect contribution to the transistor risetime for unity gain, expressed as a percentage: $100\ \mu_2/\mu_1$.

A comparison of transistor types with regard to the cutoff frequency f_t and the Miller-effect contribution to the risetime is given in Fig. 3. The constant-gain curves at the right of the diagram show how far a locus of a certain transistor for particular values of A_0 and $100\ \mu_2/\mu_1$ has to be moved to the left (i.e. towards lower frequency) to

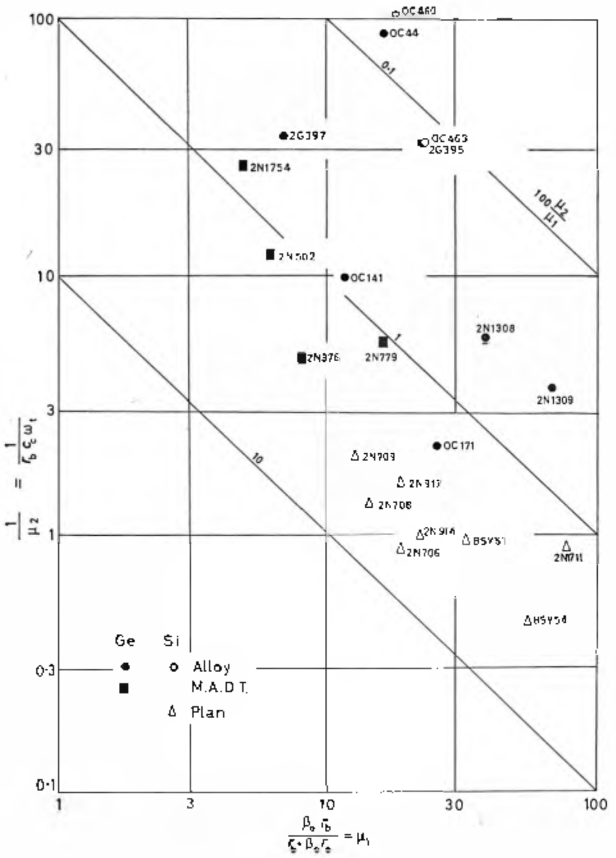

Fig. 2 Comparison of some American and European transistor types with regard to μ_1 and μ_2

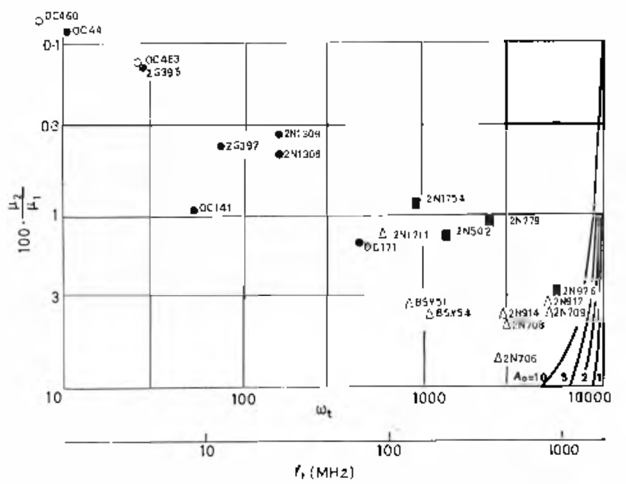

Fig. 3 Comparison of transistor types with regard to cutoff frequency f_t and the relative contribution of Miller effect to the risetime

reach the point determining the effective inherent cutoff frequency f_t of the transistor, $f_t' = f_t/(1 + A_0\ \mu_2/\mu_1)$. It can be seen that transistors with higher f_t suffer from higher Miller-effect contribution to the risetime. This effect is more evident for planar than for MADT types.

The simplified transistor equivalent circuit, neglecting the collector-to-emitter capacitance, for determining a transfer function with a single pole, has certain limits of validity. To find the error when accepting the simplified equivalent circuit, the risetime obtained will be compared with one determined by the more precise equation (3). The ratio between these two quantities

$$\frac{T_{(3)}}{T_{\text{approx}}} = 1 + \frac{P}{100}$$

leads to the relation

$$1/A_0\ \mu_1/\mu_2 = 100\left[\frac{C_L/C_c\ 1/\mu_1\ (2 + C_L/C_c\ 1/\mu_1)}{P\,(P+200)}\right]^{1/2} - 1 \quad \ldots\ldots\ldots\ldots (7)$$

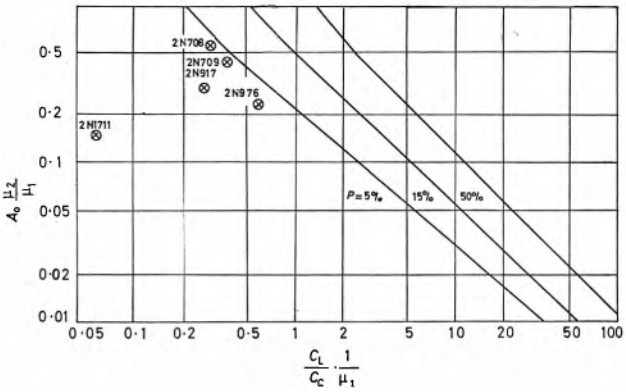

Fig. 4 Loci of the constant error when evaluating risetime using a single pole transfer function ($A_0 = 10$, $C_L/C_c = 5$)

The constant-P curves are shown in Fig. 4. The errors for 2N708, 2N709, 2N917, 2N976 and 2N1711 transistors, and for when the gain is $A_0 = 10$ and the ratio $C_L/C_c = 5$, are calculated. It can be seen that the errors are less than 5% for the conditions mentioned.

Conclusions

Besides the cutoff frequency f_t, defined as the common-emitter short-circuited collector current gain/bandwidth product and taken as the transistor figure of merit, there are two normalized transistor parameters:

$$\mu_1 = \beta_0 r_b/(r_b + \beta_0 r_e)$$

$$\mu_2 = 2\pi f_t r_b C_c = \omega_t r_b C_c$$

affecting the transistor risetime. Accepting the simplified transistor equivalent circuit, neglecting the collector-to-ground capacitance, gives an error of less than 5% when calculating the risetime for practical values of gain and collector-capacitance.

The Miller effect, which is practically the only output-condition influence on the risetime, increases as the cutoff frequency f_t increases. This effect is less evident in MADT than in planar transistors.

REFERENCES

1 Elmore, W. C.: *J. Appl. Phys. 19*, 55 (1948).
2 Giacoletto, L. J.: *RCA Rev. 15*, 506 (1959).

Linear-staircase generator

by **M. Cadwallader,** C.Eng., A.M.I.E.R.E., *Marconi Instruments Ltd,*

The staircase-generator circuit which is described is of the switched binary weighted-resistor type, often used for digital-analogue conversion. A new design method for the switching-transistor circuits gives a linearity error of only ±0·035%, with normal transistor supply voltages. A novel summing amplifier contributes to the good linearity and the temperature coefficient of 0·01% per degC. Some applications of the circuit as a nonlinear waveform generator are given.

(Voir page 731 pour le résumé en français: Zusammenfassung in deutscher Sprache auf Seite 732)

The generation of a linear staircase is a common requirement in many electronic systems. Digital-analogue and analogue-digital converters are frequently based on a circuit which can generate a linear staircase. Staircases with a large number of steps are good approximations to a linear ramp, and, because the circuits are directly coupled, the mean rate of change may be made as low as required, without the use of bulky components. Staircase generators may be used to generate various waveforms by suitable modulation of the input signal. This article describes a circuit using silicon planar transistors, which has good linearity and low thermal drift without the need for high supply voltages. The excellent performance of the circuit is obtained by careful analysis and design of the saturated-transistor switches and by the use of a novel summing amplifier.

Basic circuit

The input pulse train is fed into a chain of n binary stages; the outputs of the binaries are used to operate transistor switches which connect appropriate binary weighted resistors to a current-summing amplifier. The output of the amplifier is linearly related to the instantaneous count of the binaries[1,2]. The maximum number of staircase levels is 2^n, where n is the number of binaries. The maximum current into the summing amplifier occurs when all the transistor switches are closed, and is given by

$$I_S = V_S/R \sum_{k=1}^{k=n} 2^{k-1} \quad \ldots\ldots\ldots\ldots (1)$$

Equation (1) neglects transistor saturation voltage; the basic circuit is shown in Fig. 1.

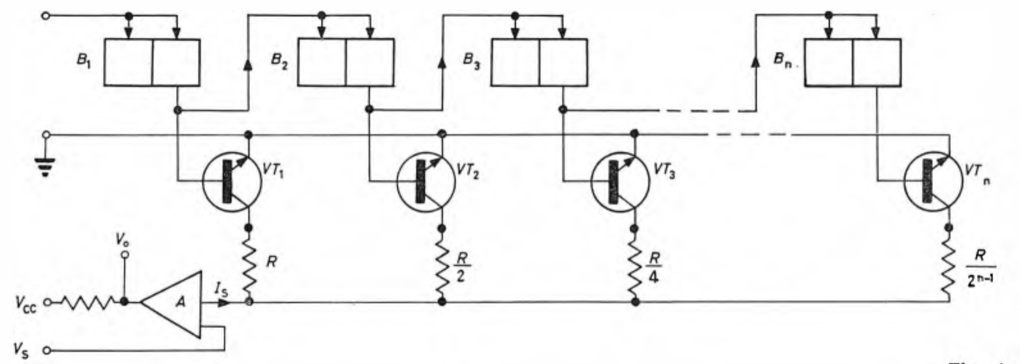

Fig. 1 Basic circuit

Transistor switches

The collector-emitter saturation voltage (V_{CEsat}) for epitaxial planar transistors is low and may be calculated from the expression[3]

$$V_{CEsat} = KT/q \ln \frac{\alpha_I \{1 - I_C/I_B [(1-\alpha_N)/\alpha_N]\}}{1 + I_C/I_B (1 - \alpha_I)} \quad \ldots\ldots (2)$$

where K = Boltzmann's constant
T = absolute temperature
q = charge on an electron
and $KT/q = 0{\cdot}026$V at room temperature.

Equation (2) neglects the voltages developed across the volume resistance of the semiconductor material; this is justified for the circuits to be considered.

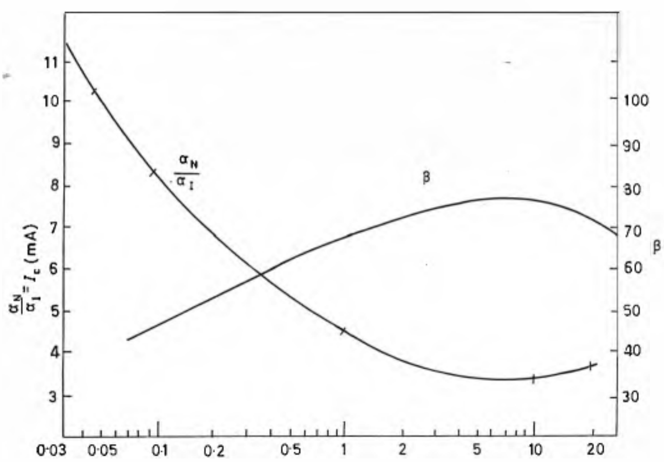

Fig. 2 Normal and inverse gain (transistor BSX20)

The common-base normal and inverse current gains, α_N and α_I, respectively, are functions of the collector current. Fig. 2 shows α_N/α_I and β_N as a function of I_C for the BSX20 transistor. Equation (2) may be written as

$$V_{CEsat} = KT/q \ \ln \phi$$

By keeping ϕ constant for all the switching transistors, V_{CEsat} will not cause any linearity error. If ϕ is calculated for the most significant switch, a base current can be calculated to give the same value of ϕ for the less significant switches; i.e.

$$I_B = \frac{I_C \{\phi(1-\alpha_I) + \alpha_I [(1-\alpha_N)/\alpha_N]\}}{\alpha_I - \phi} \quad \ldots\ldots (3)$$

The common-emmitter current gain for the saturated transistor is lower than that measured under normal test conditions. Both the normal and inverse gains are reduced to approximately $0{\cdot}4\beta_{unsat}$.

The thermal drift due to the transistor-switch saturation voltage varying with temperature is given by

$$\delta V_{CEsat} = \frac{86 \times 10^{-6} \ln \phi}{V_S} \text{ \% per degC} \quad \ldots\ldots (4)$$

An additional advantage of operating at a fixed ϕ for all the switching transistors, is that, since the saturation voltages will all have the same temperature coefficient, compensation can be applied using a similar saturated transistor.

Summing amplifier

A simple current-summing amplifier could consist of a single transistor connected as a common-base stage. However, this simple amplifier would be inadequate in two respects: the input resistance would not be low enough and the output would be subject to thermal drift. A circuit which overcomes the problem of thermal drift is shown in Fig. 3. The additional transistor VT_1 provides tempera-

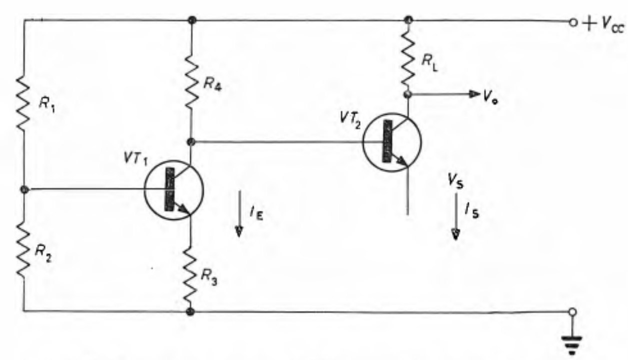

Fig. 3 Temperature-compensated common-base summing amplifier

ture compensation for the common-base amplifier VT_2 Transistor VT_1 compensates for changes in base-emitter voltage, collector-base current and current gain with change of ambient temperature. The relative circuit values are derived in Reference 4, where the circuit is used as a stable current generator.

Reference 4 gives the following relative values:

$$R_3 = R_4 \quad \ldots\ldots (5)$$

for compensation of base-emitter voltage, and

$$\frac{R_1 R_2}{R_1 + R_2} = 2R \Big/ \sum_{k=1}^{k=n} 2^{k-1} \quad \ldots\ldots (6)$$

for compensation of leakage current and current gain.

To ensure tracking of the base-emitter voltages with temperature, the emitter current I_E of transistor VT_1

should ideally be the same as that of VT_2. The best compromise is to make I_E equal to half the peak current of VT_2; i.e.

$$I_E = I_S/2 \quad \ldots\ldots\ldots\ldots\ldots\ldots \quad (7)$$

Although optimum compensation is only obtained when the input current is equal to I_E, the circuit gives good compensation over the whole range of input currents. A linearity error will be introduced by the finite input resistance of the common-base amplifier shown in Fig. 3. The input resistance may be made zero (or even negative) by providing feedback between the output and the junction of R_1 and R_2, as shown in Fig. 4. As the current into the amplifier changes from zero to I_S, the base-emitter voltage of transistor VT_2 increases by δV_{BE}; a further error is introduced by the change in base current in R_4. The total

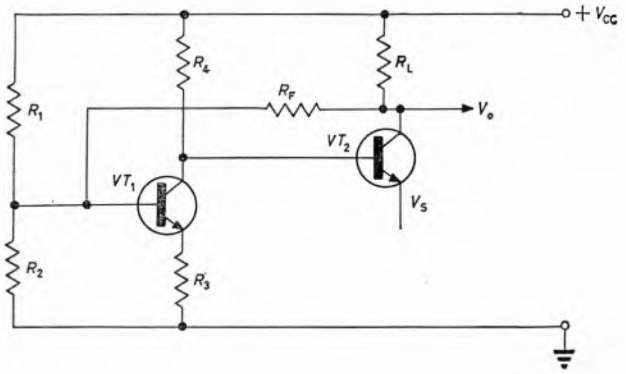

Fig. 4 Low-impedance summing amplifier

error voltage v_e is given by

$$v_e = \delta V_{BE} + \frac{I_S R_4}{1+\beta} \quad \ldots\ldots\ldots\ldots\ldots \quad (8)$$

where β is the common-emitter large-signal current gain. If R_P is the resistance of R_1, R_2 and the input resistance of transistor VT_1 all in parallel, R_F is given by

$$R_F = R_P\,\{V_0/v_e - 1\} \quad \ldots\ldots\ldots\ldots \quad (9)$$

where $$V_0 = \frac{I_S R_L \beta}{1+\beta} \quad \ldots\ldots\ldots\ldots\ldots\ldots \quad (10)$$

Part of R_F may be adjustable to cover the range of transistor gain.

For all normal circuit values, the circuit will be stable. A necessary condition for stability is that

$$\frac{R_L R_P}{R_F R_E + R_P R_E} < 1 \quad \ldots\ldots\ldots\ldots\ldots \quad (11)$$

where $$R_E = R_1 \Big/ \sum_{k=1}^{k=n} 2^{k-1} \quad \ldots\ldots\ldots\ldots\ldots\ldots \quad (12)$$

It is not possible to obtain zero input resistance over the whole range of input current, owing to the variation of transistor gain. An improvement can be effected by adding a fixed current to the input, thereby reducing the change in gain. The resulting pedestal voltage at the output can be backed off if necessary.

Performance

The base current for the switching transistors was calculated using equation (3), after fixing the ratio of I_C/I_B at 2 for the most significant switch. The circuit was built

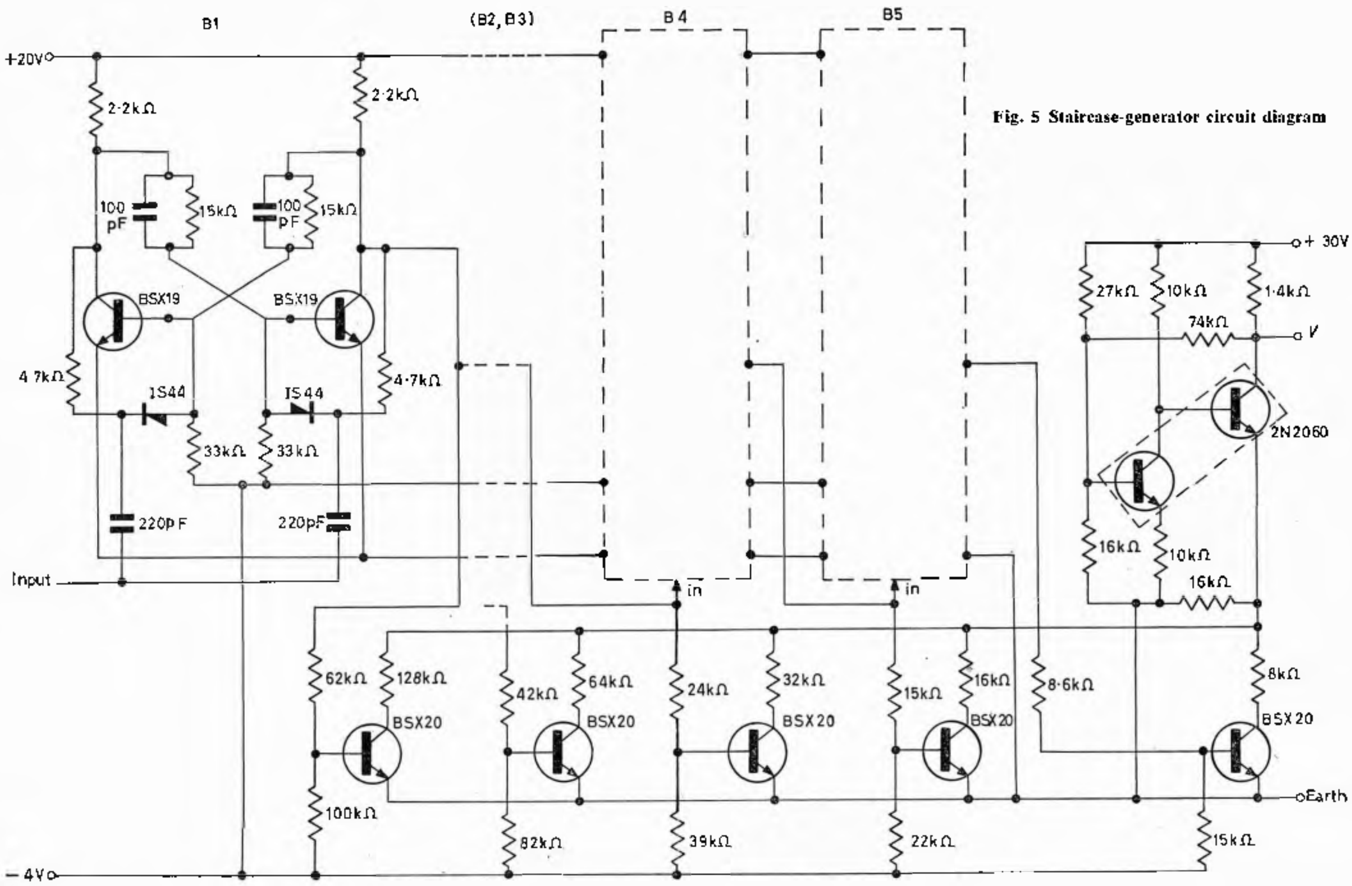

Fig. 5 Staircase-generator circuit diagram

using the nearest preferred values for the resistors. The range of measured values for V_{CBsat} was 87·2 to 92·7mV, giving a linearity error of $\pm$0·028%. The binary weighted resistors had accuracies of $\pm$0·02% for the two most significant and $\pm$0·05% for the remainder. The measured overall linearity error of the staircase was $\pm$0·035%. The summing amplifier had a thermal drift of 0·0035% per deg C. The overall drift with temperature of the complete circuit in Fig. 5 was 0·01% per degC (percentage of full scale) for temperatures between 20 and 80°C. The upper frequency of the circuit as built was approximately 200 kHz.

Applications

By suitably modulating the repetition rate of the input pulse train, it is possible to generate a number of non-linear waveforms. The waveforms considered here are all generated by feeding a voltage which is a function of the output to a voltage-controlled multivibrator[5]. The multivibrator generates the input pulse train. In the system shown in Fig. 6(a), the output is fed directly to the voltage-controlled multivibrator, giving the output shown in Fig. 6(b). When n is large, the output will be a good approximation to e^x or e^{-x}, depending on which side of the binaries are used to operate the transistor

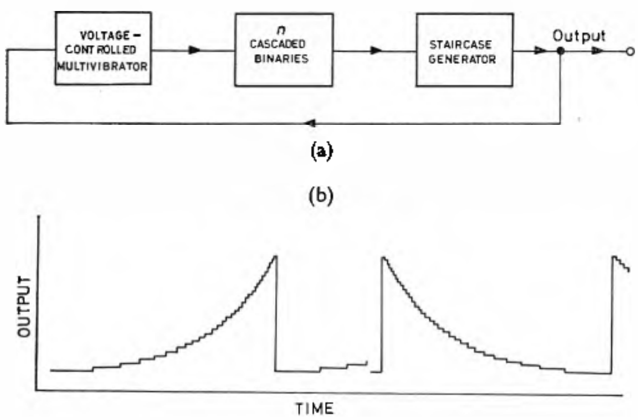

Fig. 6 (a) System for generating a logarithmic waveform (b) Output waveforms for (a), showing outputs for connexion to both sides of binaries

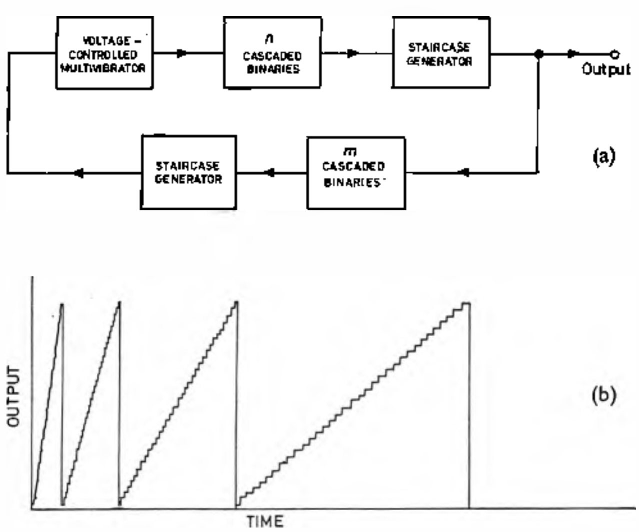

Fig. 7 (a) System for generating m linear staircases of decreasing slope (b) Output of (a) for $m = 4$

switches. The maximum-to-minimum slope ratio is entirely a function of the multivibrator maximum-to-minimum frequency range.

The system shown in Fig. 7(a) requires two staircase generators to generate 2^m linear staircases of increasing or decreasing slope (where m is the number of feedback binaries). The feedback binaries are arranged to switch on the flyback edge of the output staircase. The system shown in Fig. 8 (a) is an extension of the system shown in Fig. 7 (a). A summing amplifier of the type used in the staircase generator is used to sum the output waveform

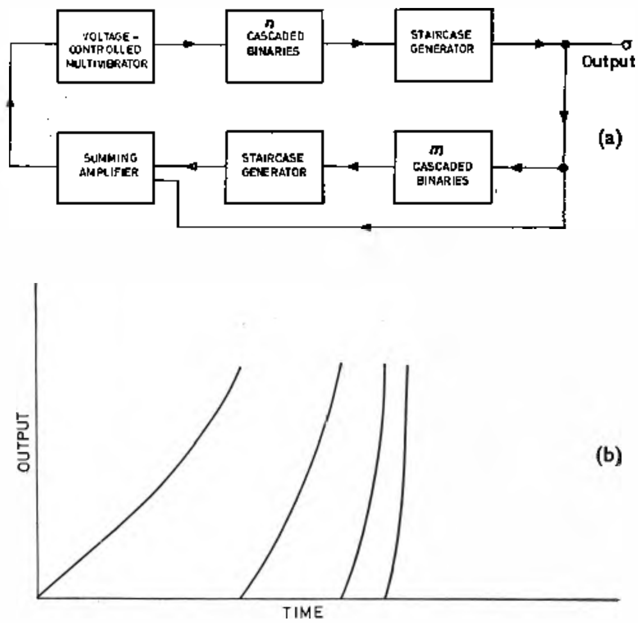

Fig. 8 (a) System for generating m exponentials of increasing slope (b) Output of (a) for $m = 4$

and the output of the feedback generator. The resultant output waveform is a series of 2^m exponentials of increasing or decreasing slope. Exponential waveforms of the type shown are useful when a logarithmic sweep is required. The directly coupled circuits allow very slow sweep rates without bulky components.

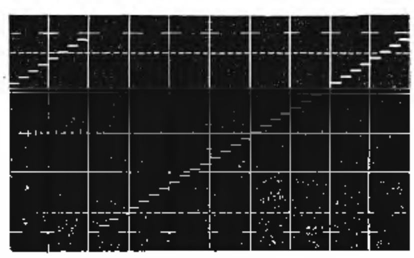

Fig. 9 Output waveform

REFERENCES

1 HAKIM, S. S.: A transistor staircase generator, *Electronic Engng.* 34, 413 (July 1962)

2 ARON, N.: Precise converter takes current analog of digital voltage pulses, *Electronics* (10 Aug. 1962)

3 EBERS, J. J., and MOLL, J. L.: Large-signal behaviour of junction transistors, *Proc. Inst. Radio Engrs.* 42, 1761-1771 (Dec. 1954)

4 CADWALLADER, M.: A precision voltage-controlled time delay circuit, *J. I.E.R.E.* (Feb. 1967)

5 COOPER, J. J.: A wide-band voltage controlled square wave generator with linear characteristics, *Electronic Engng.* 35, 427 (Sept. 1963)

Averaging of heart-rate responses in rats following electrical brain stimulation

by **William J. Mundl,** *Allan Memorial Institute, McGill University, Montreal, Quebec, Canada*

Electrical stimulation of certain parts of an animal's brain has been found to produce characteristic changes in heart rate. A system is described which yields an output curve representing the averaged heart-rate responses of an unrestrained rat to repeated stimulations. Instruments are developed for converting time intervals between successive heart beats to a voltage suitable for processing by computer.

(Voir page 731 pour le résumé en français: Zusammenfassung in deutscher Sprache auf Seite 732)

The electrical stimulation of certain structures in the brain of an animal is an important experimental approach in the field of brain research. Application of electric current to a specific part of the brain may elicit specific reactions in overt behaviour or a characteristic response in the automatic nervous system. This article describes how an averaging computer is employed to measure changes in heart rate (h.r.) of a rat as a direct effect of brain stimulation. In order to investigate h.r. responses, it has been found that beat-by-beat determinations are required[1]; such measurements carried out by hand are extremely laborious.

As a rule, physiological measurements are not easily obtained from small unrestrained animals; their size and agility cause many difficulties when electrodes are attached, or when cables are connected to the electrodes later, if the electrodes have been attached under anaesthesia. Moreover, their movements produce undesired artifacts in the signals under study. However, reliable and artifact-free recordings of h.r. can be obtained if certain precautions, such as subcutaneously implanted wire electrodes, low-noise connecting cables, and amplifiers with limited response to interference signals, are implemented[2].

A fast-responding electrocardiotachograph (e.c.t.g.) is a convenient means of observing a change in h.r. as a result of stimulation; but care is to be observed when evaluating the recording, because such a change could be caused by a random movement of the animal. An averaging computer, if synchronized to the onset of stimulation, and provided that a number of similar stimulations are applied to one animal, will produce a clear graphical display of the response of the subject under test. Fig. 1 shows h.r. changes following stimulation in different parts of the rat brain. Stimulation consisted of a 0·5s train of rectangular pulses of 0·5ms pulse length and 100Hz pulse-repetition frequency, and was supplied by a Grass model-S4 stimulator with stimulus-isolation unit. The electrodes were made of a twisted pair of 0·01in-diameter platinum wires with only the tips making contact with the brain tissue. Stimulation current was measured with an oscilloscope connected across a 1kΩ resistor. Distortion of the rectangular pulses caused by the metal-to-electrolyte (i.e. electrode-to-tissue) interface was prevented by using a pulse-restoration method described previously[3]. The left-hand side of Fig. 1 shows the response to one stimulus, while the curves on the right-hand side show the averaged responses to 15 stimuli. It should not be concluded that these curves are necessarily characteristic of h.r. changes from stimulations of the various areas denoted in the Figure; such a conclusion must await further collection of data.

The e.c.t.g. was designed to have a logarithmic response to time intervals between heart beats; this has the advantage that the rate of the change in h.r. corresponds to a linear change in output amplitude. Thus, basal h.r. of the subject is of no importance and averaged response curves obtained from different animals can be compared directly.

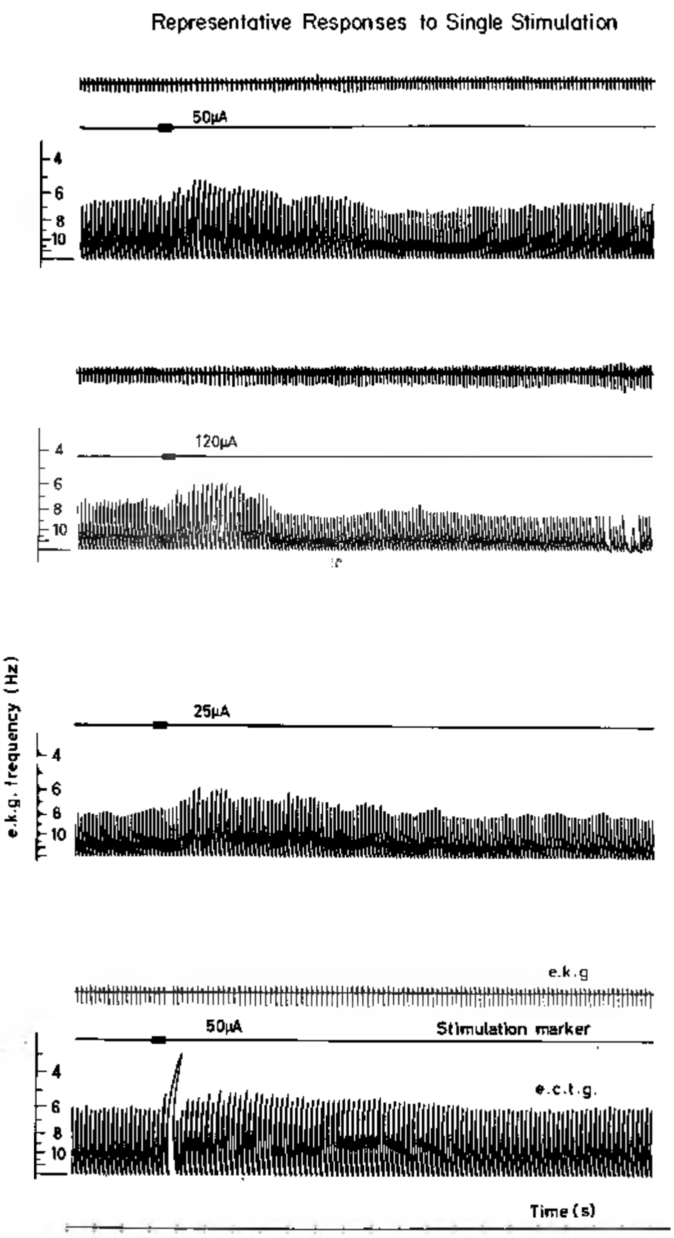

System description

The functional diagram is shown in Fig. 2. The output from an electrocardiograph (e.k.g.) preamplifier is applied to the logarithmically responding e.c.t.g. which furnishes two outputs: one is a sawtooth-like signal representing an exponential charging curve of a capacitor, its peak amplitude being a function of the time interval between successive heart beats; the other is a voltage that envelopes the e.c.t.g. spikes of the first output and follows changes in amplitude immediately (henceforth referred to as 'peak following'). The e.c.t.g. voltage spikes cannot be applied to the averaging computer, because it integrates the incoming signal and would thus obliterate amplitude changes, as the peak of a spike constitutes only a very small

Fig. 1 Changes in heart rate following electrical brain stimulation

Responses of different animals to one stimulation are shown on the left. Response curves obtained from the computer are shown on the right and represent the average of 15 responses. Interstimulation periods were random and ranged from 35 to 55s. The electrode placements, verified by histology, are noted at the right

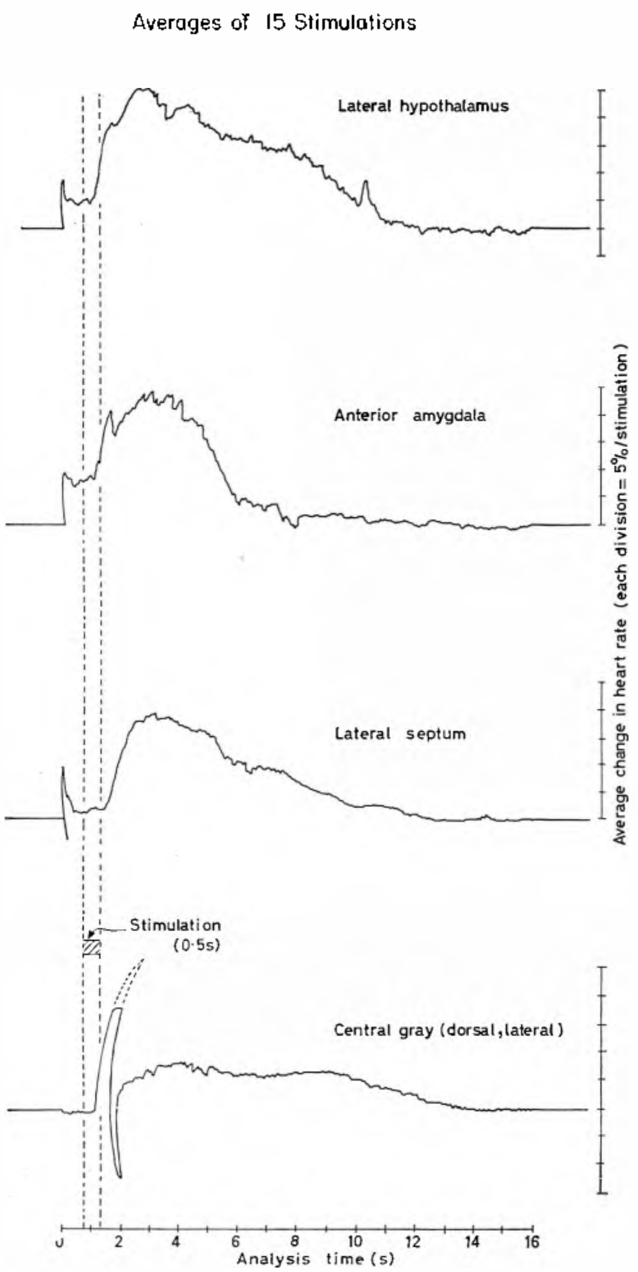

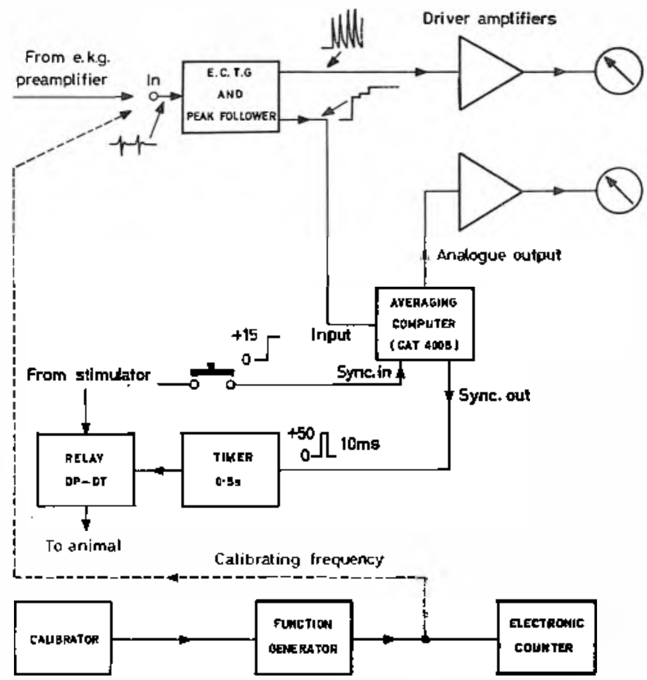

Fig. 2 Functional diagram

The peak follower and the calibrator constitute new developments; the 0·5s timer comprises a Schmitt trigger, a monostable multivibrator and a transistor to drive the relay; all other units are commercially available

fraction of the overall area under the spike. Therefore the signal produced by the peak follower is ideal for processing by the averaging computer. The peak follower is the most significant development in the system being described.

The averaging computer is a CAT model-400B* and operates basically as follows. The incoming signal frequency-modulates an internally generated standard frequency of 100kHz. This modulated frequency is electronically counted over a given time interval and the count is subsequently transferred to a ferrite memory with 400 storage channels, designated 'ordinates'. Over a predetermined analysis time, the signal can thus be stored as 400 sequential counts; a following analysis cycle will add new counts to the stored ones. In this way, with a sufficiently large number of analysis cycles, random fluctuations of the signal tend to even out, while equal signal changes synchronized to the onset of the analysis cycle always add equal counts to certain ordinates. This makes the averaging computer an excellent instrument for separating synchronous variations of the signal from random variations.

The timing sequence of the system is initiated by a pushbutton applying a positive voltage to the external trigger input of the computer (Fig. 2); this starts one analysis cycle. During recording of the data shown in Fig. 1, the analysis time was 16s; i.e., over this time, 400 counts are made and stored in the corresponding 400 ordinates of the memory, each count representing signal amplitude. When the scan reaches the 20th ordinate (which is after 0·8s), a synchronizing pulse triggers the timer, thereby energizing the relay for 0·5s. Stimulation is then applied through the relay contacts to the animal. After a number of stimulations, the summated h.r. responses are written out in analogue form (Fig. 1). The use of a variance computer to work in conjunction with the averaging com-

* Computer of Average Transients, Technical Measurement Corporation, White Plains, New York.

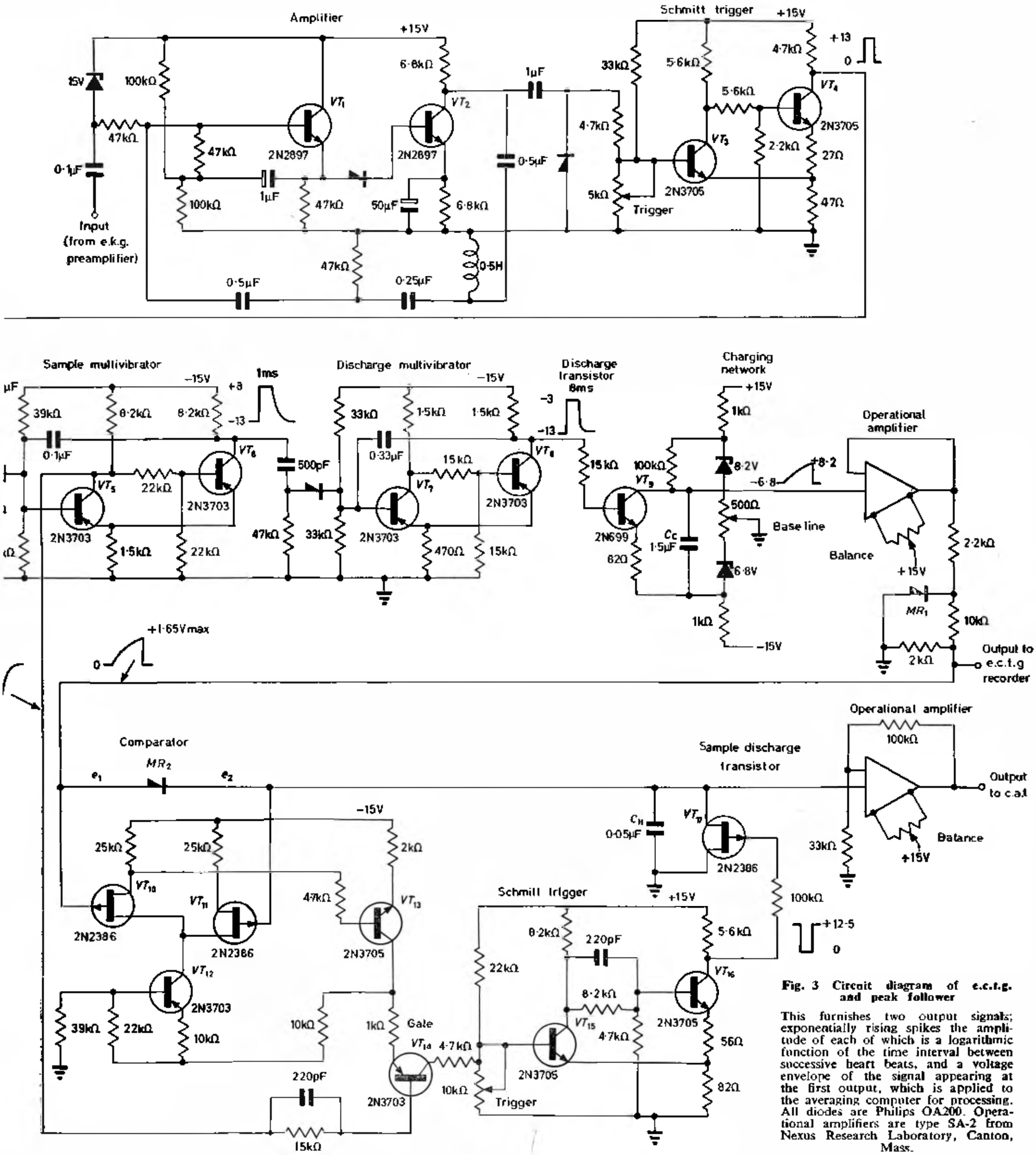

Fig. 3 Circuit diagram of e.c.t.g. and peak follower

This furnishes two output signals; exponentially rising spikes the amplitude of each of which is a logarithmic function of the time interval between successive heart beats, and a voltage envelope of the signal appearing at the first output, which is applied to the averaging computer for processing. All diodes are Philips OA200. Operational amplifiers are type SA-2 from Nexus Research Laboratory, Canton, Mass.

puter is projected for future experiments; at present, the degree of smoothness of the response curves is an indication of variance.

The e.c.t.g. is calibrated with the function generator, whereby an electronic counter serves as monitor. The calibrator was designed for calibrating the averaging computer; it generates a varying analogue voltage, which is used to program the output frequency of the function generator (f.g.) and, in addition, it generates trigger signals to synchronize the f.g. frequency with the analysis cycle of the computer. The circuits of the e.c.t.g., the peak follower and the calibrator are described below; all other instruments employed in the system are standard laboratory equipment.

The e.c.t.g. and peak follower

Time intervals between successive heart beats are represented by a voltage rising exponentially across capacitance C_c in the charging network (Fig. 3). This capacitor is discharged by VT_9 at the occurrence of a heart beat. The time constant of the charging network (C_c in series with a 100kΩ resistor) has been chosen to respond logarithmically to time intervals[4] within a range of e.k.g. frequencies of 3 to 11Hz. This range covers by a sufficiently wide margin all e.k.g. frequencies of rats encountered in this laboratory. The amplifier was designed to reject stimulation signals by frequency-dependent feedback from VT_3 to the base of VT_1. The Schmitt trigger and the discharge multivibrator serve to provide an 8ms trigger pulse to the discharge transistor VT_9. An operational amplifier connected as voltage follower offers a high input impedance to the charging network, preventing unwanted discharge of C_c. With the baseline adjustment, the e.c.t.g. spikes (i.e. voltage build-up across C_c) can be shifted relative to earth, whereby the clipping diode MR_1 eliminates the negative part which represents only the higher frequencies beyond the range of interest. This allows for an effective use of the pen excursion. A more detailed outline of the operation of the e.c.t.g. was made in a previous article[5].

The e.c.t.g. signal is then applied to the peak follower, which consists of the comparator, gate, Schmitt trigger, sample-discharge transistor and operational amplifier (Fig. 3). The signal appears across the holding capacitor C_H, where it is required to remain from spike to spike. The voltage drop across MR_2 is constant and will therefore be neglected in the following discussion. Only a negligible amount of the charge leaks away, since only devices offering high impedances are connected to C_H. Whatever the amplitude of a spike applied to C_H, the voltage across it must be made to assume the new value immediately. If the applied voltage e_1 is higher than the voltage stored e_2, the capacitor will simply be charged to the new value; an error, although small, occurs because of the time constant comprising C_H and the resistances between it and the output of the operational amplifier. This time constant is approximately 0·6ms and is short compared with a minimum pulse length of 100ms (e.k.g. frequency of 10Hz) of e_1. Suppose now that $e_1 < e_2$, i.e. an e.c.t.g. spike of smaller amplitude than the voltage stored across C_H arrives; C_H can only assume the new value when it is forcibly discharged by the sample-discharge transistor VT_{17}. This discharge process operates as follows. Two field-effect transistors at the input of a differential amplifier sense the voltage difference across MR_2, but not the forward voltage drop which is part of the quiescent state of the circuit. If $e_2 > e_1$, current through VT_{11} is decreased, thereby decreasing the voltage drop across VT_{12}. VT_{12} is a constant current source and serves as a large common source resistance for VT_{10} and VT_{11}. The source of VT_{10} becomes more positive, resulting in an increase in drain current and a positive voltage swing at its drain. This positive swing is amplified by VT_{13} and applied as negative voltage swing to gate transistor VT_{14}, through which it will only be transmitted when the sample multivibrator puts out a pulse. The following Schmitt trigger is then activated by cutting off conduction of VT_{15}. The ensuing output pulse at VT_{16} enables VT_{17} to discharge C_H, but only to a point at which e_2 reaches the value of e_1, as at this time the output of the comparator ceases, restoring the Schmitt trigger to its resting state (VT_{15} conducting).

Voltage swings between -8V and -10V occur at the drains of VT_1 and VT_2. These transistors must be matched for nearly equal transconductance. Voltage e_2 is applied to a voltage-follower operational amplifier with a gain of 3. The balance control adjusts the input offset current and should be set to effect a slight discharge of C_H.

Calibrator

The calibrator, although not essential for the operation of the system, is a convenient means of assessing the

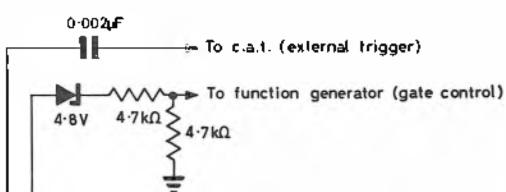

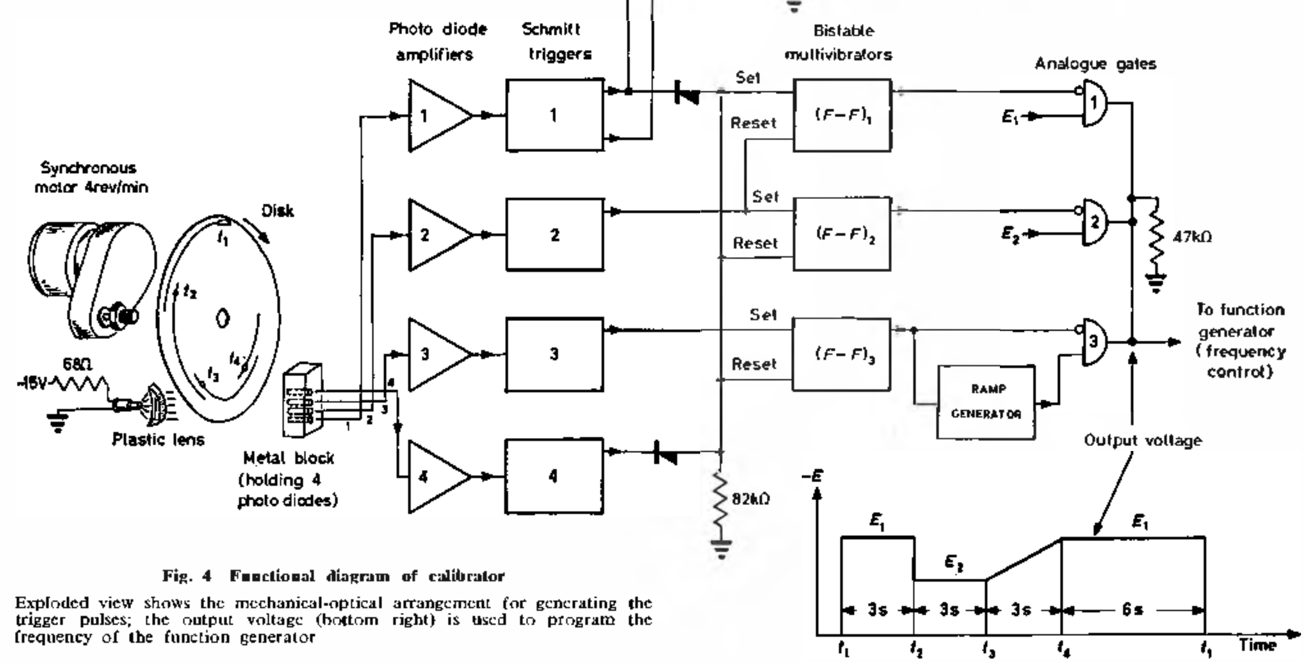

Fig. 4 Functional diagram of calibrator

Exploded view shows the mechanical-optical arrangement for generating the trigger pulses; the output voltage (bottom right) is used to program the frequency of the function generator

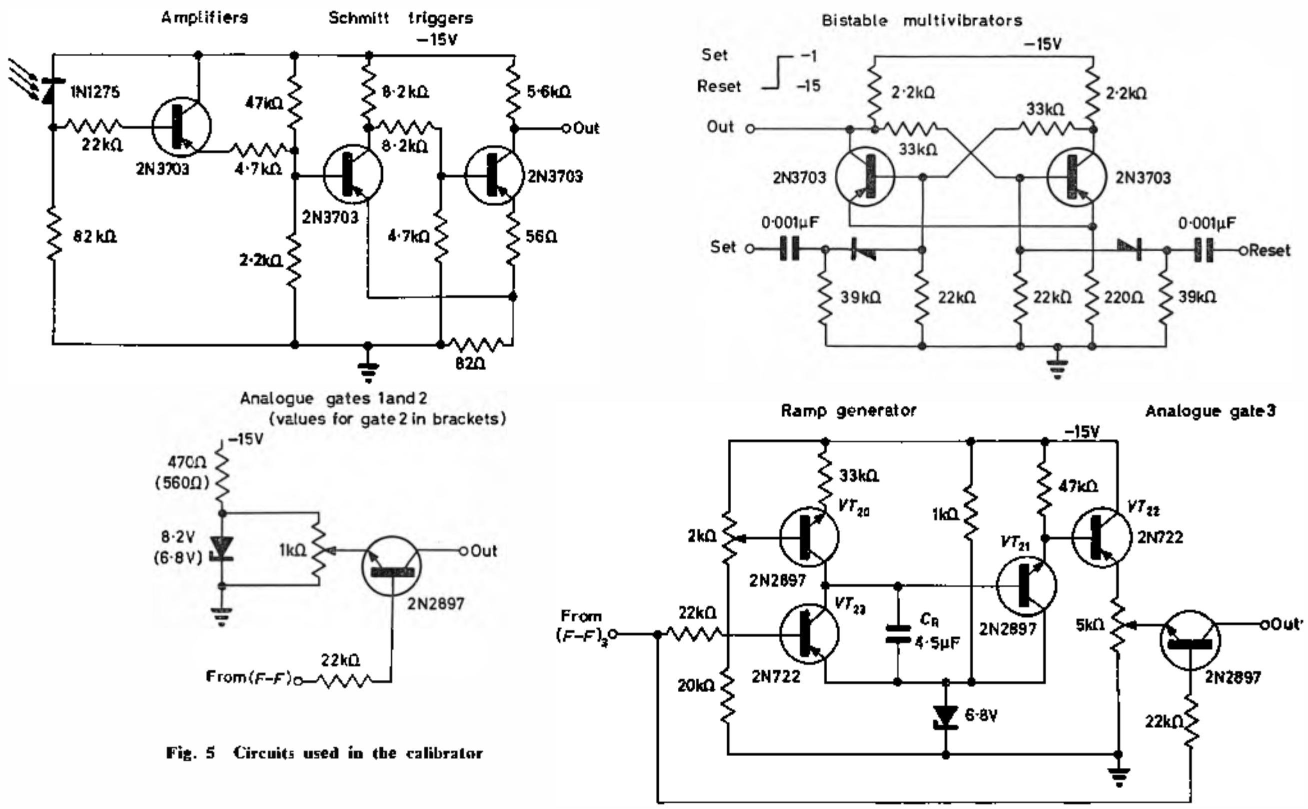

Fig. 5 Circuits used in the calibrator

response of the system and its long-term stability. The output voltage of the calibrator programs the frequency of the function generator in such a way as to stimulate an h.r. response. A metal disk attached to the shaft of a synchronous timing motor furnishes the timing sequence for the changes in output voltage (Fig. 4). Whenever one of the holes in the disk moves past its corresponding photodiode, a transmission path for the light beam is established, which produces a signal to a Schmitt trigger. An exploded view of this mechanical and optical arrangement is shown in Fig. 4 and is self-explanatory. Hole t_1 is elongated to hold Schmitt trigger 1 in the ON state for 0·25s for the following reason. The external gate signal for the f.g. is obtained from the collector of the first stage of Schmitt trigger 1, and is at zero level when in the ON state, thereby switching off the output of the f.g. for 0·25s. However, since the f.g. frequency is phase-locked to the onset of the external gate voltage, the f.g. output ceases only after the cycle during which the external gate signal becomes zero is completed. Thus the 0·25s OFF time is for this completion and allows the f.g. to start a new phase-locked cycle at the end of this 0·25s period.

Fig. 5 shows the circuits employed in the calibrator. The analogue gates consist of transistors in the common-base configuration. Sufficient base current assures a saturated mode of operation in the ON state, resulting in a minimum of collector-emitter resistance. Output levels E_1 and E_2 are set to provide two frequency levels which are representative of an h.r. response (7 and 6Hz, respectively). The ramp generator provides a gradual transition from level E_2 to E_1 over 3s. The output of the ramp generator (Fig. 5) is held at the E_2 level because of VT_{23} conducting and preventing any charging of C_R. At time t_3 $(F\text{-}F)_3$ changes state and supplies -1V to VT_{23}, switching it off. Capacitor C_R charges at a constant rate, because VT_{20} acts as a constant-current source. The charging current is controlled by a 2kΩ potentiometer at the base of VT_{20} and is adjusted so that the voltage across C_R reaches the E_1 level at time t_4. At this time $(F\text{-}F)_3$ is reset and $(F\text{-}F)_1$ set. Resetting $(F\text{-}F)_3$ discharges C_R and closes gate 3. Setting of $(F\text{-}F)_1$ opens gate 1 and results in an output of E_1. VT_{21} and VT_{22} are two complementary emitter followers. The high input impedance of VT_{21} limits leakage from C_R.

The computer is calibrated by repeatedly applying the programmed output frequency. Each frequency change from 7 to 6Hz (14·28%) results in an analogue output of the computer similar to the output of the calibrator (Fig. 4); e.g. applying the calibration 10 times to the computer shows an amplitude change in its analogue output proportional to a 142·8% frequency change or a 14.28% change per single calibration cycle. On the basis of this information, scales to facilitate evaluating the recordings can be constructed.

Acknowledgments

The development of this apparatus was supported in part by grants to R. B. Malmo from the following sources: National and Medical Research Councils and Defence Research Board of Canada, and U.S. National Institute of Mental Health and National Science Foundation. Grateful acknowledgment is made to R. B. Malmo for suggesting this developmental research and to R. Bloomberg for his assistance.

REFERENCES

1 MALMO, R. B.: Heart rate reactions and locus of stimulation within the septal area of the rat, *Science*, *144*, 1029 (1964)
2 MUNDL, W. J.: A cardio preamplifier for the free-roving rat, *Psychophysiology*, *2*, 75 (1965)
3 MUNDL, W. J.: Restoring rectangular pulses of stimulation current, *Electroenceph. clin. Neurophysiol.*, *20*, 527 (1966)
4 TOVE, P. A., and CZEKAJEWSKI, J.: Pulse period meter with short response time, applied to cardiotachometry, *Electronic Engng.*, *36*, 290 (1964)
5 MUNDL, W. J.: A cardiotachograph with logarithmic response for use with rats, *Psychophysiology*, *3*, 220 (1966)

Characteristics of asynchronous pulse-length-modulation systems

First in a series of articles on feedback modulation systems

by **P. D. Sharma,** M.E., Ph.D., *Indian Institute of Technology, New Delhi, India*

Using simple nonlinear circuits, two new approximations based on ±1 or ±1/0-slope linear segments are developed. A simple differentiation of these linear-segment approximations gives rise to ±1 or ±1/0 pulses whose widths and repetition periods are modulated in accordance with the slope of the signal waveform being approximated, thus giving rise to asynchronous pulse-length-modulation (a.p.l.m.) and asynchronous bipolar pulse-length-modulation (a.b.p.l.m.) systems. The laws of modulation, dynamic ranges, bandwidth requirements and quantizing noise characteristics of these systems are calculated.

(Voir page 731 pour le résumé en français: Zusammenfassung in deutscher Sprache auf Seite 732)

Signals with only discrete amplitude levels have several advantages over continuous ones with respect to signal processing and message transmissions. In particular, while handling the 2-level signals, the linearity of the circuits is not important and power amplification can be carried out with high efficiency. The conversion of continuous signals into discrete ones (without using synchronous sampling) may be accomplished in general by passing them through a nonlinear device (comparator) such as a Schmitt-trigger or a squaring circuit, and the original continuous signal may be recovered by linear filtering. This method, though extremely simple to instrument, leads to severe harmonic distortion in the recovered signal, and hence is not of great value for practical

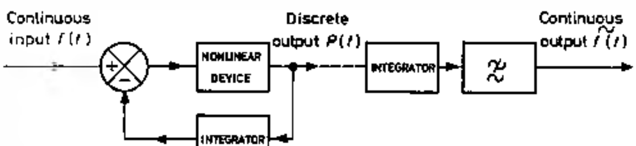

Fig. 1 Block schematic of continuous-to-discrete conversion system

purposes. The distortion produced in the nonlinear coder can be reduced considerably by using a negative-feedback loop containing a low-pass device such as an integrator, as shown in Fig. 1. The effect of this feedback loop is to introduce certain types of modulation on the discrete output of the nonlinear device; the modulation systems so derived are referred to here as asynchronous pulse-modulation systems. These systems may be divided into the following four classes:

(i) *Asynchronous p.l.m.*, where the system output consists of ±1 pulses, the instantaneous widths and time periods of the pulses being determined by the message slopes.

(ii) *Asynchronous bipolar p.l.m.*, where the system output consists of ±1/0 pulses whose widths and repetition periods are functions of the input message slopes.

(iii) *Asynchronous* $\Delta - M$, $(A - \Delta M)^1$, where the comparator output consists of ±1 pulses of constant narrow width, the interval between the consecutive pulses being determined by the message-input slope.

(iv) *Asynchronous binary s.q.p.c.m.*, where the output consists of constant-width 1/0 pulses, the instantaneous interval between the successive pulses being determined by the message slopes.

Other systems may also be obtained using more sophisticated networks in the feedback loop, and the general performance of these systems may be predicted from the results of the above four simple systems, the first two of which are being studied in detail in this article. The main criteria for the efficiency of any modulation system are its quantizing noise, bandwidth requirements and the dynamic range, and these characteristics of a.p.l.m. and a.b.p.l.m. systems are described in this article. These asynchronous systems are useful in such applications as storage of analogue signals, single-channel message transmission and nonlinear control systems.

Dynamic range and bandwidth requirements

Important characteristics of a.p.l.m. and a.b.p.l.m., such as the laws of modulation, the average number of output pulses required for a proper approximation of the given input signal, the channel bandwidth required and the dynamic range, will be studied in detail in this section. Quantizing noise, which is also an important characteristic of these systems, will be considered in the next section.

Asynchronous p.l.m.

In this system, the message input $f(t)$ is approximated to by a series of linear segments having alternately positive and negative slopes of equal magnitude, and a simple differentiation of the linear segments produces positive or negative pulses of equal height but of varying widths and frequency. Thus the given message slope may be approximated to by positive or negative pulses and only the zero crossings of these pulses need be transmitted accurately by the channel. The mathematical model of this system may be expressed as

$$\tilde{f}(t) = \sum_{n} (-1)^n \rho_0 R(t - t_n) \quad \ldots\ldots\ldots\ldots \text{(1a)}$$

$$\tilde{f}'(t) = \sum_{n} (-1)^n \rho_0 u(t - t_n) \quad \ldots\ldots\ldots\ldots \text{(1b)}$$

where $R(t - t_n)$ is a unit ramp occurring at $t = t_n$ and ρ_0 is the magnitude of the slope of the approximating linear segments. A typical example of a linear-segment approximation based on the above mathematical model is shown in Figs. 2(a), (b) and (c). The error $\epsilon(t)$ defined as $[f(t) - \widetilde{f(t)}]$ has a triangular waveform of fixed height but varying basewidths, and the slope approximation $\widetilde{f(t)} = P(t)$, as given by equation (1b), shows large variations in pulsewidths and a comparatively lesser variation in instantaneous time periods.

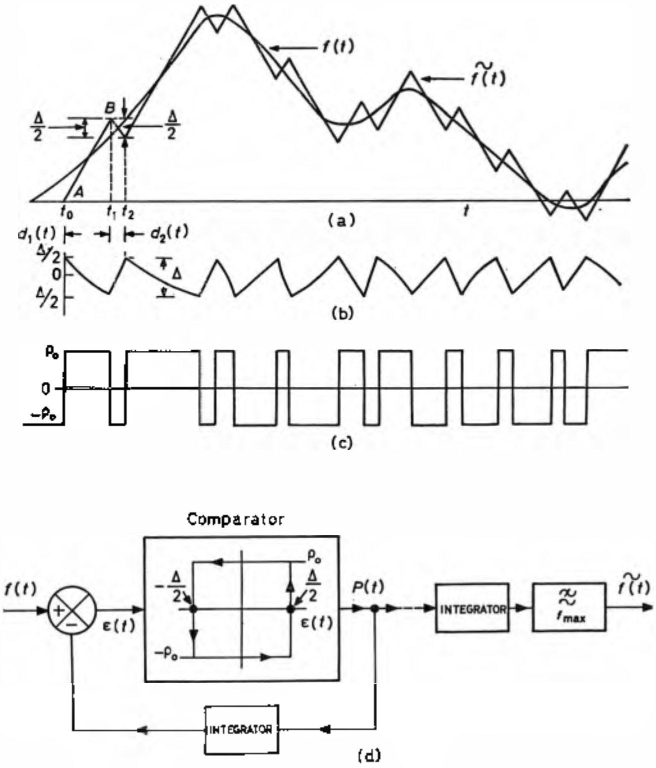

Fig. 2 Typical waveform approximation in a.p.l.m.
(a) Linear-segment approximation
(b) Error waveform
(c) Slope approximation $\widetilde{f'(t)} = P(t)$
(d) Block schematic of coder and decoder

Theoretical calculation of the instantaneous pulsewidths $d_1(t)$ of the positive pulse, and $d_2(t)$ of the following negative pulse, and the instantaneous time period $T(t)$ may be carried out by assuming $f(t)$ to be linear over one complete cycle of $P(t)$ in Fig. 2(a). Thus, from the figure, the slope of the line AB is given by

$$d_1(t) = \frac{f(t_1) + \Delta/2 - f(t_0) + \Delta/2}{d_1(t)} \quad \ldots\ldots\ldots (2)$$

On simplification, equation (2) gives

$$d_1(t) = \frac{\Delta}{\rho_0 - f'(t)} \quad \ldots\ldots\ldots\ldots\ldots\ldots (3)$$

where $f'(t)$ is the instantaneous slope of $f(t)$. Similarly $d_2(t)$, the instantaneous width of the negative pulse, is given by

$$d_2(t) = \frac{\Delta}{\rho_0 + f'(t)} \quad \ldots\ldots\ldots\ldots\ldots\ldots (4)$$

and the instantaneous period is

$$T(t) = d_1(t) + d_2(t)$$
$$= \frac{2\Delta\rho_0}{\rho_0^2 - (f')^2(t)} \quad \ldots\ldots\ldots\ldots\ldots\ldots (5)$$

Maximum and minimum values of $d_1(t)$ and $d_2(t)$ are given by

$$d(t)_{\max} = d_1(t)_{\max} = d_2(t)_{\max} = \frac{\Delta}{\rho_0 - |f'(t)_{\max}|} \quad \ldots . (6a)$$

$$d(t)_{\min} = d_1(t)_{\min} = d_2(t)_{\min} = \frac{\Delta}{\rho_0 + |f'(t)_{\max}|} \quad \ldots . (6b)$$

Since the system is assumed nonoscillating, there will be no pulse output when the input is absent. A typical coder of this system, shown in Fig. 2(d), consists of a difference circuit followed by a symmetrical comparator with hysteresis, whose output is integrated and compared with the input, thus giving an equal slope approximation of the waveform $f(t)$. At the decoder, also shown in Fig. 2(d), rectangular output of the comparator is integrated and filtered to obtain the approximated message $\widetilde{f(t)}$. It is seen from Fig. 2 that, for a good approximation to the message waveform $f(t)$, the slope ρ_0 of the linear segments should be greater than or equal to the maximum slope of $f(t)$. For a sinusoidal signal $f(t) = A \sin \omega_m t$, therefore, $|\rho_0| \geqslant A\omega_{\max}$.

The number of pulses required to approximate the above sinusoidal signal is given by

$$n_s = 2 \frac{2A}{\left[\dfrac{\Delta}{\rho_0 - f'(t)} - \dfrac{\Delta}{\rho_0 + f'(t)}\right]\rho_0} f_m \text{ per second}$$

$$= (2A/\rho_0\Delta)\left[\frac{\rho_0^2 - (f')^2(t)}{f'(t)}\right] f_m \text{ per second} \quad \ldots\ldots\ldots (7)$$

and the corresponding number of zero crossings of the error waveform of Fig. 2b is

$$\mu_s = 2n_s = (4A/\rho_0\Delta)\frac{\rho_0^2 - f'^2(t)}{f'(t)} \quad f_m \text{ per second} \ldots (8)$$

The average number of pulses required to approximate a Gaussian input of average slope $\overline{|f'(t)|}$, is given by

$$n_g = \overline{|f'(t)|} \cdot \frac{\rho_0^2 - \overline{|f'(t)|}^2}{2\rho_0\Delta\,\overline{|f'(t)|}} = \frac{\rho_0^2 - \overline{|f'(t)|}^2}{2\rho_0\Delta}$$

and the corresponding number of zero crossings of the error waveform is

$$\mu_g = 2n_g = \frac{\rho_0^2 - \overline{|f'(t)|}^2}{\rho_0\Delta} \quad \ldots\ldots\ldots\ldots (9)$$

If it is required to use this system for purposes of transmission, $P(t)$ will be the transmitted signal, and the minimum bandwidth $B_{\min}$ required for satisfactory recovery of the message at the decoder is

$$B_{\min} = \frac{1}{2d(t)_{\min}} = \frac{\rho_0 + |f'(t)_{\max}|}{2\Delta} \quad \ldots\ldots (10)$$

If $d(t)_{\min}$ is fixed by bandwidth considerations, as shown above, the system will be unable to follow input signals with slopes in excess of $|f'(t)_{\max}|$ given by equation (10), and this value of $f'(t)$ represents the overload slope input for the system. Equation (10) shows that the overload input amplitude A for a sinusoidal input frequency $\omega_{\max}$ is given by $A = (2\Delta B_{\min} - \rho_0)/\omega_{\max}$ and is thus inversely proportional to the signal frequency. It is also seen from Fig. 2(a) that the system will fail to operate for input levels lower than $\Delta/2$, and with this as the lower limit of allowable input levels, the system dynamic range for $\omega_{\max}$ is $2(2\Delta B_{\min} - \rho_0)/\Delta\omega_{\max}$. The linearity characteristics of the system may thus be drawn if $B_{\min}$, $\omega_{\max}$ and ρ_0 are known.

As an example, let it be required to calculate the number of zero crossings of the error waveform and the dynamic range of an asynchronous p.l.m. system required to handle a 1V p-p sinusoidal signal of any frequency in the range 0-3·2kHz, when the channel bandwidth allowed is 100kHz. Noting that $|f'(t)_{max}| = \rho_0 = 10^4$, as discussed earlier, and using equation (10), it is seen that

$$\frac{1}{2 \times 100 \times 10^3} = \frac{\Delta}{10^4 + 10^4}$$

and hence $\Delta = 0{\cdot}1$ and the dynamic range for $f_m = 3{\cdot}2$kHz is 20dB. Considering a sinusoidal input signal with $f_m = 800$Hz, the value of μ_s obtained from equation (8) is

$$= \frac{4 \times 0{\cdot}5}{10^4 \times 0{\cdot}1 \times 0{\cdot}5 \times 4 \times 800} \; (10^8 - 1600^2) \times 800$$

$$\simeq 10^5 \qquad\qquad (4A\, f_m = 1600)$$

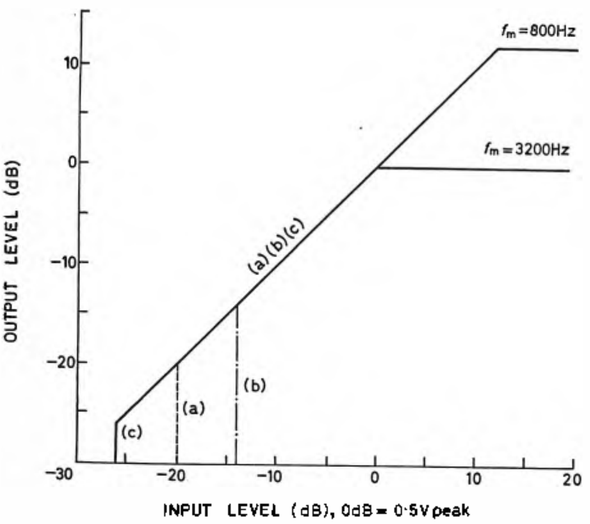

Fig. 3 Input-output relation of different asynchronous systems for sinusoidal inputs (f_m = 3200 and 800Hz and channel bandwidth = 100kHz)
(a) $\Delta - \Delta M$ and a.p.l.m.; (b) a.b.s.q.p.c.m.; (c) a.b.p.l.m.

where $f'(t)$ has been taken as the average slope of the sinusoidal signal in question. The present system can handle $\sqrt{3}$V p-p of a Gaussian signal of bandwidth 0-3200Hz and corresponding number of zero crossings obtained from equation (9) is

$$\mu_z = \frac{10^8 - (1120 \times \sqrt{3})^2}{10^4 \times 0{\cdot}1}$$

$$\simeq 10^5$$

It is seen from the above calculations and the discussions regarding the system overload that, for the given bandwidth, the overload input for $f_m = 3200$Hz is 0·5V peak, and for other values of f_m it is simply $(0{\cdot}5 \times 3200)/f_m$. Also the lower limit of the dynamic range is 0·05V peak, and the complete linearity characteristics for two values of f_m are shown in Fig. 3, curve *a*.

Asynchronous bipolar p.l.m.

In this system, the message input $f(t)$ is approximated by a series of linear segments having alternately positive and zero slopes when $f(t) > 0$ and alternately negative and zero slopes when $f'(t) < 0$. A simple differentiation of this linear-segment approximation produces a bipolar pulse output where the heights of the pulses are constant but their widths and repetition periods vary in accordance with the slope of the message signal. The mathematical model of this system may be expressed as

$$\tilde{f}(t) = \sum_n \gamma \rho_0 R(t - t_n) \quad \ldots\ldots\ldots\ldots\ldots \quad (11a)$$

$$\tilde{f}'(t) = \sum_n \gamma \rho_0 u(t - t_n) \quad \ldots\ldots\ldots\ldots\ldots \quad (11b)$$

$$\text{where } \gamma = \begin{cases} +1, \text{ if } f'(t) > 0 \text{ and } [f(t) - \tilde{f}(t)] \geqslant \Delta/2 \\ -1, \text{ if } f'(t) < 0 \text{ and } [f(t) - \tilde{f}(t)] \leqslant \Delta/2 \\ 0, \text{ in all other cases} \end{cases}$$

A typical approximation based on the above mathematical model is shown in Figs. 4(a), (b) and (c). The error $\epsilon(t)$ defined as $[f(t) - \tilde{f}(t)]$ has a triangular waveform of fixed height but varying basewidths and the slope approximation $\tilde{f}'(t) = P(t)$ as given by equation (11b), shows large variations in the widths of the pulses and relatively lesser variations in the instantaneous time periods.

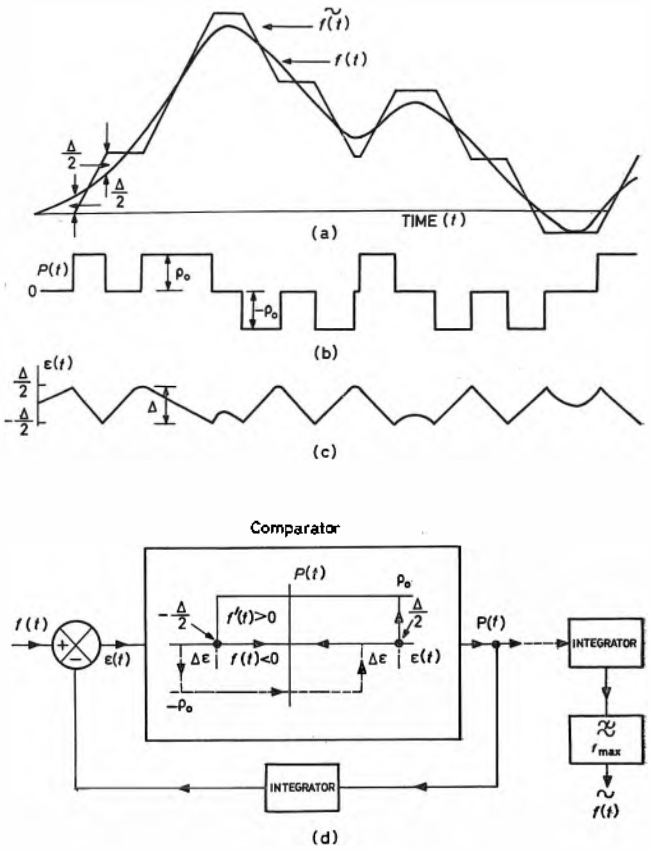

Fig. 4 Typical waveform approximation in a.b.p.l.m.
(a) Linear-segment (±1/10 slopes) approximation
(b) Slope approximation $\tilde{f}'(t) = P(t)$
(c) Error waveform
(d) Block schematic of coder and decoder

The length $d_1(t)$ of the positive- or negative-slope segments and $d_2(t)$ of the zero-slope segments may be determined by the same technique as that used in the case of a.p.l.m., and the result is

$$\left.\begin{aligned} d_1(t) &= \frac{\Delta}{\rho_0 - |f'(t)|} \\ d_2(t) &= \frac{\Delta}{|f'(t)|} \end{aligned}\right\} \quad \ldots\ldots\ldots\ldots \quad (12)$$

and

$$T(t) = d_1(t) + d_2(t) = \frac{\Delta\rho_0}{|f'(t)|\,[\rho_0 - |f'(t)|]} \quad \ldots\ldots \text{(12a)}$$

where ρ_0 is the magnitude of the slope of the approximating positive or linear segments. Since $|f'(t)|$ is very nearly equal to ρ_0 for a full-load input signal, $d_2(t)$ will always be less than $d_1(t)$, and minimum pulsewidth in the approximation is given by

$$d(t)_{min} = d_2(t)_{min} = \frac{\Delta}{|f'(t)_{max}|} \quad \ldots\ldots\ldots\ldots \text{(13)}$$

Equation (12) shows that $d_2(t)$ is inversely proportional to $|f'(t)|$, while $d_1(t)$ tends to increase if $|f'(t)|$ is increased, and *vice versa.* This behaviour is also seen in Fig. 4. The block diagram of a typical a.b.p.l.m. coder and the complementary decoder is shown in Fig. 4(d). The coder consists of a difference circuit followed by a 3-level comparator, whose output is integrated by an ideal integrator and compared with the input, thus giving the desired approximation for $f(t)$. At the decoder, the bipolar output of the comparator is integrated and filtered to obtain $f(t)$. It is seen from Fig. 4 that, for a good approximation of the message waveform $f(t)$, the slope $\pm\rho_0$ of the linear segments should be greater than or equal to the maximum slope of $f(t)$. For a sinusoidal signal $f(t) = A \sin \omega_m t$, therefore, ρ_0 should be greater than or equal to $A\omega_{max}$.

The number of pulses required to approximate the above sinusoidal waveform is

$$n_s = 2\,\frac{2A}{\left(\dfrac{\rho_0\Delta}{\rho_0 - |f'(t)|}\right)}\,f_m \text{ per second}$$

The number of zero crossings of the error waveform is

$$\mu_s = \frac{8A\,[\rho_0 - |f'(t)|]}{\rho_0\Delta} f_m \text{ per second} \quad \ldots\ldots \text{(14)}$$

For bandlimited Gaussian input of average slope $\overline{|f'(t)|}$ the number of pulses required for approximation is

$$n_g = \frac{\overline{|f'(t)|}\,[\rho_0 - \overline{|f'(t)|}]}{\rho_0\Delta} \text{ per second}$$

and the number of zero crossings of the error waveform is given by

$$\mu_g = \frac{2\,\overline{|f'(t)|}\,[\rho_0 - \overline{|f'(t)|}]}{\rho_0\Delta} \text{ per second} \quad \ldots\ldots \text{(15)}$$

If it is desired to use this system for purposes of transmission, $P(t)$ will be the transmitted signal and the minimum channel bandwidth required will be

$$B_{min} = \frac{1}{2d(t)_{min}} = \frac{|f'(t)_{max}|}{2\Delta} \quad \ldots\ldots\ldots\ldots \text{(16)}$$

where the value of $d(t)_{min}$ has been taken from equation (13). If d_{min} is fixed by the bandwidth considerations indicated in equation (16), the system will be unable to follow the input signals with slopes in excess of $|f'(t)_{max}|$ given by equation (16) and this value of $f'(t)$ represents the overload slope input for the system. As seen from the above equation, the overload input amplitude A for a sinusoidal input of frequency ω_{max} is given by $A = (2\Delta B_{min})/\omega_{max}$ and is thus inversely proportional to the signal frequency. It is also seen from Fig. 4(a) that the system will fail to operate for input levels lower than $\Delta/2$, and with this as the lower limit of allowable input levels, the system dynamic range for ω_{max} is $4B_{min}/\omega_{max}$. The linearity characteristics of the system may thus be drawn if B_{min} and ω_{max} are given.

As an example, let it be required to calculate the number of zero crossings of the error waveform and the dynamic range of the a.b.p.l.m. system required to handle a 0·5V peak sinusoidal signal of any frequency in the band 0-3·2kHz when the channel bandwidth allowed is 100kHz. Noting that $|f'(t)_{max}| = \rho_0 = 10^4$, as discussed earlier, and using equation (16), it is seen that $1/(2\times 100\times 10^3) = \Delta/10^4$, and hence $\Delta = 0{\cdot}05$, giving a dynamic range of 26dB for $f_m = 3{\cdot}2$kHz. Considering a sinusoidal signal with $f_m = 800$Hz, the value of μ_s obtained from equation (14) is

$$\mu_s = \frac{8 \times 0{\cdot}5\,(10^4 - 1600)}{10^4 \times 0{\cdot}05} \times 800$$
$$\simeq 64\,000$$

where $f'(t)$ has been taken as the average slope of the sinusoidal signal in question [i.e. $\overline{|f'(t)|} = 1600$]. The present system can handle $\sqrt{3}$V p-p of a Gaussian signal of bandwidth 0-3200Hz, and the corresponding number of zero crossings obtained from equation (15) is

$$\frac{2 \times 1120 \times \sqrt{3}\,(10^4 - 1120 \times \sqrt{3})}{10^4 \times 0{\cdot}05} \simeq 64\,000$$

It is seen from the above calculations and discussions regarding the system overload that, for the given bandwidth, the overload input for $f_m = 3{\cdot}2$kHz is 0·5V peak, and for other values of f_m it is simply $(0{\cdot}5\times 3200)/f_m$. Also the lower edge of the dynamic range is 0·025V, as discussed earlier and the complete linearity characteristics for two values of f_m are shown in Fig. 3, curve *c.*

Quantizing-noise characteristics

The spectrum of the triangular error waveforms[3] of a.p.l.m. and a.b.p.l.m. is given by

$$N_e(f) = \frac{0{\cdot}05\,\Delta^2\,\mu}{f^2 + \mu^2} \quad \ldots\ldots\ldots\ldots \text{(17)}$$

where μ is the number of zero crossings per second of the error waveform. If the bandwidth of the message signal is f_{max}, the noise power falling in the message band is given by

$$N = \frac{0{\cdot}05\,\Delta^2}{\mu} f_{max} \quad \ldots\ldots\ldots\ldots \text{(18)}$$

The signal power can be calculated from the given peak value of the input and the signal/noise ratio may then be obtained by using equation (18). Assuming an input power S, the signal/quantizing-noise ratio at the decoder output is given by

$$\frac{S}{(K\Delta^2/\mu)\,f_{max}} \quad \ldots\ldots\ldots\ldots \text{(19)}$$

For a given channel bandwidth B_{min} and message bandwidth f_{max}, Δ is determined by the highest signal amplitude to be handled, and is thus independent of other input levels. As seen from equations (9) and (15), μ is proportional to the input level $\sqrt{S}$ (say, σ) in the case of a.b.p.l.m. (since $\overline{|f'(t)|}$ is usually small compared with ρ_0 and is proportional to σ) but independent of it in the case of a.p.l.m. (for the same reasons as for a.b.p.l.m.). Incorporating this behaviour of μ in equation (19), it is found that the signal/quantizing-noise ratio changes by 9dB for each 6dB change in σ for a.b.p.l.m., while for a.p.l.m. the corresponding change in the ratio is only 6dB.

As an example, let it be required to calculate the signal/quantizing-noise ratios a.p.l.m. and a.b.p.l.m. systems when the channel bandwidth allowed is 100kHz and the systems are required to handle a $\sqrt{3}$V p-p Gaussian signal of bandwidth 0-3·2kHz. The signal power for both systems is

$$S = [(\sqrt{3})/8]^2 = 3/64W$$

The values Δ and μ for the two systems have been calculated in the previous section, and the noise power N falling in the message band may be calculated from equation (18). Thus, for the a.p.l.m. system,

$$N = \frac{0{\cdot}05 \times (0{\cdot}1)^2}{10^5} \times 3200$$

and the signal/quantizing-noise ratio is 34·77dB. The ratio for a.b.p.l.m. may be calculated in a similar manner, and the result is found to be 38·77dB. These values increase (or decrease) by 9dB for each octave increase (or decrease) in the channel bandwidth B, since Δ is inversely, and μ directly, proportional to B.

Discussions

Possibilities and various characteristics of a.p.l.m. and a.b.p.l.m. have been discussed in this article. The more important properties, i.e. the dynamic range and the signal/quantizing-noise ratio, have been discussed in detail. Based on the equations (10) and (16), the dynamic ranges of the two systems for the mean audio frequency of 800Hz are shown in Fig. 5. For comparison, similar characteristics of asynchronous and asynchronous binary s.q.p.c.m. are also shown in the same figure. Using equation (8), the theoretical signal/quantizing-noise ratios of the asynchronous systems for different channel bandwidths are also shown in Fig. 5. The variation of this ratio with input level as obtained from equation (19) and subsequent discussions are shown in Fig. 6 for a channel bandwidth of 100kHz and a message bandwidth of 3·2kHz. Since the signal/quantizing-noise ratio is inversely proportional to

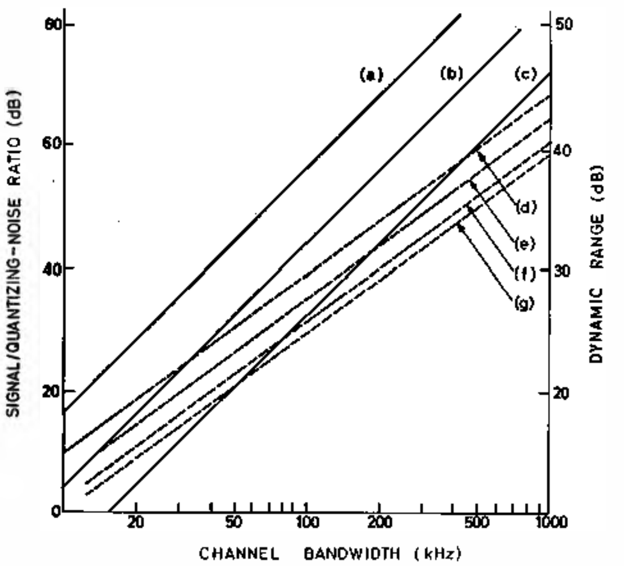

Fig. 5 Dynamic range (f_m = 800Hz) *vs.* bandwidth and signal/quantizing-noise ratio (for Gaussian inputs) *vs.* bandwidth characteristics of asynchronous systems

(a) Dynamic-range characteristics of a.b.p.l.m.
(b) Dynamic-range characteristic of a.p.l.m. and $A-\Delta M$
(c) Dynamic-range characteristic of a.b.s.q.p.c.m.
(d) Quantizing-noise characteristic of a.b.p.l.m.
(e) Quantizing-noise characteristic of a.p.l.m.
(f) Quantizing-noise characteristic of $A-\Delta M$
(g) Quantizing-noise characteristic of a.b.s.q.p.c.m.

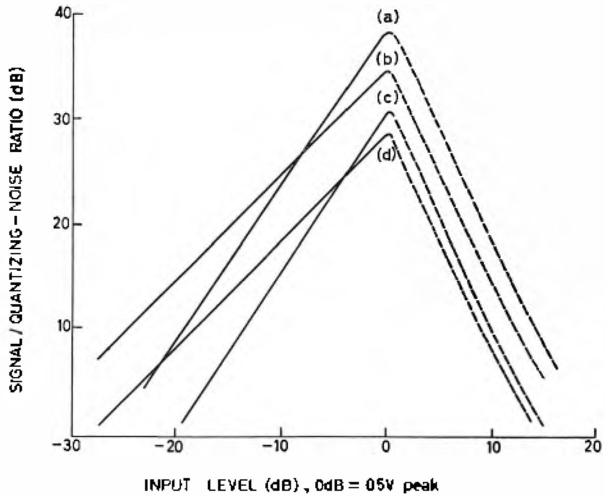

Fig. 6 Signal/quantizing-noise ratio *vs.* input characteristics of asynchronous systems for a channel bandwidth of 100kHz and bandlimited (0-3·2kHz) Gaussian inputs

(a) a.b.p.l.m.; (b) a.p.l.m.; (c) $A-\Delta M$; (d) a.b.s.q.p.c.m.

Δ^2/μ, it improves by 9db for each octave increase in the channel bandwidth. It is seen from the curves that for a ratio of 40dB, a.b.p.l.m. requires a minimum bandwidth of 100kHz and others require bandwidths between 150-250kHz. The dynamic ranges for the mean message frequency of 800kHz and B = 100kHz are 32, 38, 32, and 26dB for $A-\Delta M$, a.b.p.l.m., a.p.l.m. and a.b.s.q.p.c.m., respectively.

Thus it is evident that in comparison with the synchronous pulse-modulation systems, i.e. p.l.m. and p.p.m.[3], the asynchronous systems are somewhat inefficient. However, the asynchronous systems produce fewer pulses when the modulating signal has a falling spectrum and the average number of pulses is less than that of a corresponding synchronous system. This will conserve the r.f. video-signal power and the average channel bandwidth required will be less, especially in cases of speech and television signals with large pauses and some d.c. components. The poor signal/quantizing-noise ratio characteristics of the asynchronous systems may be improved considerably by introducing a secondary loop where only the message part of the coder output is fed back. The effect of this additional feedback loop is to reshape the quantizing-noise spectrum in such a way that its value in the message band is considerably reduced, and a peak characteristic is produced outside the message band. However, when large feedback is given, it is found that the system tends to oscillate, but the improved signal/noise-ratio properties are still maintained[4].

Acknowledgments

The author owes a special debt of gratitude to Prof. J. Das of I.I.T., Kharagpur, for constant guidance and encouragement at all stages of the work. He is also thankful to Prof. C. S. Jha and Prof. P. V. Indiresan of I.I.T., Delhi, for valuable discussions.

REFERENCES

1 INOSE, H., *et al.*: Asynchronous delta modulation system, *Electronics Letters*, 2, 95 (March 1966)
2 BENNET, W. R.: Spectra of quantized signals, *Bell Syst. Tech. J.*, 27, 446 (1948)
3 DAS, J.: Some effects of bandwidth limitation on p.s.m., p.l.m. and p.p.m. signals, *Proc. IEE*, monograph 532E (July 1962)
4 DAS, J., and SHARMA, P. D.: Rectangular wave modulation—A hybrid p.l.m.-f.m. system, *Electronics Letters*, 2, 7 (Jan. 1966)

Open-limit calculus

by **C. G. Mayo,** M.A., B.Sc., F.I.E.E., and **J. W. Head,** M.A., F.Inst.P., M.I.E.E., C.Eng., F.I.M.A.

If two or more processes or quantities derived by closing limits occur simultaneously in a calculation, it is sometimes critically important which limit is closed first. If the limits are closed in the correct order no difficulty will occur, and with the Fourier integral no special techniques will be required. Due attention is paid here to the possibility that a problem may be so formulated that a critically important limit has been inadvertently closed prematurely.

(Voir page 731 pour le résumé en français: Zusammenfassung in deutscher Sprache auf Seite 732)

A student usually first meets the idea of a limit in connection with the process of differentiation. The idea of average speed has been familiar at a much earlier age, but now the concept of instantaneous speed is introduced. This concept is very difficult to get across to an individual, and still more to a class, when they meet it for the first time. The students concerned are quite right to put up a kind of unconscious resistance to the idea; for the concept of a closed limit (in many apparently different forms, such as absolute zero, infinity, pure differentiation, integration, resistance, inductance, capacitance etc.) is responsible for many unnecessary difficulties in the study of natural phenomena. These difficulties are not inherent in the phenomena, but in the manner of thought associated with these concepts.

It must be made clear from the beginning that there are two complementary and fundamentally different ways of specifying what it is wished to discuss—a 'metrical' way, analogous to the average speed mentioned above, and a 'nominal' way, corresponding to the idea of instantaneous speed. 'Metrical' and 'nominal' specifications are therefore fully compared and contrasted in the following section.

Metrical and nominal specification

Examples of nominal specification in ordinary life are: a loaf of bread, a dozen eggs, £1, a 1in board or a 1in-diameter shaft. These nominal specifications can be used only when no critical comparison of items is envisaged; they vary widely in their accuracy and their validation. A loaf of bread is validated by legal penalties for short-weight; a £1 note has no definite buying power but is legal tender; a steel rod having a nominal diameter of 1in might have an actual diameter specified (metrically) as being between 0·999 and 1·001in. Such nominal specifications would be useless on an assembly line. Metrical specification is then required, and equations must be replaced by inequalities. Thus if a 1in shaft has to be fitted into a 1in collar, a 'metrical' specification is needed that the diameter d inches of the shaft satisfies

$$1-\eta-\varepsilon < d < 1-\eta; \quad \varepsilon, \eta > 0 \quad \text{(1a)}$$

while the diameter D inches of the collar satisfies

$$1 < D < 1+\zeta; \quad \zeta > 0 \quad \text{(1b)}$$

To secure a fit, the critically important point is that the greatest permitted d be less than the least permitted D. If the sign of equality occurs, it indicates usually that nominal specification is being used. Occasionally it indicates that a change of nomenclature is convenient, as in

$$a^2-b^2=(a-b)(a+b) \quad \text{(1c)}$$

in which both sides are alternative names for the same entity or thing. It may happen that either name is the more convenient; both are exactly the same. We can speak of a nominal specification as 'exactly' 12 eggs or 'exactly' £1, but a metrical specification of 'exactly' 12in is nonsense, since this really means 12·00000... in and requires infinite information.

Although in science and technology nominal values can thus only be used when there is no critical comparison, it is always possible to unclose a prematurely-closed limit if we are unexpectedly confronted with a critical comparison. The expression py or dy/dt is a nominal or conceptual derivative of y; it can be regarded as derived by the closing of any one of the three limits

$$\lim_{\delta t\to 0}(\delta y/\delta t); \quad \lim_{\epsilon\to 0}(p+\epsilon); \quad \lim_{\nu\to 0}(1/p+\nu)^{-1} \quad \text{(2)}$$

each of which is a metrical entity before the limit is closed. Again, we use freely the nominal or conceptual ideas of 'pure' capacitance, 'zero' impedance or admittance, and all is well as long as we always remember the existence of at least residual associated resistance (as in Fig. 1, discussed below).

In pure mathematics, however, a nominal specification implies that the limit has been closed. If we are given that

$$b=a \text{ and } c=a \quad \text{(3)}$$

the implication is that

$$b=c \quad \text{(4)}$$

and no information is available about the signs of any of the quantities $(b-c)$, $(c-a)$ and $(a-b)$. This information may be critically important, as in the case of the shaft and collar already discussed.

If ϵ is arbitrarily small and positive, the equation

$$b=a+\epsilon$$

is in effect a shorthand for the inequalities

$$a < b < a+\epsilon$$

and it is possible to retain the exactness of pure mathematics if we refrain from closing limits too soon. We may even have to 'unclose' them, as the conceptual expression dy/dt or py was 'unclosed' by means of expressions (2).

The engineer's point of view

Let us first consider what restrictions must be put on a function (of time) so that it can be regarded as 'admissible' for the purpose of describing natural phenomena. We must then consider how the repeated application of some of the above-mentioned conceptual processes, like pure differentiation, may turn an 'admissible' function into an 'inadmissible' one. In some situations we can, and frequently do get away with the use of closed limits, especially if there is only one conceptual or closed-limit operation involved in the problem under discussion. But when two such entities are involved simultaneously, as in the famous question 'what happens when an irresistible force is applied to an immovable body?', we have a situation about which it is impossible to talk sense because the situation is inadequately specified. We must determine metrical processes analogous to the above-mentioned conceptual processes, and differing from them to an arbitrarily small extent, such that the application of any combination of these metrical processes to an 'admissible' function always gives an 'admissible' result. Success in this task means that we need never bother about mathematical complications and monstrosities such as functions having an infinite number of discontinuities in a finite range, discontinuities more complicated than an isolated step, Lebesgue integration, distribution theory etc. Such matters can be relegated to the status of a game, analogous to chess—very enjoyable for those who like mathematical abstractions for their own sake, without caring how little they make the work of others easier.

Admissible functions of time

A minimum qualification for an admissible function $h(t)$ of time might be expressed in the form that $h(t)$ is everywhere finite, and is of limited extent. This means either that $h(t)$ is zero when t is outside certain limits, or, if $h(t)$ is different from zero for all t, then $h(t)$ must tend to zero as t tends to $\pm\infty$. Furthermore, $h(t)$ must have an ultimately smooth fine structure. However, these points are most easily specified and understood with the help of Fourier theory. In the language of this theory, $h(t)$ must have no components at zero or infinite frequency.

By definition, if $F(\mathrm{p})$ is the Fourier transform of $h(t)$

$$h(t) = (1/2\pi \mathrm{j}) \int_{-\mathrm{j}\infty}^{\mathrm{j}\infty} e^{\mathrm{p}t} F(\mathrm{p})\, \mathrm{dp}; \quad F(\mathrm{p}) = \int_{-\infty}^{\infty} e^{-\mathrm{p}t} h(t)\, \mathrm{d}t \quad \ldots . (5)$$

Both integrals in equation (5) are infinite integrals, so that their evaluation involves the closing of limits associated with p and t, respectively. A necessary condition of convergence and hence usefulness of these integrals is

$$F(\mathrm{p}) \to 0 \text{ as } \mathrm{p} \to \pm \mathrm{j}\infty \quad \ldots\ldots\ldots\ldots (6a)$$

$$h(t) \to 0 \text{ as } t \to \pm\infty \quad \ldots\ldots\ldots\ldots (6b)$$

Condition (6a) ensures that

$$h(t) = \tfrac{1}{2} \lim_{\epsilon \to 0} \, [h(t+\epsilon) + h(t-\epsilon)] \quad \ldots\ldots\ldots (7)$$

while condition (6b) ensures that $F(\mathrm{p})$ remains finite as p tends to zero. Note that proceeding to the limit for p tending to $\pm\infty$ sometimes presents great difficulty and sometimes ambiguity. Sometimes there appears to be no definite limit; closer inspection reveals, however, that in such cases a second quantity or process, derived by closing a limit, is involved. The solution lies in 'unclosing' this prematurely closed limit before attempting to close the limit for p.

Application of conceptual processes to admissible functions

Suppose that a particular function $h(t)$ qualifies for admissibility by tending to zero as t tends to $\pm\infty$ and that it has a Fourier transform $F(\mathrm{p})$ defined by equation (5) such that $F(0)$ has a finite value a while for large values of p, the expression $\mathrm{p}F(\mathrm{p})$ tends to a constant limit K. Then if we differentiate $h(t)$, the Fourier transform of the derivative $h'(t)$ is $\mathrm{p}F(\mathrm{p})$, which tends to zero with p but tends to K, and not zero, when p tends to infinity, so that $h'(t)$ fails to qualify as an admissible function. Again if $I(t)$ is the integral of $h(t)$ (with lower limit of integration at $-\infty$), the Fourier transform of $I(t)$ is $F(\mathrm{p})/\mathrm{p}$. This expression tends to zero as p tends to infinity, but tends to infinity as p tends to zero; so that $I(t)$ is again an inadmissible function in spite of the fact that $h(t)$ is admissible. Clearly, admissible functions $h(t)$ which can be repeatedly differentiated and/or integrated are few and peculiar.

These difficulties are overcome by replacing conceptual differentiation, integration etc. by analogous metrical processes, as indicated below in a critical situation requiring accurate and detailed specification and calculation. Many situations, however, are not critical in this sense, and for these situations nominal or quantized concepts greatly simplify the relevant mathematical work. In electrical technology, likewise, the concepts of pure resistance, capacitance etc. are often extremely helpful, as long as they are used with care and we never allow ourselves to forget their idealized nature.

Metrical differentiation and integration

The cure for the difficulties associated with conceptual differentiation, integration etc. is best found by means of physical intuition. If we replace the conceptual idea of instantaneous velocity by that of average velocity over the shortest time-interval that we can measure in the situation under discussion, we know exactly what we are talking about. Likewise, a nominally 'pure' unit capacitance in practice necessarily has at least residual series resistance (say, ν ohms) and shunt conductance (say, ϵ mhos) associated with it. It is thus better represented in terms of Fig. 1.

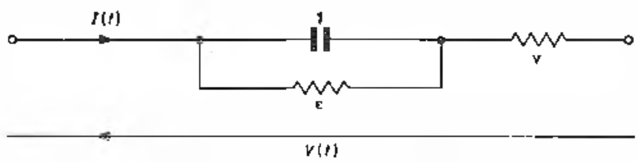

Fig. 1 Residual elements associated with a unit capacitance

In science (the study of observables), all actual observations are averages, probabilities and similar quantities. Instantaneous velocity, position etc. are not observed or observable. We expect that the simplest formulation of our observations will be in terms of ideal concepts like Maxwell's equations. But using such idealizations involves 'contraction' of information by the formation of various mean or average values, for example contraction of tensors, mean values of vectors, scalar products of vectors, formation of moments, centroids, frequency components etc.

Ideally, a pure unit capacitance can be regarded as an integrator of all current $I(t)$ applied to it, and as a differentiator of all voltage $V(t)$ applied to it; both ways of regarding it are equivalent expressions of what a capacitance does. When the residual elements are taken into account, however, the essential fact is that the impedance Z of the circuit of Fig. 1 is

$$Z = \frac{1}{\mathrm{p}+\epsilon} + \nu \simeq \frac{1}{\mathrm{p}+\epsilon} \ldots\ldots\ldots\ldots\ldots (8)$$

while the admittance Y or $1/Z$ is

$$Y = 1/Z = \frac{p + \epsilon}{1 + \nu p + \nu\epsilon} \simeq \frac{p}{1 + \nu p} \quad \ldots\ldots \quad (9)$$

In equations (8) and (9), p denotes the conceptual differentiation operator d/dt, and $1/p$ means the conceptual integration operator with lower limit minus infinity, so that for all operands $h(t)$ that can be associated with a genuine physical situation (representable by means of a passive electrical network),

$$pp^{-1}\,h(t) = p^{-1}p\,h(t) = h(t) \quad \ldots\ldots\ldots\ldots \quad (10)$$

By operational calculus or otherwise, we can deduce from equation (8) that the formula for $V(t)$ when $I(t)$ is

$$V(t) = e^{-\epsilon t} \int_{-\infty}^{t} e^{\epsilon\tau}\, I(\tau)\, d\tau \quad \ldots\ldots\ldots\ldots \quad (11)$$

while that for $I(t)$, when $V(t)$ is given, is correspondingly

$$I(t) = (1/\nu)\, V(t) - (1/\nu^2)\, e^{-t/\nu} \int_{-\infty}^{t} e^{\tau/\nu}\, V(\tau)\, d\tau \quad \ldots\ldots \quad (12)$$

If $I(t)$ is the admissible function $h(t)$, $V(t)$ given by equation (11) has the Fourier transform

$$F(p)/(p+\epsilon), \text{ instead of } F(p)/p \quad \ldots\ldots\ldots \quad (13)$$

and thus, for all finite p, the change in this Fourier transform is arbitrarily small; but there is now a limit a/ϵ for the transform when p tends to zero, a being $F(0)$ which must be finite because $h(t)$ itself is admissible. Thus the process of 'metrical integration' described by equation (11) gives an admissible output $V(t)$ for an admissible input $I(t)$. Again, if $V(t)$ is the same admissible function $h(t)$, the corresponding output $I(t)$ obtained from equation (12) has the Fourier transform $pF(p)/(1+p\nu)$ instead of $pF(p)$. Hence, when p tends to infinity, this Fourier transform tends to zero instead of to K, and thus $I(t)$ is admissible as well as $V(t)$. Hence the process of metrical differentiation described by equation (12) also gives an admissible output $I(t)$ for an admissible input $V(t)$. Repeated metrical differentiation and/or integration will not destroy admissibility because the argument above for a single metrical differentiation or integration can be repeated indefinitely.

The mathematician's point of view

Given, as before, that $F(p)$ is the Fourier transform of $h(t)$, so that equations (5) apply, we note first that the infinite limits of integration indicate that a limit has been closed. The limiting values of $F(p)$ and $h(t)$ in equations (6a) and (6b) are necessary conditions for the integrals to converge, and imply that $h(t)$ has a smooth fine structure, as specified in equation (7). Conditions (6a) and (6b) happen also to be the requirements that $h(t)$ shall be a function admissible for the representation of natural phenomena, although this fact is unimportant from the pure-mathematician's point of view.

Now the limiting processes involved in equations (5) happen to be abnormally sensitive, and frequently abnormally difficult to evaluate in specific cases. There are very few analytic functions (of time) which are as well behaved as $\exp(-k^2t^2)$. This noble expression has a nonzero value for any real finite value of t positive or negative (k being real) and tends to zero as t tends to $\pm\infty$; it has a Fourier transform. But most of the straightforward functions we encounter in our student days (hereinafter called 'teaching functions' for brevity) fail to meet the requirement that they must be adequately specified for all values of time, not only those in which we happen to be interested. Thus the expression e^{at} (real part of $a > 0$) behaves excellently at its beginning when t is negative, but it has no finite end and is thus inadmissible unless 'tailored' as explained below. Likewise the expression e^{-at} behaves excellently at its end when t is arbitrarily large and positive, but it has no finite beginning. An admissible function can be made up from teaching functions like this in much the same way as a tailor makes a garment from a roll of cloth. The scissors are the Heaviside step function $H(t - t_0)$ defined, as in Fig. 2, by

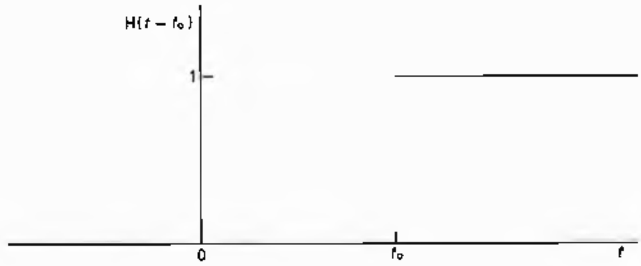

Fig. 2 Heaviside step function $H(t-t_0)$ (zero for $t < t_0$; unity for $t > t_0$)

$$H(t - t_0) = 1(t > t_0) \quad \ldots\ldots\ldots\ldots \quad (14)$$

$$H(t - t_0) = 0(t < t_0) \quad \ldots\ldots\ldots\ldots \quad (15)$$

The value of $H(0)$ is not defined because it is not relevant. If we are ever under the delusion that we need to know it, the truth is that we have wrongly specified or formulated the problem under discussion. Thus the expressions

$$e^{at}\, H(-t) \text{ or } e^{-at}\, H(t) \quad \ldots\ldots\ldots\ldots \quad (16)$$

are admissible in the sense that they have both a beginning and an ending; their only defect is the abrupt discontinuity when $t = 0$. This discontinuity is merely a convenient artefact from the engineer's point of view. It is tacitly understood that any actual circuit contains at least residual elements which round off the theoretical discontinuity, so that a theoretically discontinuous input gives an output which may change extremely rapidly (e.g. when a switch is closed) but it is practice continuous and repeatedly differentiable. But from the mathematician's point of view, the tailored functions (16) cannot be differentiated; other such functions cannot be integrated. Very few will tolerate repeated differentiation and/or integration; for if $h(t)$ has a Fourier transform $F(p)$ which tends to zero as p tends to infinity and to a finite limit when p tends to zero, there is no guarantee that $p^nF(p)$ or $p^{-n}F(p)$ will do so. This is a very severe limitation on the use of Fourier integrals, and has led mathematicians into various attemps to widen the applicability of the Fourier integral by means of Stieltjes or Lebesgue integrals and other less well known techniques. It is here indicated, however, that the difficulty is due to the schoolboy error of closing limits in the wrong order.

When a limit has to be taken which involves a nominal expression already in closed-limit form, it may be necessary to revert to the unclosed, or metrical, form of this expression to correct the order in which the limits are closed, and recover the information lost by the premature closure, as was in effect done when considering equations (3) and (4). Again, if

$$h(t) = (1/2\pi j) \int_{-j\infty}^{j\infty} e^{pt}\, dp/p \quad \ldots\ldots\ldots\ldots \quad (17)$$

we have an indeterminate form, although it is given in many textbooks as $H(t)$. But

$$h_1(t) = (1/2\pi j)\int_{-j\infty}^{j\infty} e^{pt}\,\frac{dp}{p+\epsilon} = e^{-\epsilon t}\,H(t) \;\ldots\ldots\; (18a)$$

$$h_2(t) = (1/2\pi j)\int_{-j\infty}^{-\infty} e^{pt}\,\frac{dp}{p-\epsilon} = -e^{-\epsilon t}\,H(-t) \;\ldots\; (18b)$$

and if the limits in equations (18a) and (18b) are closed by making ϵ tend to zero, the results differ by unity.

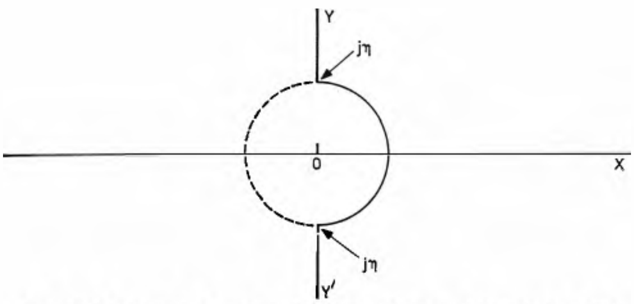

Fig. 3 Indentation of imaginary axis for the integral in equation (17)

If we try to evaluate the integral (17) by indenting the contour, as in Fig. 3, leaving the imaginary axis for a small semicircle between the points $-j\eta$ and $+j\eta$, we obtain a result half way between; namely

$$h(t) = \tfrac{1}{2}\,[H(t) - H(-t)] \;\ldots\ldots\ldots\; (19)$$

But by this process of indentation, what we have evaluated is not $h(t)$ given by equation (17), but

$$h_3(t) = (1/2\pi j)\left[\int_{-j\infty}^{-j\eta} e^{pt}\,dp/p + \int_{j\eta}^{j\infty} e^{pt}\,dp/p\right] \ldots\ldots\; (20)$$

omitting the integral

$$h_4(t) = (1/2\pi j)\int_{-j\eta}^{j\eta} e^{pt}\,dp/p = (1/2\pi j)\int_{-j\eta}^{j\eta} dp/p \;\ldots\ldots\; (21)$$

which (for η sufficiently small to permit the factor e^{pt} to be replaced by unity) is $\pm\frac{1}{2}$, since either semicircle connecting the points $-j\eta$ and $j\eta$ in Fig. 3 can be used. Alternatively, equation (17) is often expressed in terms of Dirichlet's integral:

$$h(t) = (1/\pi)\int_0^{\infty} \frac{\sin \omega t}{\omega}\,d\omega = \tfrac{1}{2}\,[H(t) - H(-t)] \;\ldots\; (22)$$

but here also we have omitted the critically important and indeterminate integral (21). Similarly the integral

$$h_5(t) = (1/2\pi j)\int_{-j\infty}^{j\infty} e^{pt}\,dp \;\ldots\ldots\ldots\ldots\; (23)$$

is indeterminate. On the other hand, if ν is positive, however small,

$$h_6(t) = (1/2\pi j)\int_{-j\infty}^{j\infty} e^{pt}\,\frac{dp}{1+\nu p} = (1/\nu)\,e^{-t/\nu}\,H(t) \;\ldots\; (24)$$

$$h_7(t) = (1/2\pi j)\int_{-j\infty}^{j\infty} e^{pt}\,\frac{dp}{1-\nu p} = -(1/\nu)\,e^{t/\nu}\,H(-t) \;\ldots\; (25)$$

without any difficulty or ambiguity at all.

Conclusions

From the point of view both of the engineer and of the pure mathematician, difficulties encountered in calculating with ideal, nominal or quantized quantities expressed in closed-limit forms are easily evaded with no loss of precision by replacing conceptual entities in closed-limit forms by the corresponding metrical or open-limit forms. If this is done, there is no need to study techniques involving anything more than straightforward differentiation and ordinary Riemann integration, and no discontinuity more complicated than an isolated step need be considered.

Acknowledgment

The authors wish to express their thanks to the Director of Engineering of the British Broadcasting Corporation for permission to publish this article.

Continuously tunable laser radiation

Scientists in the Quantum Physics Division of the Ministry of Technology Signals Research and Development Establishment, Christchurch, Hampshire, have recently discovered a method of generating high-powered narrowband optical frequencies which can be continuously tuned in the 0·5-0·8μm spectral range. In the past, laser outputs have been restricted to discrete frequencies; this discovery offers a method of filling the gaps in the spectrum where laser frequencies do not occur. This is thought to be the first observation of intense tunetable outputs at higher frequencies than the laser frequency.

The effect was first observed when a lithium niobate crystal was being temperature-tuned for the efficient addition of a neodymium laser frequency to another frequency generated by the laser in a cell of benzene. The frequency of the tunable output was shown to be independent of the liquid in the cell and to depend only on the temperature of the lithium niobate. At temperatures above 200°C a fine structure could be resolved on the tunable frequency. All the observed frequencies can be accounted for if it is assumed that they originate from an upconversion of the following type:

$$\underset{\text{(tunable)}}{\omega_{\text{observed}}} = \underset{\text{(fixed)}}{\omega_{\text{pump}}} + \underset{\text{(tunable)}}{\omega_{\text{infrared}}}$$

where the fixed pump frequencies can be either the laser, the Stokes or the antiStokes stimulated Raman emissions. It is apparent that, at a given temperature, the three pump frequencies upconvert different infrared frequencies. In an effort to make a positive identification of this proposed mechanism, a search was made for a tunable source at the ω_{infrared} frequency. No such frequency has yet been detected. With the crystal at a constant temperature, the output intensity at 0·585μm has been shown to vary exponentially with the laser field strength and to have a line width of less than 8cm^{-1}. Since the output frequency is independent of the material in the cell and depends only on the temperature of the crystals, it was concluded that the only function of the cell was to increase the power density of the laser beam by the beam-trapping mechanism. The power/wavelength curve shown was observed

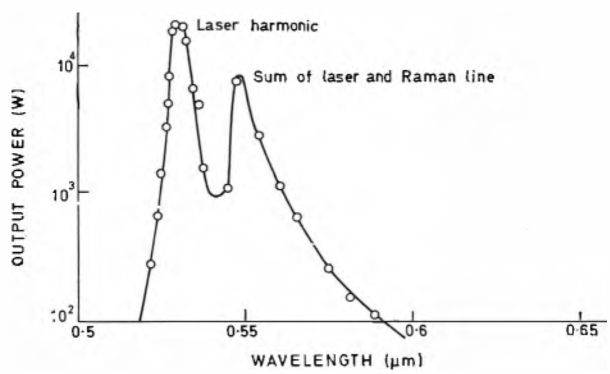

when a 20cm cell of CS_2 was placed between the laser and the crystal. The output power is limited only by the ability of the crystal to withstand high-power laser pulses without damage, and in these tests the apparent power density of the laser was limited to $4{\cdot}5\text{MW/cm}^2$.

Possible applications for this discovery lie in the field of optical communication, spectroscopy and photochemistry.

Accurate triangle-sine converter

by **G. Klein** and **H. Hagenbeuk,** *Philips Research Laboratories, Eindhoven, Netherlands*

By means of a hybrid integrated circuit of thin-film nickel-chromium resistors and monolithic diode arrays, an accurate instantaneous triangle-sine conversion is obtained for frequencies up to 1MHz. From a symmetrical triangle, a sinewave can be obtained with less than 0·1% distortion.

(Voir page 731 pour le résumé en français: Zusammenfassung in deutscher Sprache auf Seite 732)

Particularly in instrumental electronics, an accurate instantaneous triangle-sine converter is of great value, since triangles can be generated with greater flexibility than sinewaves. This may be illustrated by the following example. An earlier article[1] described a generator of symmetrical triangles and rectangles which allowed for a frequency sweep of more than four decades, while maintaining a perfect symmetry and amplitude constancy. If such a generator is now combined with an instantaneous triangle-sine converter, a sinusoidal signal of good amplitude stability and low distortion is obtained whose frequency can be controlled by an external signal. Such a combination can thus serve as a voltage/current-controlled frequency modulator with a frequency sweep of 10^4.

Known methods for the instantaneous conversion of triangles into sinewaves all have some disadvantages. The method employing the inverse function generator[2] is very accurate but only applicable up to some tens of kilohertz, as it uses a sampling technique. Among the methods using the nonlinear characteristics of passive or active elements, the one employing a field-effect transistor, as proposed by Middlebrook and Richer[3], seems to give the best results. By this method, a distortion of approximately 1% can be obtained, but it requires some critical adjustments and is also highly temperature-sensitive. The third and most common method makes use of resistor-diode networks with which a well defined nonlinear resistance is made[4]. In most published circuits employing this method, separate networks are required for the positive and negative halfcycles. This implies that, if low distortion is required, the tolerances in the corresponding resistances of the two networks should be made very small. Because of the stringent requirements thus imposed on the components, the sinewave is usually approximated to in no more than six steps and this makes the sinewave more like a broken line. One of the great disadvantages of this is that such a signal cannot be differentiated properly.

The circuit to be described here uses a resistor-diode network also. One of its main features is that the same network is used for the positive and the negative halfcycles, so that, even if a distortion of the order of 0·1% is required, large tolerances (5-10%) in the resistances are allowed, provided that sufficient steps are taken in the approximation. This makes the circuit particularly suitable for realization in integrated form. Other features are that no critical adjustments have to be made and that the sinewave has a small distortion and is very smooth.

The principle of the circuit is given in Fig. 1. If the height V_p of the two equal but antiphase triangles is made to be several volts, only one of the transistors will be conducting during each halfcycle, and the circuit will then act as an emitter follower. If it is assumed for the moment that the common emitter follows the bases perfectly and that the conductance Y in the emitter lead can be varied proportionally with $\cos x$ (where $x = (\pi/2)\, V_e/V_p$, with V_e the instantaneous voltage of the common emitter), the current through the conducting transistor will vary proportionally with $\sin x$. Thus half sinewaves, half a period out of phase with each other, will appear on the collectors, so that a full sinewave can be obtained between the collectors.

The conductance $Y(x) = Y_0 \cos x$ can be achieved in the manner shown in Fig. 2. The resistor-diode branches are connected to the direct voltages $V_1 \ldots V_n$, which are all derived from one direct voltage V_p, corresponding to the height of the triangles. The internal resistance of these points is low compared with the branch resistors. At zero

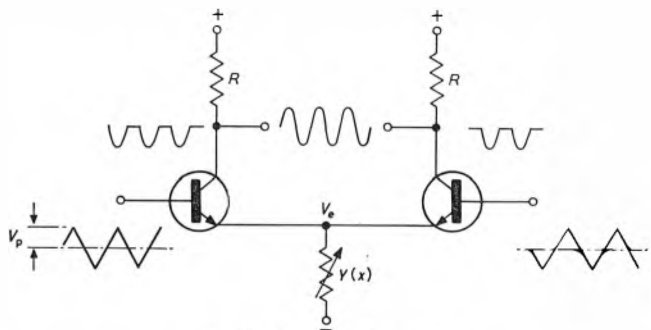

Fig. 1 Principle of convertor

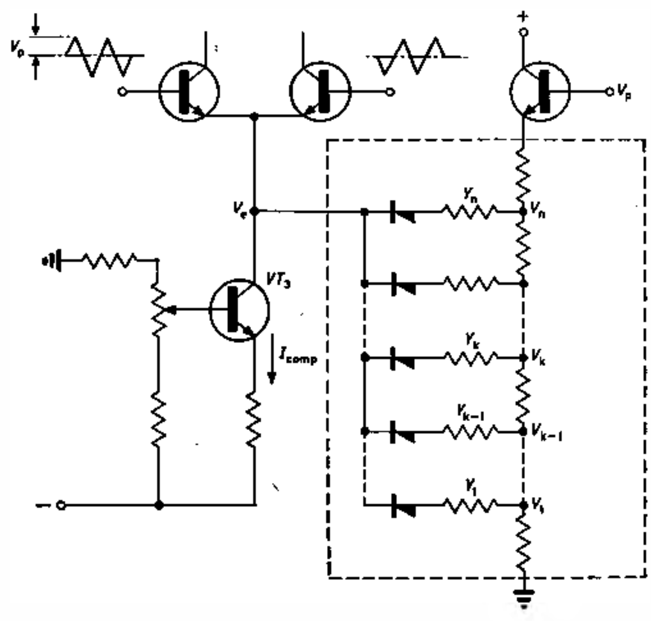

Fig. 2 $Y(x) = Y_0 \cos x$

signal, all diodes are conducting, but as V_e goes more positive the diodes stop conducting one after the other; and when $V_e = V_p$ the differential conductance through the resistor-diode network becomes zero. By selecting the proper values for the conductances $Y_1 \ldots Y_n$ in the branches, the cosine function can thus be obtained. If Y_o is the conductance at zero signal, and assuming perfect diodes, the value of Y_k should be $Y_o(\cos x_{k-1} - \cos x_k) \simeq Y_o(x_k - x_{k-1}) \sin x_k$, with $x_k = (\pi/2)\ V_k/V_p$. The current source VT_3 is used for compensation of the current through the network for zero signal.

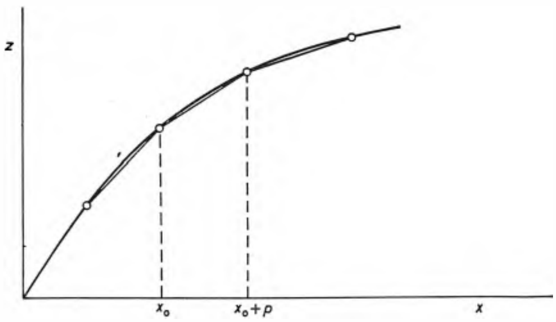

Fig. 3 Linear approximation of sinewave

Before dealing with the circuits in detail, the accuracies required for the resistors and diodes in the branches and for the voltages $V_1 \ldots V_n$ will be examined. Referring to Fig. 3, if the linear approximation of a sinewave $z = \sin x$ fits exactly at the points x_o and $x_o + p$, the maximum deviation between these points occurs at $x = x_o + \frac{1}{2}p$ and is approximately equal to $\frac{1}{8}p^2 \sin x_o$. In order to keep the deviation everywhere smaller than 0·1%, p should be approximately 0·1 or 5° for large x_o, and can be increased to 10° for smaller x_o. In practice, the quality of a sinewave is primarily judged by its behaviour at the peaks, and in order to obtain perfect smoothness the approximation should preferably be made smaller than the calculated 5°. In the practical circuit there were 21 branches and these were divided into 90° in the following way: 15 × 5°, 3 × 3°, 2 × 2° and 2 × 1°. Assuming that all other parameters are ideal, it is clear that this approximation is ample for high accuracy.

Next, the influence of a deviation in one of the branch conductances is examined. Assuming perfect compensation for zero signal, the deviation in the current caused by a deviation ΔY_k in the conductance Y_k will be (Fig. 4, top)

$$\Delta I_x \propto x\ \Delta Y_k\ , \text{ for } x < x_k$$
$$\Delta I_x \propto x_k\ \Delta Y_k\ , \text{ for } x \geqslant x_k$$

and this deviation should be compared with the amplitude of the sinewave which is proportional to Y_o. From Fig. 4, it is clear that ΔY_k does not cause any even harmonics. Regarding the odd harmonics, for small values of x_k the deviation approaches the rectangular form, in which the amplitude of the nth harmonic is proportional to $1/n$. For large x_k, the deviation approaches the triangular form, in which the nth harmonic is proportional to $1/n^2$. From this it follows that the ratio between the heights $x_k \Delta Y_k$ and Y_o is a good measure of the introduced harmonic distortion. With a possible deviation of 10% in Y_k and $Y_k/Y_o = p \sin x_k$, this ratio is smaller than $0{\cdot}1\ p\, x_k^2$. From this it follows that a deviation in one of the upper resistors has the greatest influence, in particular when p is still 0·1 or 5°. With $x_k \simeq 1$ and $p = 0{\cdot}1$, the ratio would be 0·01.

The above calculation applies to the unfavourable situation where the zero crossing remains perfect but the amplitude changes. In a practical circuit, where simple adjustments for both amplitude and zero signal have been made, however, the opposite effect occurs. Here a deviation ΔY_k will have no effect on the amplitude, as this is solely determined by the current I_{comp} delivered by VT_3 (in Fig. 2) and the deviation in the current will then be the compliment of the one just dealt with (Fig. 4, bottom). Except for large values of x_k, the harmonic distortion due to this deviation will always be considerably smaller than that in the previous case.

Next, the influence of a deviation in the breaking points, i.e. the points where the conductance of one of the branches changes over, is considered. When a sinewave $z = \sin x$ is approximated by a number of broken lines (Fig. 5) starting at the points $x_1 \ldots x_n$, and if the line starting at x_k is replaced by a line with the same slope but starting at the point $x_k - \Delta x_k$, the deviation in z will be $p\, \Delta x_k \sin x_k$. The greatest deviation thus occurs for large values of $p \sin x_k$. In this circuit, this product has a maximum value for $p = 0{\cdot}1$ and $x_k \simeq 1$. In order to keep the deviation there below 0·1%, the breaking points should be defined to within 1% of the peak voltage V_p.

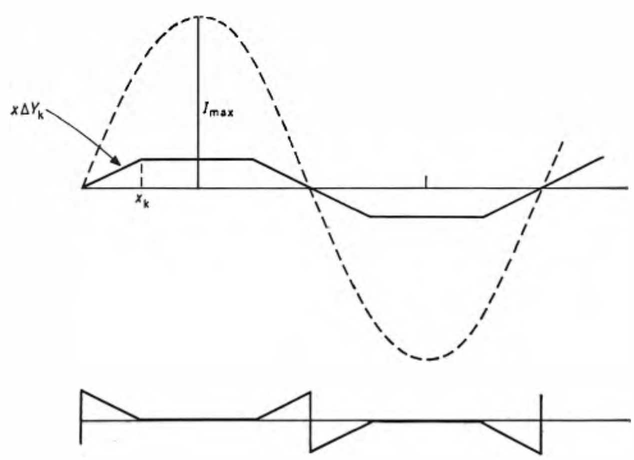

Fig. 4 Deviation in branch conductances
(a) with constant zero-crossing
(b) with constant amplitude

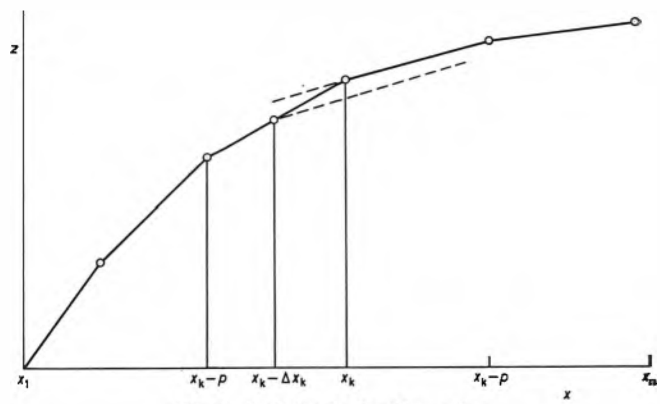

Fig. 5 Deviation in breaking points

Deviation in the positions of the breaking points can be caused by deviations or changes in the voltage divider and in the I/V characteristics of the diodes. In a voltage divider (Fig. 6), a deviation ΔR_m in one of the resistors R_m causes a deviation ΔV_k in the voltage V_k, which is always smaller than $(\Delta R_m/R_{tot})\ V_p$, where R_{tot} is the

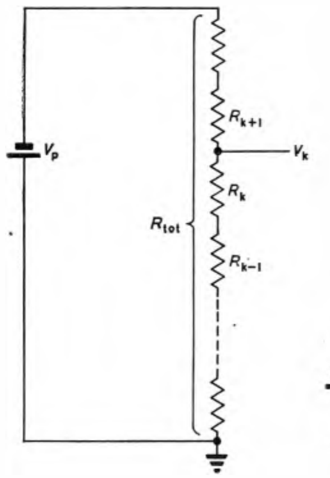

Fig. 6 Deviation in voltage divider

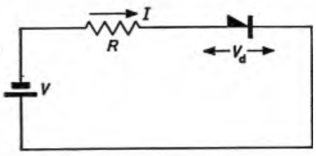

Fig. 7 Diode-resistor branch

total resistance of the divider. As the largest steps in the approach correspond to 5°, a relative deviation of 10% in one of the resistors will cause a ΔV_k which is always less than 1% of V_p. From Fig. 7, which gives the situation for one branch, the influence of the diode characteristic is calculated. For the diode,

$$I = I_o [\exp (V_d/V_o) - 1]$$

where V_d is the voltage across the diode and $V_o = kT/q \simeq$ 25mV. Thus

$$V_d = V_o \ln (I/I_o + 1)$$

and

$$V = IR + V_o \ln (I/I_o + 1)$$

From this, $$\Delta V = R\Delta I + \frac{V_o}{I/I_o + 1} \Delta I/I_o$$

or $$\Delta V/\Delta I = R + \frac{R_o}{\alpha + 1}$$

where $R_o = V_o/I_o$ and $\alpha = I/I_o$.

With silicon diodes, I_o is usually of the order of 10^{-9} to 10^{-10}A and thus R_o will be of the order of 10^7 to $10^8\Omega$, which is much larger than any of the values R of the series resistor ($< 10^5\Omega$). By eliminating $\alpha + 1$, the relation between V and the differential resistance $\Delta V/\Delta I$ is obtained:

$$V = V_o \left[\frac{1}{k-1} - \ln (k-1) + \ln (R_o/R) \right] - I_o R$$

where $$k = \frac{\Delta V/\Delta I}{R}$$

This relation is shown in Fig. 8, where $\ln (R_o/R)$ has been given the value 16. From this it is seen that the change-over from maximum to minimum conductance is not only very smooth, as required, but also takes place in a rather narrow region around the voltage $V_o \ln (R_o/R)$. As the resistors are all of the same order of magnitude, this voltage will not differ very much for the various branches. Moreover, with given diodes, the optimum value of the resistors R can be determined experimentally, so that the influence of these differences is still reduced. In this way the possible deviation in the breaking points due to the diode characteristic can be kept well below the required 0·1V.

From Fig. 8 it is also seen that, in the conducting state, the diode resistance only contributes appreciably in a small voltage region ($\simeq$ 0·2V) to the total branch resistance. As long as a great number of branches conducts, this will have little effect, so that a correction for this has only to be made in the upper branches in Fig. 2.

The temperature-dependence of the basic circuit in Fig. 2 can be completely predicted and thus, if wanted, compensated for. By using thin-film nickel-chromium resistors, the temperature coefficient of the resistors can be made sufficiently small if an overall accuracy of 0·1% is intended. The difference in drift between the two stages of the difference amplifier can be kept below 10μV/degC, while the common drift is about 2·5mV/degC. Approximately the same change occurs in the voltage across the conducting diodes, thus giving a partial compensation. For the emitter follower used with the voltage divider, and for the current source, the change of approximately 2·5mV/degC in the base-emitter voltage corresponds to relative changes of approximately 5×10^{-4}.

From all these considerations, it follows that, even without taking any special measures, the basic circuit in Fig. 2 should give good results. The shaded part lends itself excellently to integration: no accuracy is required provided that sufficient components are used. The integrated circuit used consisted of 43 thin-film nickel-chromium resistors and three monolithic chips, each containing 7 diodes. The optimum values of the resistors were determined experimentally, taking into account the loading of the voltage divider and the properties of the diodes. In order to make Y_o equal to 1mmho, the resistors in the branches were given values between 12 and 100kΩ. The resistors of the voltage divider were given a value of 11Ω/deg, thus making the total emitter resistance 1kΩ.

Fig. 9 shows the integrated circuit; the actual size is 2 × 2cm. The resistors of the voltage divider are at

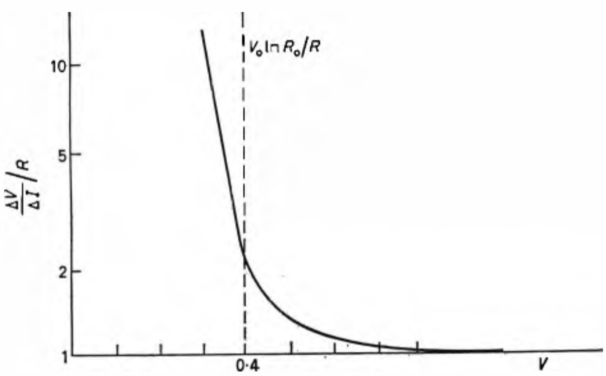

Fig. 8 Branch resistance as function of applied voltage

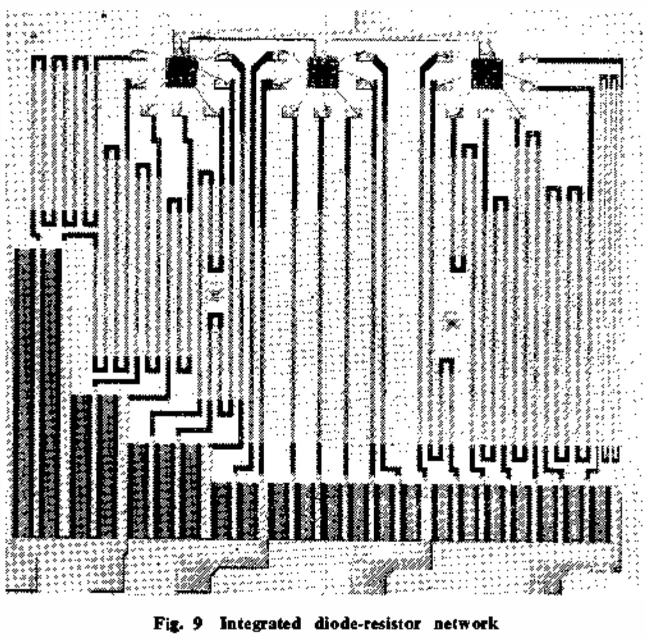

Fig. 9 Integrated diode-resistor network

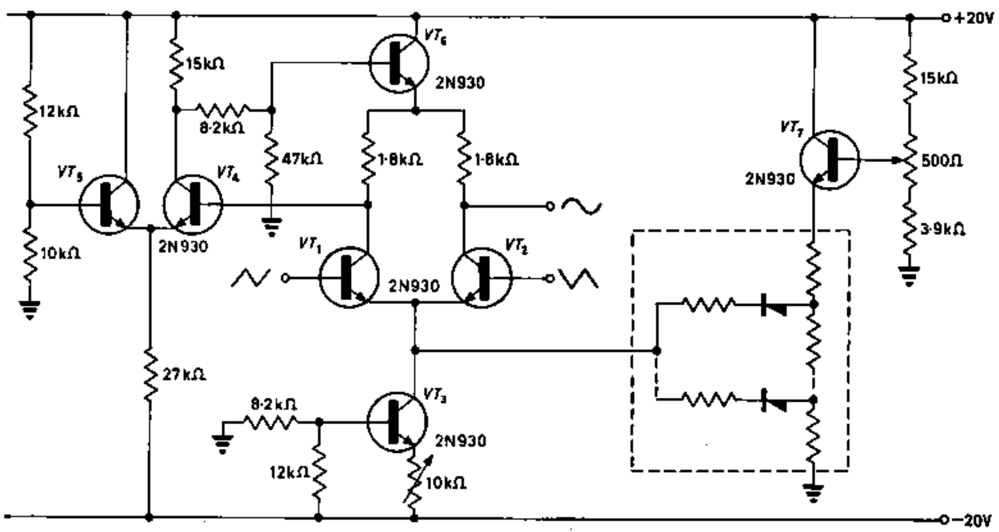

Fig. 10 Practical circuit of converter

the bottom, while the branch resistors are in the middle. Their upper sides are connected to the anodes of 3 × 7 diodes. The cathodes of these diodes are all connected to the top terminal.

A practical circuit, basically the same as that in Fig. 2, with which the properties of the network were measured, is given in Fig. 10. By means of the feedback circuit VT_4, VT_5 and VT_6, a full sinewave is obtained on one of the collectors. The distortion varied from 0·2% for low frequencies to 0·8% for some hundreds of kilohertz. Fig. 11 shows a 50kHz sinewave and an enlargement of the brightened part, showing the smoothness of the peak. Furthermore, the distortion can be made completely insensitive to changes in the height of the triangles by allowing the base voltage of VT_7 in Fig. 10, and thus the voltage across the voltage divider, vary with the height of the triangle. Here, with the height of the triangles stabilized within 0·1%, this precaution was not necessary. The influence of changes in the ambient temperature on the performance of the integrated network was very small indeed: a change from 20 to 50°C increased the distortion by no more than 0·1%.

Apart from the frequency limitation, there is only one shortcoming in the simple circuit shown in Fig. 10: the takeover of the current by the transistors VT_1 and VT_2 from each other at zero signal. Fig. 12 shows the two possibilities for different values of the compensating current I_{comp}. Depending on whether this current is too large or too small, a jump or a flat part occurs. A good approximation is obtained by making the compensating current so much larger than the current through the network that the slope of the takeover is equal to Y_0. However, the takeover in a difference amplifier is not completely linear and this gives a small deviation, as can be seen from Fig. 13, where a sinewave is shown with the optimum value for I_{comp} and a 10-times enlargement of the central part. A possibility for improvement of this point is given in Fig. 14. By means of feedback, the common emitter is now forced to follow the positive-going triangle much more accurately. Fig. 15 shows an output signal obtained in this way and a 40-times enlargement of the central part. For this circuit a distortion below 0·1% was obtained, and this might well be caused by a slight inequality of the two triangles. To show the smoothness of the sinewave, Fig. 16 gives a reproduction of the sinewave after passing a differentiating network, the frequency characteristic of which is given in Fig. 17, where f_0 is the frequency of the sinewave.

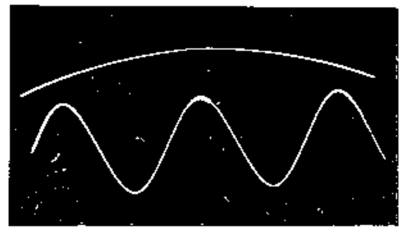

Fig. 11(a) 50kHz sinewave (b) Enlargement of brightened part

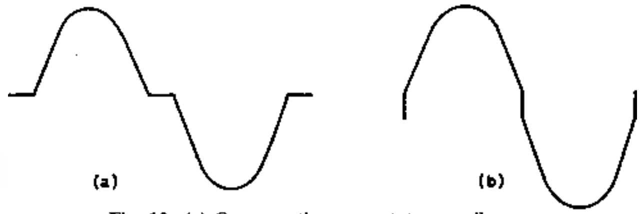

Fig. 12 (a) Compensating current too small (b) Compensating current too large

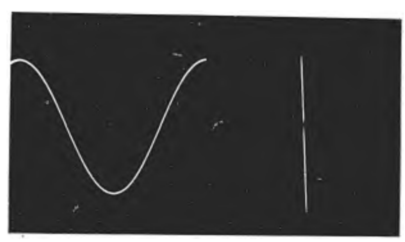

Fig. 13 Left: optimum value of compensating current. Right: 10-times enlargement of central part

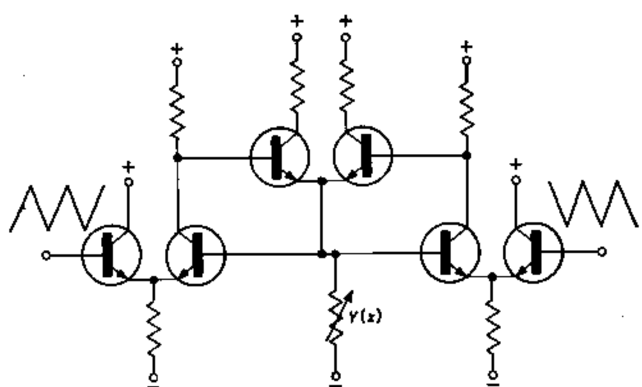

Fig. 14 Improvement of circuit

Thus all harmonics up to 1000 f_0 were amplified with a factor 3-20 compared with the fundamental.

The integrated form of the circuit brings the total stray capacitance C_{par} of the common emitter down to

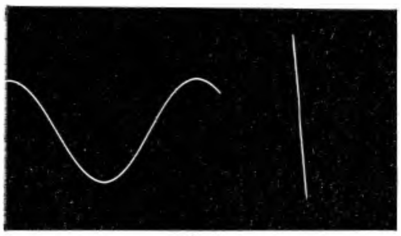

Fig. 15. Left: Output signal in Fig. 14
Right: 40-times enlargement of central part

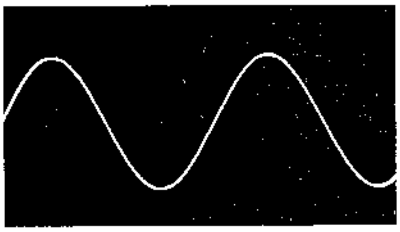

Fig. 16
Differentiated sinewave

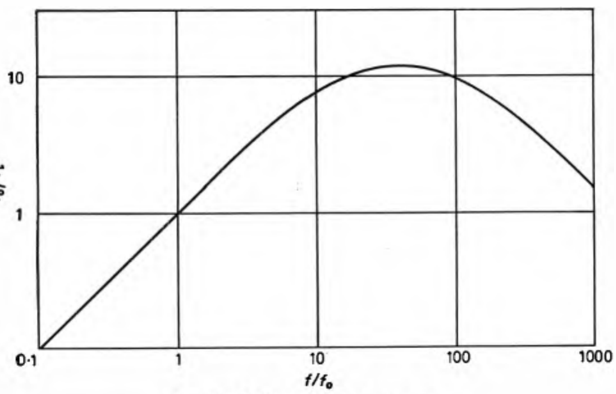

Fig. 17 Differentiating network

some picofarads (Fig. 18). Above the frequency for which the admittance of this capacitance becomes, say, 1% of the total conductance Y_o, the total distortion will increase rapidly. Thus the maximum frequency ω_{max} at which the circuit can be used will be determined by

$$\omega_{max}\ C_{par} \simeq 10^{-2} Y_o$$

With $Y_o = 10^{-3}$mho and $C_{par} = 3$pF, this gives an upper frequency of approximately 0·5MHz. By reducing the impedance level and hence Y_o, this maximum frequency can still be increased. A great reduction in the impedance level will, however, impair the simplicity of the circuit, so that it can be said that, with simple circuits like those in Figs. 10 and 14, an accurate triangle-sine conversion is possible up to 1MHz.

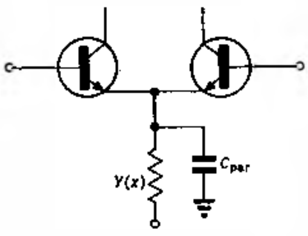

Fig. 18 Influence of stray capacitance

Acknowledgment

The integration of the integrated network was done by W. G. Gelling and the authors would like to thank him for his co-operation.

REFERENCES

1 KLEIN, G., and HAGENBEUK, H.: Accurate triangular-wave generator with large frequency sweep, *Electronic Engng. 37*, 388-390 (June 1967)
2 KLEIN, G., and DEN HERTOG, J. H.: A sinewave generator with periods of hours, *ibid. 31*, 320 (June 1959)
KLEIN, G., and ZAALBERG VAN ZELST, J. J.: *Instrumental electronics*, Centrex Publishing Co., Eindhoven, Netherlands.
3 MIDDLEBROOK, R. D., and RICHER, I.: Non-reactive filter converts triangular waves to sines, *Electronics* (8th March 1965)
4 RITCHIE, C. C., and YOUNG, B. W.: The design of biased-diode function generators, *Electronic Engng. 31*, 347 (June 1959)

New concept in microelectronics

SGS-Fairchild's c.c.s.l. (compatible current-sinking logic) approach to the use of microcircuits without restrictions to the limitations of specific logic families combines the most important features of three distinct families, all categorized as current-sinking (i.e. accepting current into their outputs from the circuits they are driving), all employ positive NAND logic, and all are compatible—logically and mechanically. Every c.c.s.l. element can drive and be driven by every other c.c.s.l. element, regardless of family identity. There are three families within the SGS-Fairchild current-sinking group: t.t.μl. (transistor-transistor micrologic), d.t.μl. (diode-transistor micrologic) and l.p.d.t.μl. (low-power diode-transistor micrologic). By crossing distinct family boundaries within this compatible logic group, system optimization is easily obtained.

All three families use a single 5V power supply and are guaranteed to perform compatibly when the specified rules for interconnecting between logic forms are observed. The power-supply pin is the same for all elements, and pin configurations for the same functions are identical throughout. All three families are available in the same two encapsulations—flat and dual-in-line. Also, all three families are manufactured using the same planar technology; so that, within the same working environment, they will maintain a uniform stability over a period of time.

Until now, circuit designers have been confronted with the task of selecting one particular family of integrated circuits with which to build a system. Inevitably, this has led to compromise, since each family has been optimized with respect to one specific consideration: high speed or low power, say. With c.c.s.l., design engineers are freed from this form of compromise; for example, advantage can be taken of the speed of t.t.μl. and the very low power requirements of l.p.d.t.μl. in the same system. As a result, application needs can be considered at each stage and not in terms of what any one family can offer.

Current-sinking and -sourcing

The two most common basic types of logic circuit are current-sinking and current-sourcing. The terms sinking and sourcing indicate that the output of the circuit acts as a current sink (i.e. receives current) or a current source (i.e. current flows from it). The output of a logic circuit, such as a gate, has two meaningful states. When it is higher than a certain level the output is said to be high, or in the 1 state; when it is lower than another level it is said to be low, or in the 0 state (or *vice versa*). In a system, the output of one gate (the driving gate) is connected to inputs of other gates (the driven gates). Current flows in the conductor which connects the output of one gate to the inputs of others. In the case of current-sinking logic, when the output of the first gate is low, current flows out of the inputs of the driven gates and into the output of the driving gate. This current sinks into the output of the driving gate. Hence the term current-sinking logic. Common examples of this sinking logic are d.t.l. and t.t.l.

In d.t.l., the two logic states are high when the output transistor of a gate is not conducting, and low when the output transistor of the gate is conducting and saturated. When the output transistor of the gate is saturated, the output voltage is typically 0·2V. Current flows from the positive voltage supply, through the input resistor and out of the input diode of the following gate. This current flows into the output terminal of the driving gate. When the output transistor of the gate is not conducting, the input diode of the following gate is reversed-biased and only a very small leakage current flows out of the output terminal. The major current flow in this circuit is into the output terminal, hence current-sinking.

Common basis

All SGS-Fairchild c.c.s.l. elements are derived from three basic gate circuits. The d.t.μl. gate is a medium-speed gate (t_{pd} = 25ns) derived from the well known diode-transistor-logic technique). In this gate, however, one of the two level-shifting diodes has been replaced by a transistor, and as a result the speed of the gate has been increased for the same power dissipation. The fan-in extension obtained by adding external diodes at the input, and the possibility of performing the wired-OR function at the output without any additional elements (which allow two levels of logic per gate) gives the d.t.μl. gate good logic flexibility.

By taking advantage of the wired-OR function when designing a system, not only can the total number of elements used be decreased, but the propagation delay through the logic chain can be lowered, thus improving the speed of the system.

High speed

The t.t.μl. gate is also derived from basic diode-transistor logic. In this case the input diodes have been replaced by a multi-emitter transistor to increase the speed of the input node; furthermore, two cascaded emitter-followers replace the collector resistor of the d.t.l. gate, providing a large amount of drive current when the output goes high, thus greatly improving speed with capacitive loads. The physical layout of the resistors and transistors in t.t.μl. gates has been designed to obtain maximum speed (t_{pd} = 6ns, typically) with only a relatively small increase in power dissipation (P_{tot} = 11mW/gate).

Low power

The l.p.d.t.μl. gate is again a modification of basic diode-transistor logic, but additional transistors have been incorporated to decrease the power dissipation to a minimum while still retaining a reasonable speed. Power drains of less than 1mW/gate are obtained by using resistor values of about 10 times those for a d.t.μl. gate while still maintaining a t_{pd} of only 60ns. This has been achieved by the use of a dual-emitter transistor at the output and by replacing both level-shifting diodes with transistors. In this way, large charging currents are supplied during the transition periods to speed up operation, while, during the steady state, the supply current is limited to a very small value by the large resistors used. Fan-in extension can be obtained with the l.p.d.t.μl. gate. The output stage can be used either with active pull-up to obtain maximum speed and fan-out or with resistive pull-up to perform the wired-OR function. These two modes of operation can be obtained simply by interconnecting the relevant output pins.

Complex elements

There are a number of c.c.s.l. complex-function elements already in an advanced state of development. With these, stage-by-stage system optimization will be further improved and the reduction of the number of packages in a system further simplified. A number of these functions are briefly described below.

A 2-bit full adder intended for use in parallel adders with serial carry will have a sum output available in both true and complementary form. The carry outputs are such as to allow the direct coupling of the two sections of the 2-bit adders. A 16-pin version will allow both true and complementary entry for 1 bit. Having decimal outputs *via* a d.t.μl. gate, allowing output ORing, a converter from 1-2-4-8 binary code to decimal is in development. Encapsulated in a 16-pin dual-in-line package, a 4-bit shift register will have provision for both serial and parallel entry with a gating input provided for the parallel entry; separate outputs are provided for each bit. A 14-pin version will also be available.

With a single asynchronous reset to clear all flipflops, inhibiting at the same time the clock input, a 1-2-4-8 decade counter with a typical speed of 16MHz is also in development. It will include four preset inputs per unit individual setting of each stage. This individual setting has been designed to avoid ripple-through of the counter during presetting. A divide-by-16 version of this counter will also be available.

Micromatrix—the future

As improving semiconductor-production techniques begin to meet systems designers' requirements for more complex integrated circuits, so the demand for custom-designed circuits increases. Owing to the multifunction capabilities of l.s.i. elements, the quantity required of each element can be low, even for relatively large-quantity users of integrated circuits. Integrated circuits have so far been offered either as standard products, or as custom devices for the user with large equipment production who was willing to pay the circuit-design costs. Micromatrix is a large-scale-intgeration technique, fully compatible within the c.c.s.l. concept, being developed by SGS-Fairchild to bridge the gap between these two alternatives. It is intended to satisfy the need for special complex circuits, even when the quantity required is relatively low, by accommodating the special circuit design at the last possible moment, thus ensuring short design time and minimizing chip size and testing, since these will finally determine the cost to the equipment manufacturer.

A Micromatrix is an array of cells all diffused in the same chip, each cell consisting of an isolated region containing components that can be interconnected to form fundamental logic functions such as gates, flipflops etc. Basic wafers are diffused by normal mass-production techniques and will be held in stock. The customer's special circuit design is incorporated during the final metallization process. This approach has the advantage not only of eliminating the design and engineering cost required for the diffusion mask, wafer processing and evaluation of a customer's specific circuit, but also of providing more thoroughly characterized devices with a large volume of data from which reliability predictions can be made. The number of basic array types can be quite large, varying according to the number of cells, speed and power required. Even within a specific class, arrays can be designed either for general-purpose logic or for a specific function, such as active memory; in the latter case, for example, the cell will be specially designed to perform the bistable functions. Micromatrix becomes practical only if a 2-layer metal-interconnexion technique is used; area-consuming diffusion crossovers in use up to now would make the concept useless.

Only three masking operations (first-lay metal, insulating-layer holes, and second-layer metal) are required to custom-connect each array. This approach is different from the test-and-connect or discretionary wiring approach, since no testing is done at the cell level. The elimination of pads for cell testing allows the use of the minimum possible chip size, ensuring a reasonable yield, and therefore lower costs. The Micromatrix interconnexion pattern will be designed on the basis of customer logic specification. The procedure will be similar to the layout of a conventional double-sided printed circuit. A systematic approach using a regularised grid of possible interconnexion paths will reduce to a minimum the time required to generate the artwork.

The first Micromatrix in development is an array made up of eight cells. It will be compatible with all the SGS-Fairchild c.c.s.l. family; this is very important since such complex circuits will always be used together with standard less-complex elements, such as gates, buffers, flipflops etc.

Precision temperature-controlled environments for ultrasonic fused-quartz delay lines

by **D. Howorth**, B.Sc. (Tech.), M.I.E.E., A.M.C.T., **C. R. Caine**, B.Sc., and **L. T. E. Ward**,
British Broadcasting Corporation Research Department, Tadworth, Surrey

This article describes the design and construction of an environment suitable for a 2·5ms ultrasonic delay line which is accurately controlled in temperature. It also comments on the design of such environments in general

(Voir page 731 pour le résumé en français: Zusammenfassung in deutscher Sprache auf Seite 732)

Ultrasonic fused-quartz delay lines having delays of the order of 2 or 3ms can be cascaded to give a delay of one television-field, obviously suitable for use in television applications. These ultrasonic delay lines, which are band-pass devices operating at carrier frequencies between 10 and 50MHz, have a considerable insertion loss[1]. This is caused partly by the inefficiency of the transducers which convert the input electrical signal into an acoustic wave, and *vice versa,* and partly by the losses in the fused-quartz transmission path; the latter can be considerably reduced by operating the delay line at a temperature in the region of 70°C. In addition to a reduction in insertion loss with increase in temperature, the delay is also reduced; this is because the elasticity and density of the fused quartz are changed in such a way as to increase the velocity of propagation of the acoustic wave, and this more than offsets any increase in the transmission-path length caused by expansion. The temperature coefficient of delay for fused quartz is approximately 75 parts/10^6 per degC, and, in order to achieve the stability of delay necessary for television applications, the operating temperature must be controlled to within close tolerance limits. In the British 625-line system, the field period is 20ms and the permissible tolerance on delay is $\pm$15ns (approximately 1/6th of a picture element); the required stability is therefore $\pm$0·75 parts/10^6, and in order to achieve this, the temperature must be maintained within a tolerance of $\pm$0·01 degC.

This article describes a temperature-controlled environment developed for use with a 2·5ms delay line*, eight of which are to be used to produce a delay of one field period of the British 625-line system. The development may be conveniently divided into three sections:

(i) the design of a uniform-temperature enclosure with the minimum of heat loss;

(ii) the design of a servocontrolled heating system which maintains a uniform temperature within the enclosure and compensates for the inevitable loss;

(iii) the design of an ancillary heating system to bring the delay line up to operating temperature as quickly as possible, together with protection circuits which ensure that the delay line cannot be destroyed by overheating in the case of a failure of either heating system.

* *The delay line in question is manufactured by MEL Equipment Co. Ltd and has the type number YL 2104/09.*

The design of a temperature-controlled environment for a 2·5ms ultrasonic delay line

Uniform-temperature enclosure with minimum heat loss

Enclosures with minimum heat loss consist basically of a double-walled container with a thermal-insulating material between the walls. The most effective form of enclosure is the simple vacuum flask, in which conduction is prevented by a vacuum between the walls and radiation is prevented by silvered surfaces. Unfortunately, this type of enclosure is impracticable for use with ultrasonic delay lines. The most suitable insulating material readily available is air, which has a thermal conductivity of 0·027kcalm/m^{2}hdegC; however, with air, heat loss occurs as a result of convection. In order to reduce the convection losses to a minimum, it is necessary to restrict the flow by introducing a cellular or fibrous material between the walls of the enclosure. The materials used for this purpose themselves introduce heat losses owing to their own thermal conductivity, and overall thermal conductivities of between 0·03 (kapok) and 0·035 (felt) are not uncommon. One excellent material for this purpose is expanded polystyrene, which has a thermal conductivity of approximately 0·029.

Having chosen the insulating material for the enclosure, the heat losses depend on

(i) the thickness of the insulating material, which is in turn dependent on the space available for the enclosure and the size of the delay line to be accommodated;

(ii) the operating temperature;

(iii) the ambient temperature.

The size of the 2·5ms delay line in its case, which provides the inner wall of the enclosure, is $11\frac{7}{8}\times9\times2\frac{1}{4}$in and the overall dimensions are not to exceed $16\frac{1}{4}\times13\frac{3}{8}\times6\frac{3}{8}$in; it therefore appears possible to enclose the delay line in expanded polystyrene 2in thick. The specified operating temperature of the delay line is 70°C, and, assuming an ambient temperature of 25°C, the heat loss would be approximately 5kcal/h. In order to compensate for this loss, it is necessary to fit a heater to the inner wall of the oven, dissipating approximately 6W (average). In order to avoid hot spots, which would lead to a nonuniform operating temperature of the delay line, the heater must dissipate heat uniformly over the whole of the surface area of the inner wall. The design of such a heater can be closely approximated to if the heaters are spread over a further wall of good heat conducting material, such as copper, which is isolated from the delay line by a layer of insulating material; this wall, of course, becomes the inner wall of the enclosure and reduces the thickness of the outer insulating material, so that the heat losses are increased.

Although an enclosure designed following these principles would combine minimum heat loss with a uniform operating temperature, the temperature stability would be affected by the range of ambient temperatures to which the enclosure might be subjected. An improvement in this respect can be effected by using a double enclosure which includes a wall maintained at an intermediate temperature. In order to achieve even better temperature stability, this argument can be extended *ad infinitum* and an engineering compromise must be reached which depends on the maximum size, cost and degree of stability acceptable.

A double enclosure designed for use with the 2·5ms delay line is shown in Fig. 1. The delay line, contained within an aluminium casting, is surrounded by a layer of expanded polystyrene 0·5in thick and is mounted in a copper container. Because expanded polystyrene is thermoplastic and will not bear the weight of the delay line at 70°C, four small Mycalex pillars 0·5in in diameter are used to support the delay line. Six heating elements are mounted on the outside of each of the larger sides of the copper container. The most suitable elements readily available proved to be those developed for use in a 450W domestic smoothing iron. These possess the technical advantages of being thin, causing minimum reduction of the thickness of the insulating material, and extremely reliable; in this particular enclosure, the maximum dissipation required is only 2·25W/element and the average dissipation is less than 1W.

The copper container is again surrounded by expanded polystyrene 0·5in thick and mounted within a second copper container on Mycalex pillars; this second container is also fitted with 12 heating elements, so that it can be maintained at a temperature of 60°C. The second copper container is surrounded by expanded polystyrene, in this case 1in thick, and is mounted on Mycalex pillars in a mild-steel container which forms part of the mounting chassis. It must be emphasized that the choice of dimensions used in this particular enclosure represents an engineering compromise and they may not represent the optimum dimensions which would give the best performance.

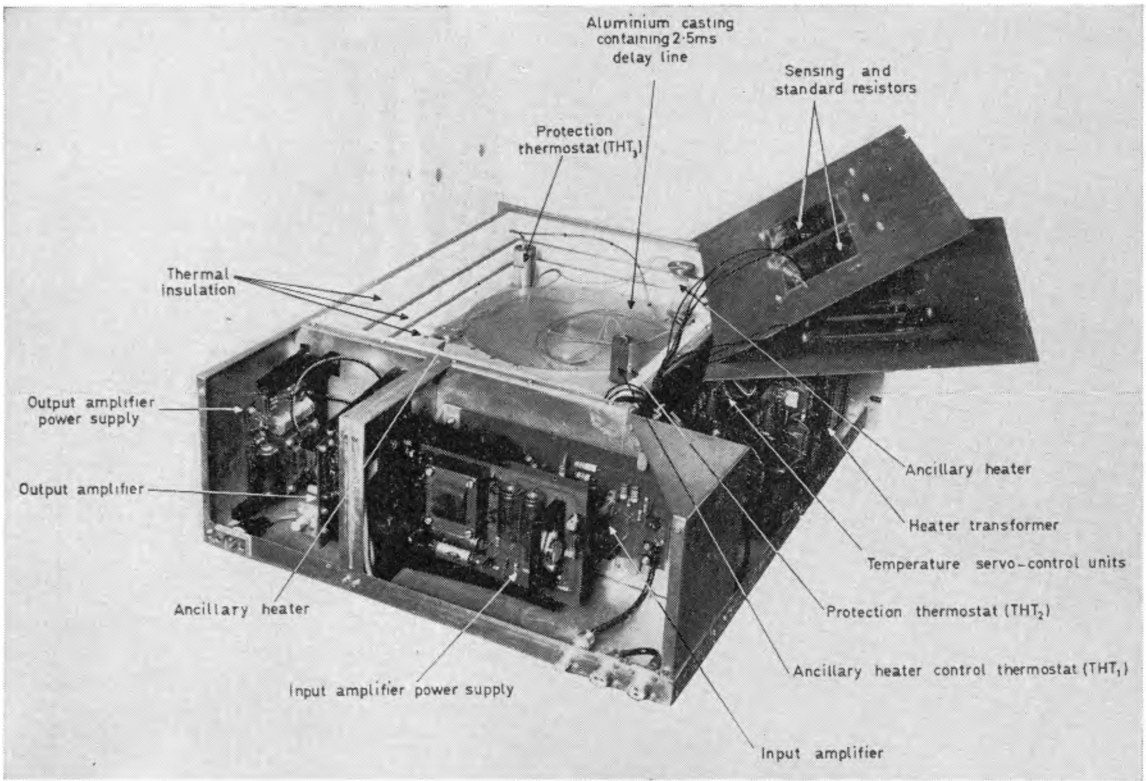

Fig. 1 2·5ms delay unit suitable for use in a television field delay

Temperature servocontrol system

The inner wall and the second wall of the enclosure are required to be stabilized at their respective operating temperatures to within a high degree of precision. In order to achieve this, two independent but similar servocontrols are provided. The temperature-servocontrol system is required to stabilize the chosen operating temperature of the 2·5ms delay line to within a tolerance of $\pm 0{\cdot}01$degC over long periods of time. In order to achieve this, it is obviously necessary to include temperature-sensitive devices inside the enclosure. Many types of temperature-sensitive device are available, such as mercury-contact thermometers and thermistors. However, in order to obtain good long-term stability and to measure the temperature over as large a surface area as possible, a temperature-sensitive resistor made of high-K nickel wire was chosen; this had a temperature coefficient of resistance of 0·005/degC, so that a change in temperature of ±0·01degC produced a change in resistance of ±0·005%.

The problem of servocontrol is principally that of providing a sufficiently sensitive resistance-measuring bridge to detect this small percentage change in resistance. An a.c. bridge was chosen for the purpose in preference to a d.c. bridge, because the small signals obtained near balance need to be considerably amplified in order to control the heater circuit, and a high-gain d.c. amplifier is liable to drift. Of the many types of a.c. resistance bridges available, the type using inductively coupled arms[2], as shown in Fig. 2, was chosen; such a bridge is relatively independent of small changes in the operating frequency and is relatively unaffected by stray capacitances across the standard and unknown resistors. Furthermore, the performance of the bridge depends principally on the turns ratio of the transformer, a factor which is unaffected by either temperature or time. The standard resistors needed for the bridge were wound using Ferry wire, which has a temperature coefficient of ±0·00002/degC. In order to avoid the small errors which might be introduced by changes in the ambient temperature of the standard resistors, these were placed inside the enclosure alongside the sensing resistors; thus, at one temperature, the resistances of both the sensing and the standard elements are equal and the output from the secondary of the bridge transformer is zero. In order to make the sensors and standards as flat and as large as possible, so as to obtain the average temperature over a large area, they were layer-wound on a 3in-square sheet of mica 0·01in thick. The sensing and standard resistors were mounted in pairs on the inside of the larger sides of each of the copper containers, immediately below the heating elements; in this way, the sawtooth of temperature which is caused by the time taken for heat to flow from the heater to the sensor is made as small as possible.

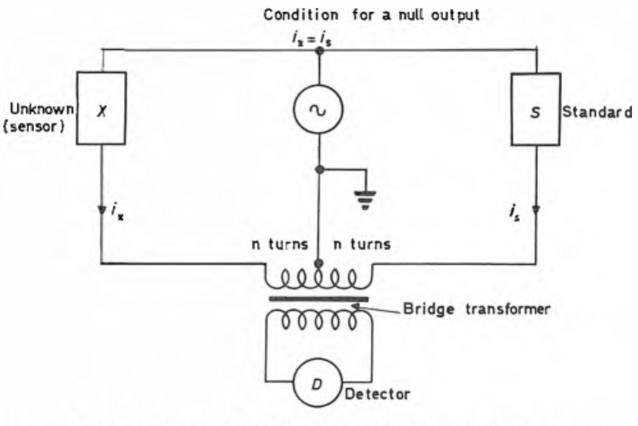

Fig. 2. Resistance bridge with inductive coupled arms

Fig. 3 shows the complete circuit diagram of the temperature servocontrol used with the 2·5ms delay line. The reference-signal input is a 5kHz sinewave having an amplitude of 10Vp-p; the use of such a frequency permits the transformers to be constructed on small ferrite pot-cores. Each standard resistor is 375Ω and, as two are used, this gives a total of 750Ω for the standard arm of the bridge. The sensing resistors are adjusted on test to equal the standards at the appropriate operating temperatures; these temperatures are 70°C in the case of the inner wall and 60°degC in the case of the second wall. The reference-signal input transformer T_3 has a number of small secondary windings which may be used to drive each side of the bridge with slightly different potentials. This causes the bridge to balance when the sensing and standard resistors are somewhat unequal and in this way the operating temperature can be adjusted over a range of ±5degC in 0·3degC steps. The output obtained from the secondary of the bridge transformer T_1 is approximately 0·3mVp-p for a change of temperature of 0·01degC. This is amplified to a level of 1Vp-p by a feedback amplifier (VT_1, VT_2 and VT_3) which has a gain of 70dB. An output, which differs only in its polarity, is obtained from the bridge irrespective of whether the temperature increases or decreases. In order to ensure that only a fall in temperature switches on the heating circuit, the output of the amplifier is applied to a phase-sensitive detector. The reference signal for this detector is obtained from the secondary of the auxiliary input transformer T_2 *via* a phase-shifting network. This is adjusted so that the rectifier provides negative-going halfcycles of the 5kHz reference signal if the temperature falls, and positive-going halfcycles if the temperature rises. The positive-going halfcycles have no effect on the circuit, but the negative-going halfcycles cause the amplifying transistor VT_4 to conduct. The positive-going halfcycles from the collector of this transistor VT_4 are applied to the gate of the thyristor rectifier TH_1 *via* an emitter follower VT_5, causing current to flow through the heating elements. This raises the temperature of the enclosure until the bridge again approaches balance, when the pulses applied to the gate of the thyristor fall to a level at which it ceases to conduct. In practice, owing to a time lag between the temperature of the heaters and the temperature of the sensors in the enclosure, the bridge passes through balance, so that small positive pulses appear at the output of the phase-sensitive detector. If this time lag is allowed to be sufficiently large, it is possible that the positive pulses will break through the amplifier (VT_4) and the emitter follower (VT_5), thus switching on the heaters and causing a thermal runaway; a similar effect can occur if the phase of the reference signal applied to the phase-sensitive detector is incorrect. Such maloperation may, of course, be avoided by a suitable protection circuit.

Ancillary-heating and protection circuits

With the type of temperature enclosure described in the previous two sections, the delay line reaches operating temperature in 8h, and the time taken to reach stability may be several days. This time can be considerably reduced if, initially, heat is applied directly to the delay line. Such a system is often described as a booster-heating system. Fig. 4 shows the circuit of the booster-heating arrangements for the 2·5ms delay line. Two 15W heaters are mounted in the aluminium casting which contains the delay line; when the relay A is energized, these are connected by A_2 in series across the supply, and heat the delay line directly. On switching on, the delay line is cold and the bimetallic strip THT_1, which is also mounted in the aluminium casting, is closed. Rectified current flows from the heater transformer through the thyristor of the temperature controller associated with the inner wall, and A is energized. The contacts of THT_1 are adjusted to open when the delay line reaches a temperature of 65°C; however, when this occurs A remains energized because of the hold-in contact A_1. The booster heaters in fact remain switched on until the temperature controller of the inner wall reaches balance. When this happens current flow through the thyristor ceases and A is de-energized. The booster heater is therefore switched off and cannot be

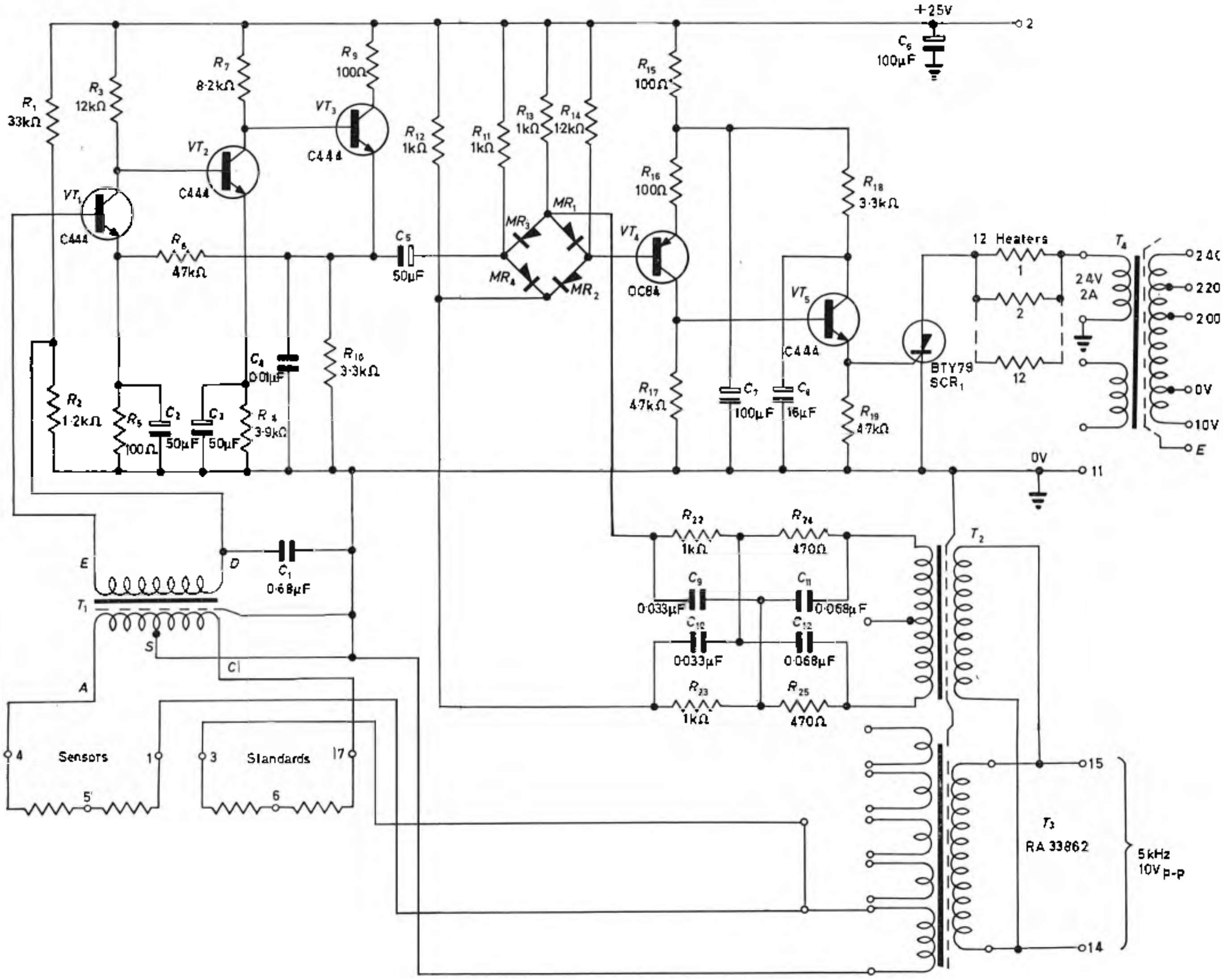

Fig. 3. Temperature servocontrol unit

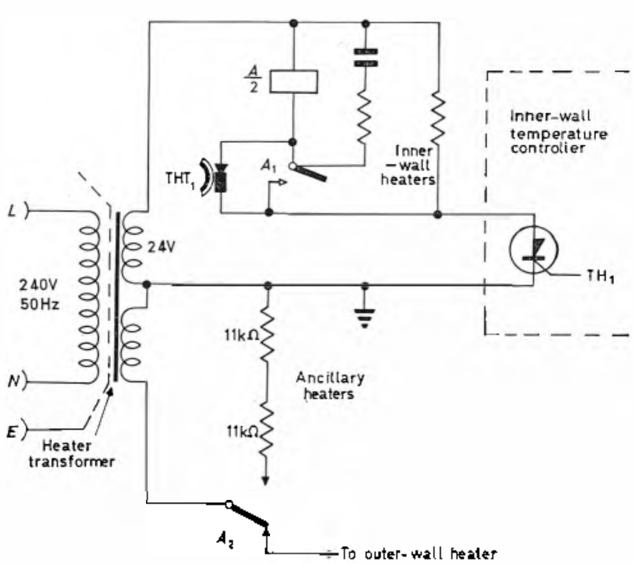

Fig. 4 Ancillary heating

reconnected until the delay line cools sufficiently for the contacts of THT_1 to reclose; this occurs at a temperature of 60°C. The dissipation of the booster heaters has been carefully chosen so that the delay line is brought up to its operating temperature at the same time as the inner wall of the enclosure.

In order to prevent the delay line being permanently damaged as a result of thermal runaway, it is necessary to include a protection device in the enclosure. The maximum temperature to which a delay line may be safely heated has not been determind; however, it is thought to be very little in excess of 100°C. The protection devices included in the 2·5ms delay line enclosure are two* bimetallic-strip thermostats connected in series with the main supply of the heater transformer, as shown in Fig. 5. These thermostats are mounted in the aluminium casting and their contacts open at a temperature of 75°C. The thermostat contacts close at a temperature of 65°C, so that, in the event of failure of the other control circuits, the delay-line temperature slowly cycles between 65 and 75°C.

* *Two are used rather than one in order to provide an additional safeguard.*

In order to warn the operator, the circuit is so arranged that when the mains supply is removed from the heater transformer a green indicator-lamp is extinguished and a red warning lamp is lit (Fig. 5).

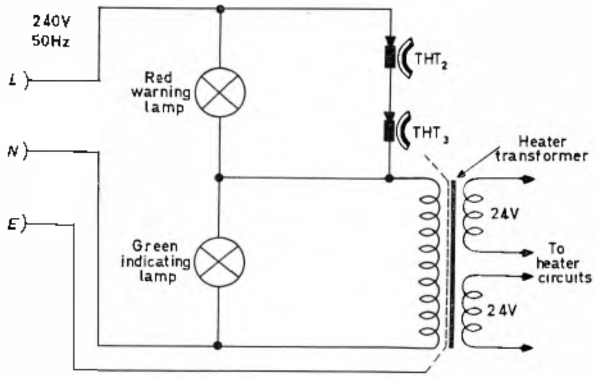

Fig. 5. Protection arrangements

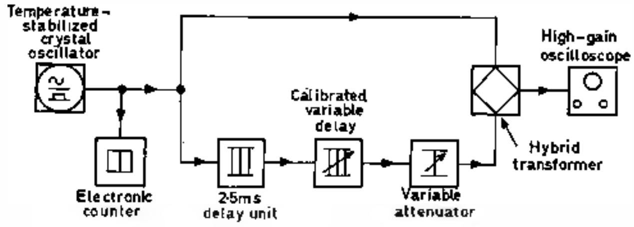

Fig. 6. Measurement of stability—method 1

change of delay which could be made by means of the variable delay was 0·5ns. The output of the hybrid transformer was displayed on a high-gain oscilloscope. By adjusting the calibrated variable delay and attenuator, the two inputs to the hybrid transformer were made equal and opposite, so that a null output was obtained. Any subsequent change in delay of the delay line which destroyed the balance could be compensated for by adjusting the calibrated variable delay. Measurements were carried out in this way after the temperature was known to have stabilized; after correction for changes in oscillator frequency, these indicated maximum changes of delay of about $\pm 0{\cdot}5$ns. These changes are equivalent to an accuracy of 2 parts/10^7, which is of the same order as the specified accuracy of the electronic counter used to measure the frequency of the oscillator. These measurements are therefore a good indication that the temperature stability is satisfactory, but no absolute conclusions may be drawn from them.

The second measurement of stability used is more directly equivalent to television. The block diagram of the circuit arrangement used is shown in Fig. 7. A 625-line sawtooth television waveform was generated by means of a crystal-controlled waveform generator and amplitude-modulated a 28MHz carrier; the line period of the waveform was checked by means of an electronic counter. The modulated carrier was fed to an electronic switch to which an operating pulse was applied so that ten television lines of the signal were fed into the delay line once per picture period (i.e. every 40ms). In the absence of the operating pulse, the switch was arranged to connect the output of the delay line back to its input, so that the ten television lines of signal were recirculated, giving an additional output every 2·5ms. A proportion of the output of the delay

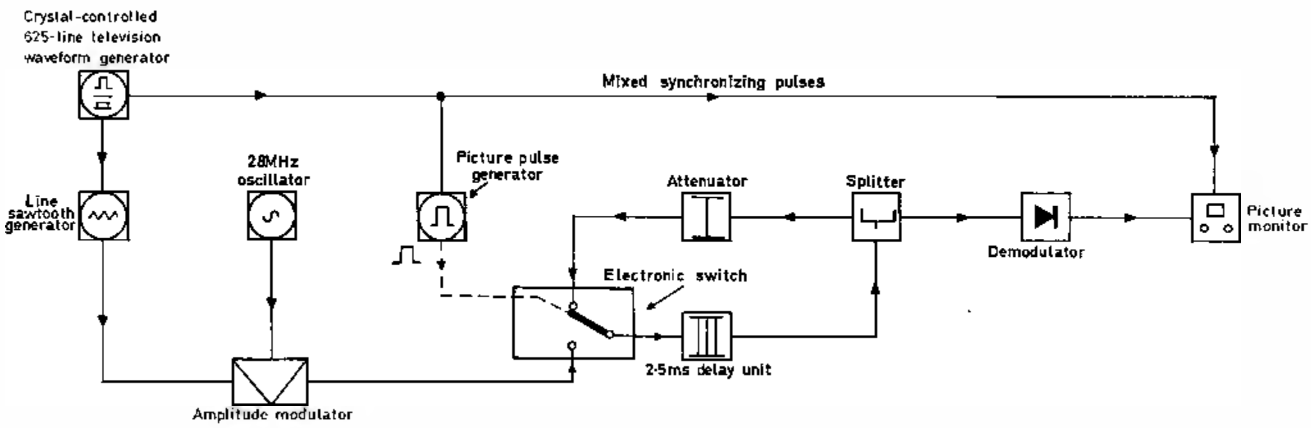

Fig. 7. Measurement of stability—method 2

Measurement of stability

The measurement of variations in temperature of about $\pm 0{\cdot}01$ degC is very difficult to carry out. Therefore, as the prime requirement for such temperature stability is to obtain a stable delay, measurements of delay stability were made. Two methods of measurement were used, the first of which is shown in block-diagram form in Fig. 6. A 28MHz sinewave was generated by means of a temperature-stabilized crystal-controlled oscillator whose frequency was monitored by means of an electronic counter. The sinewave was fed to the input terminals of a hybrid transformer along two paths; one direct and the other *via* the delay line. A variable attenuator and a calibrated variable delay were also included in the delay path. The minimum line was demodulated and displayed on an externally synchronised picture monitor. Two vertical lines were inscribed on the faceplate of the picture tube corresponding with the fast edge of the sawooth as delayed by 2·5ms and 20ms respectively. Over a period of four days, no perceptible change in the position of the fast edges of the sawteeth, relative to the inscribed lines, was observed. This indicated that the temperature stability of the delay is adequate for normal television applications.

REFERENCES

1 Brockelsby, C. F., Palfreeman, J., and Gibson, R. W.: *Ultrasonic delay lines* (Iliffe, 1963)
2 Glynne and Arvon: Bridges with inductively coupled ratio arms. Bulletin of Electrical Engineering Education No. 8, 69-73 (May 1952)

Time-amplitude and amplitude-time converters using linear ramps

(Part 2)

by **C. Riddle,** B.Sc., M.I.E.E., *Royal Armament Research and Development Establishment.*

Pulse generator with time intervals between the pulses proportional to the input voltage

The circuit of Fig. 6 can be modified so that it generates pulses at time intervals which are proportional to an input voltage. Fig. 14 shows a circuit derived from Fig. 6, but having two additional transistors which are used to limit the voltage excursion of *C* to a value equal to an input voltage *V*. This limited voltage swing is fed back to the first of two complementary transistors, to form a pulse generator, as in Fig. 6. Since the time intervals between pulses are proportional to the voltage excursions, they are also proportonal to the voltage *V*. The feedback voltage is limited in both positive and negative directions. Limiting in the positive direction is by feeding the output from the first HT101 through a 4·7kΩ resistor to the emitter of a second HT101, the base of which is preset at *V*. (The IN914 diode is inserted in series so that the resistor can swing freely in the negative direction, without being clamped by the reverse base-emitter voltage limit of the second HT101.) The junction of the 4·7kΩ resistor and the IN914 diode is taken to the base of a second C111 transistor, and the maximum positive excursion at this point is limited by the voltage *V* plus the turn-on voltages of the IN914 and the second HT101.

The negative terminal of the input voltage *V* is not connected directly to the −20V negative line, but to a slightly more positive potential derived from the network shown; the object of this is to compensate for any changes in turn-on voltage due to changes in ambient temperature. The 120/100Ω junction is at about 1·5V, derived from the 3·3V Zener voltage. This is reduced to about 0·3V at the negative input terminal, because of the voltage drop across the two IN914 diodes. Variations in voltage across these two diodes due to temperature changes are approximately equal and opposite to similar variations in the limiter circuit. This effect is not important when *V* is high, but for low *V*, the repetition frequency may be affected by large ambient changes unless some form of compensation is provided.

The feedback capacitor *C* is driven through the C111 emitter follower, and in the positive direction its excursion is therefore determined by the voltage *V*. In the negative direction, the excursion is limited by the voltage on the first HT101 collector in the cut-off condition and this is determined by the setting of the 100Ω zero potentiometer. By this means, the negative-to-positive excursion of *C* can be adjusted to be exactly equal to *V*. The remainder of the circuit is similar to Fig. 6, but some details are different. To ensure the shortest pulse length, the first C111 collector resistor is reduced to 220Ω and a capacitance-shunted 100Ω emitter resistor is inserted to ensure that the C111 does not overheat if oscillation should cease. As before, an IN914 diode is in series with the emitter, to avoid the reverse base-emitter maximum voltage limitation. Coupling between the C111 and first HT101 is by a 47kΩ resistor, shunted by 100pF to improve the waveshape. It is essential that the 100pF is discharged after each pulse before *C*; so that, at low values of *V*, the time interval between pulses is determined by *C*, and not by the discharge period of the 100pF capacitor. To ensure rapid discharge of the latter, an OA70 diode is connected across the base-emitter of the HT101. A 1MΩ base resistor ensures that the latter is always conducting

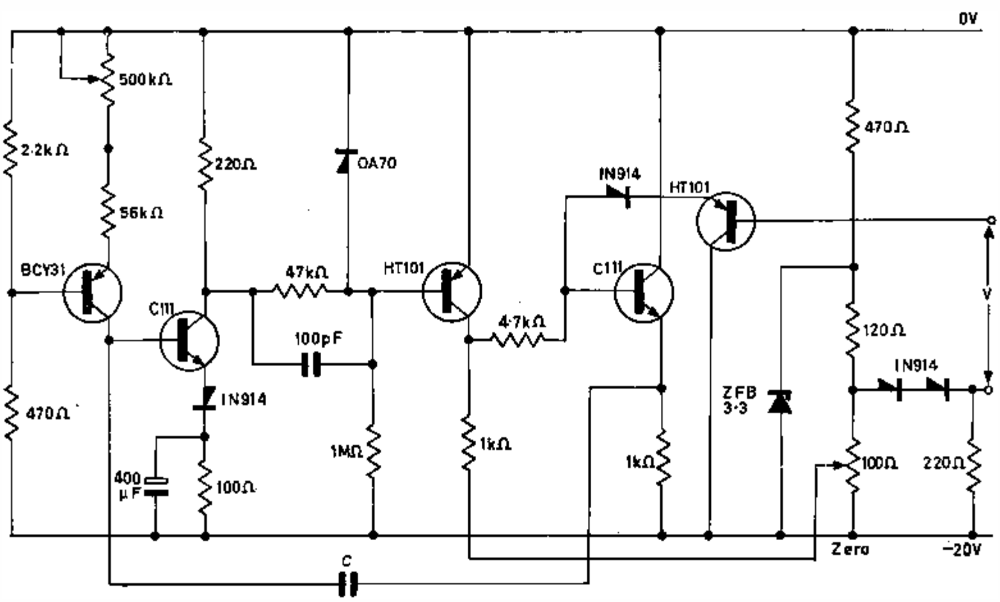

Fig. 14 Voltage time-interval generator

slightly, and that a pulse is initiated as soon as the C111 starts to conduct. (If this is omitted, the C111 collector must swing to the turn-on voltage of the HT101, which may be affected by ambient temperature variations).

A 500kΩ potentiometer is provided so that the discharge current can be varied from 30 to 300μA. Time intervals from 50μs upwards can be generated by decade switching of C, using 0·01μF as the lowest value. With 0·01μF, the range is from 50μs (V = 1·5V, discharge current = 300μA) to 5ms (V = 15V, discharge current = 30μA). The pulse length varies between 2 and 5μs. For larger values of capacitance, the times are increased *pro rata*. The zero setting can be a preset operation, and there is no change in the setting for different currents or capacitors.

With values of C lower than 0·01μF, there is some loss of charge on the capacitor in the switching-off process, i.e. the negative-going excursion on the base of the first C111 is a little less than that on the emitter of the second C111. The effect is more important than in the circuit of Fig. 6 because, for good linearity, the loss should be small compared with any excursion in the working range from about 1 to 15V. The effect can be compensated for to some extent by inserting a small resistor in series with the capacitor C. For instance, if a 150Ω resistor is used in series with a 1000pF capacitor, linear operation is restored for a discharge current of 30μA down to time interval of 50μs. If the current is increased to 300μA, some nonlinearity occurs, but this can again be corrected by adjusting the zero control. The graph in Fig. 15 shows that, provided that this special adjustment is made, linearity from 50 down to 5μs can be achieved.

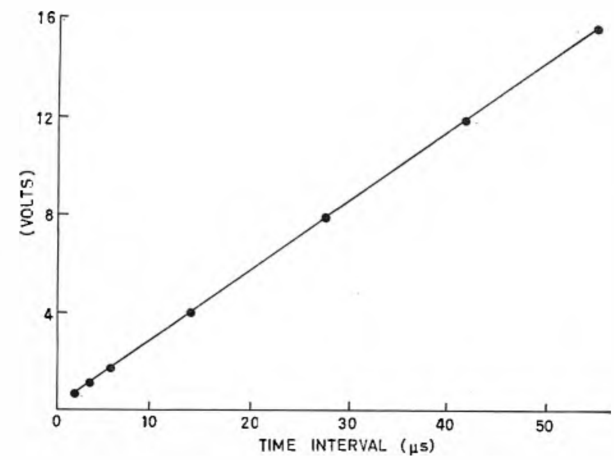

Fig. 15 Pulse generator with time intervals proportional to input voltage (C = 0·001μF, charging current = 295μA)

The circuit is self-starting under all conditions and is comparatively stable under ambient-temperature changes. Tests carried out for time intervals between 50μs and 50ms indicate that the maximum drift due to a 40 degC ambient-temperature rise is about 2%. This could probably be improved if a charging-current compensating circuit were incorporated.

Converter generating a voltage proportional to the time intervals between input pulses

A circuit of the type shown in Fig. 9 can be used to generate a voltage proportional to a time interval. Thus, if the time interval is represented by the leading and trailing edges of a positive pulse, C_3 in Fig. 9 will charge to a peak voltage proportional to the time interval, before resetting to zero on the trailing edge. A peak-reading

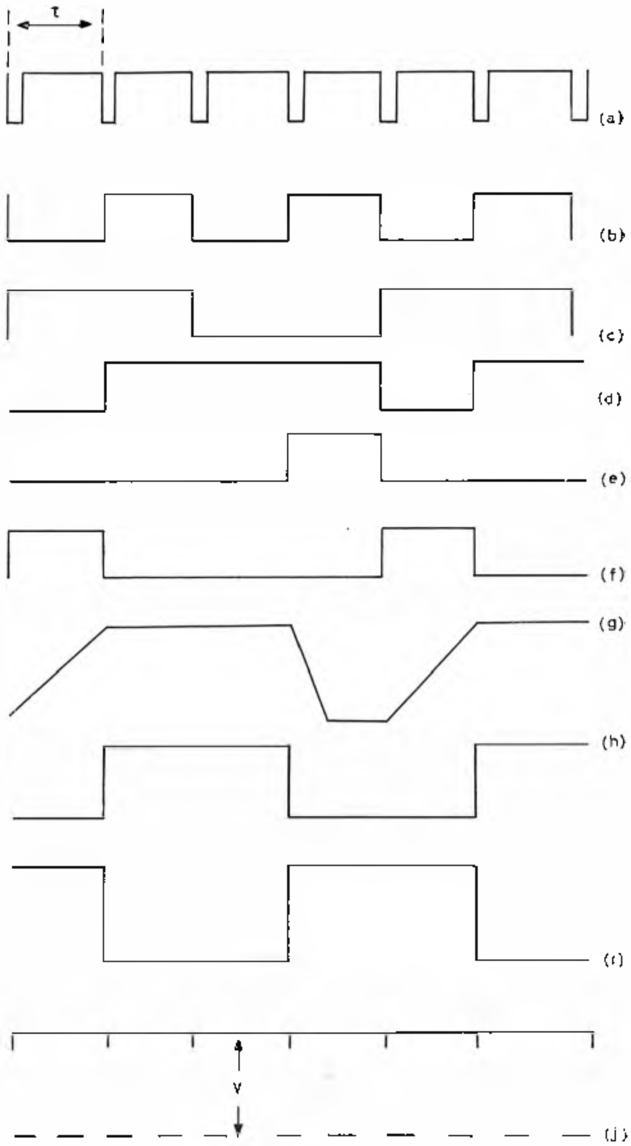

Fig. 16 Waveshapes for time-interval/voltage converter
(a) Negative-going pulse train
(b) Bistable flip-flop triggered by negative pulses from (a)
(c) Bistable flip-flop (output 1) triggered by negative pulse from (b)
(d) Waveshape (b) gated off by negative pulses from (c)
(e) Waveshape (b) gated off by positive pulse from (c)
(f) Waveshape (d) reversed in sign
(g) Positive-going ramp generated from (d) and reset from (e)
(h) Waveshape (g) gated off by positive pulses from (e) and (f)
(i) Complementary to (h), derived from another circuit initiated from (c) output 2
(j) Sum of (h) and (i) producing voltage V proportional to time interval t

voltmeter could be used to measure the voltage level. If there is a succession of pulses, this method involves integration techniques and a delay in the response. If an instant response is required, this can be achieved by employing switching and gating techniques. Fig. 16 illustrates the process and Fig. 17 shows the circuitry involved. The waveshapes in Fig. 16 are marked in Fig. 17.

The pulse train operates two identical bistable flip-flops in succession. The output from the first is gated by the output from the second in two complementary transistors, to produce the waveshapes (d) and (e) at the points indicated. Wave (d) operates the linear generator, which charges C linearly; on completion of the charge, the charging transistor is switched off but the capacitor retains its charge momentarily, because the shunt resistance at

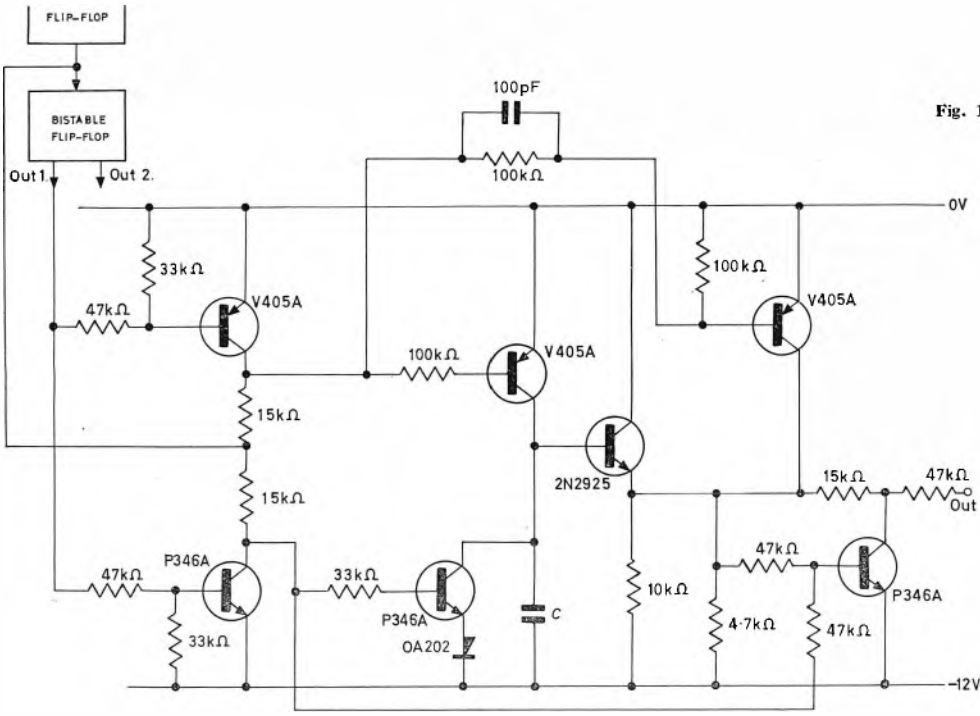

Fig. 17 Time-interval/voltage converter

this moment is very high. The next positive pulse at (c) discharges the capacitor. The discharge is about three times faster than the charge, because the 100kΩ base resistor in the charging circuit is three times larger than the 33kΩ base resistor in the discharge circuit. The capacitor is connected to the output gate *via* an emitter follower; a high gain transistor is used here to ensure that the shunt resistance across the capacitor is as high as possible. The output gate is gated off by the positive pulses on (e) and (f) to give a squarewave at (h) whose amplitude is proportional to the time interval between the input pulses.

A duplicate circuit switched by output 2 from the second bistable flip-flop can be used to generate the wave-train (i), which, when added to (h), gives an unbroken output at (j). Since the switching is not instantaneous, small spikes can be seen on the output waveform but these do not cause any significant error in the output reading. A diode is inserted in the emitter of the discharge transistor, so that the capacitor is discharged to a point slightly positive from ground. There is a similar voltage drop between the base and emitter of the 2N2925 emitter follower, so that the output is linear positive from ground, and there is no need for a separate zero adjustment. Fig. 18 is a graph showing the linearity of the device. Time intervals up to 200μs were used, using a 0·047μF charging capacitor. The output voltage was measured on the 10V range of an Avometer. The scale can be changed over a wide range by varying the charging capacitor and the charging current.

Fig. 19 is an oscillogram showing the waveshapes at (b), (g), and (j). The linear charge and discharge is displayed in (b), and the output (j) is a 3V positive output showing the small negative switching spikes.

Converter generating a voltage proportional to the repetition frequency of input pulses

A feature of all the devices mentioned is the rapid conversion from one mode to another, since integration techniques are not used. A frequency/voltage converter can be built using similar techniques, in a rather roundabout way. First, the converter of Fig. 17 is used to produce a voltage proportional to the time interval between pulses. This voltage is then used with the converter in Fig. 6 to generate pulses with a repetition frequency proportional to the input voltage. (This repetition frequency must be much higher than the original frequency). A second time-interval/voltage converter is now used to generate a voltage proportional to the time intervals between the pulses at the latter frequency. This voltage is proportional to the repetition frequency of the original pulse train. For decade switching, using a 10 : 1 linear scale, the derived frequency range must be at least twenty

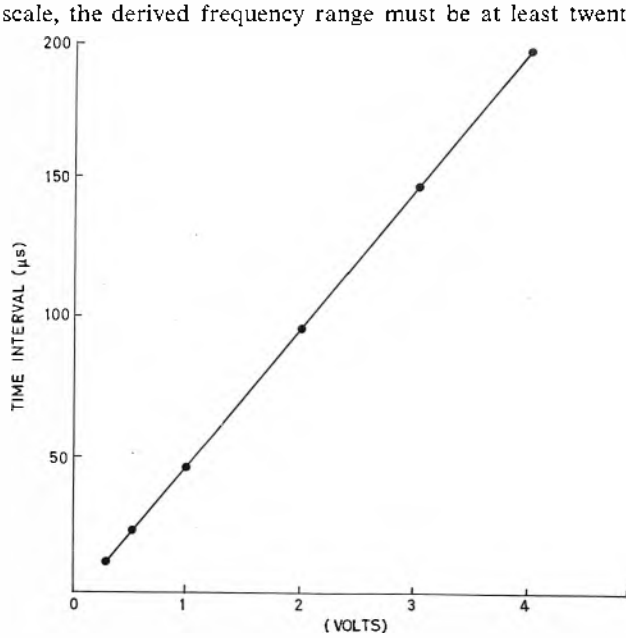

Fig. 18 Time-interval/voltage generator ($C = 0{\cdot}047\mu$F)

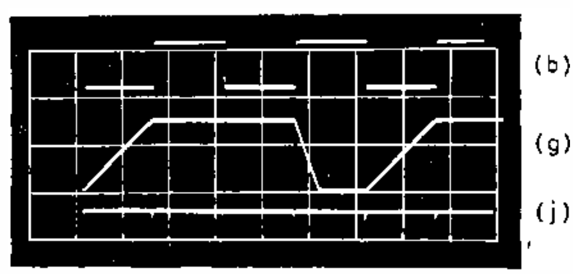

Fig. 19 Waveshapes (b), (g) and (j) of Fig. 16

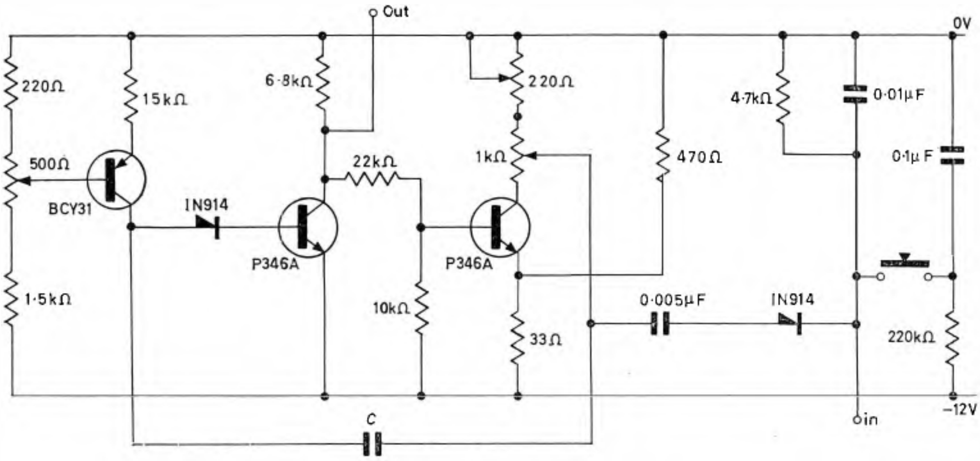

Fig. 20 Linear delay unit

times greater than the original frequency range, and this factor limits the maximum working frequency, with circuits similar to those described, to about 100kHz.

Linear delay unit

Fig. 20 shows a monostable flip-flop operated by negative input pulses. The circuit differs basically from the pulse generator of Fig. 6 in that two similar transistors are used, instead of the complementary pair. In the stable state the first P346A is fully conducting and the second is switched off. Switching is accomplished by applying a negative pulse from the 1N914 terminal to the base of the first P346A (via the capacitors and the diodes). Alternatively, a manual pressbutton can be used, in which the negatively charged 0·1μF is discharged into the 0·01μF capacitor. The diode is inserted to reduce the change of multiple triggering due to switch bounce. When the circuit is switched, the first transistor is switched fully off and the second fully on. The capacitor C is driven negative and is discharged by the BCY31 constant-current generator. The main condition for stability is that the second P346A must be nonconducting in the stable period. This is accomplished by ensuring that the first transistor is bottomed, and then connecting its collector to the following base by a voltage divider, and at the same time providing a small positive bias for the second P346A. Coupling between the second and first P346A is by a capacitor C taken from the midpoint of the collector potentiometer, as shown. The overall gain is such that switching occurs when the tapping point is at 1/10th of the full collector swing. The excursion of the capacitor C can therefore vary over a 10:1 range, and hence the switching time also alters by this amount. A preset 220Ω potentiometer allows the range to be set to any predetermined value between, say, 10:1 and 20:1. This allows decade switching to be accomplished with some overlap if necessary.

The switching time depends on C, the voltage excursion and the discharging current supplied by the BCY31. If the latter is too small, the circuit will became unstable, and will start to oscillate. If too large, it will become difficult to switch. In Fig. 20, a moderate variation in current is provided by the 500Ω potentiometer. This enables the delay time for any given capacitor to be set to the nearest convenient whole number. For instance, using a 1μF capacitor, the 220Ω potentiometer should first be set to give a range of, say, 10:1. The 500Ω potentiometer could then be adjusted so that the maximum delay is 100ms, with the corresponding minimum delay of 10ms. Decade switching of C may then be employed to provide delays down to 1μs ($C = 100$pF). If delays longer than 100ms are required, electrolytic capacitors up to 1000μF, giving delays of over 1min, can be used. The tolerances on most electrolytic capacitors are fairly wide, however, and the time delays obtained will vary accordingly.

Temperature effects

All of the circuits are subject, to a greater or lesser extent, to thermal-drift effects. Drift occurs owing to variations in stabilised-voltage levels, discharging currents, transistor base-emitter voltages, diode turnover voltages etc. A stabilised-voltage rail can be maintained constant and free from thermal drift by using a zero-coefficient Zener diode as the reference voltage. The discharging current in a transistor can be kept fairly constant, as in the BCY31 of Fig. 14, by using the highest possible base voltage, with a fairly large emitter resistor. Changes in base-emitter voltage then have a relatively small effect. If this is not possible, a complementary transistor can be used to drive the discharging transistor. Variations in the base-emitter voltages then tend to cancel out. Alternatively, a diode can be used in the zero balance, as in the circuit of Fig. 6, to provide a similar effect. Variations in turnover voltages of diodes can sometimes be nullified by adding opposite-effect diodes, as in Fig. 14.

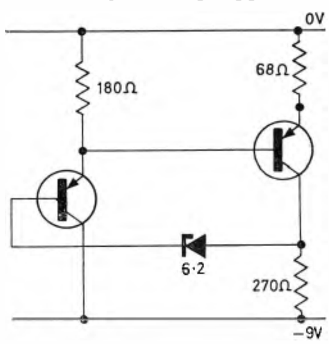

Fig. 21 Constant-current device compensated for ambient temperature changes

Also Zener diodes with positive or negative coefficients can be used, as appropriate. It may sometimes be possible, in a complex circuit to apply a simple remedy to several sources of drift; for instance, the circuit in Fig. 21 is a balancing circuit which has been used to compensate for several different additive effects in other parts of the equipment. The first transistor is a constant-current device which has been overstabilised by the second transistor. In Fig. 21 the second stage has a gain of 4, but, by suitable adjustment of the 270Ω and 68Ω resistors, any degree of over- or undercompensation can be provided.

LETTERS TO THE EDITOR

(We do not hold ourselves responsible for the opinions of our correspondents)

Zener-diode alternatives

SIR,—In looking for viable alternatives to Zener diodes at very-low-voltage levels, an interesting feature of the tunnel-diode characteristic has been investigated. When such diodes are used with currents which have exceeded the peak current, the characteristic resembles that of a normal forward-biased *p-n* junction. The typical voltage drop of 500mV at a current equal to the peak current of a germanium tunnel diode is, however, much nearer to that expected for a conventional silicon diode. The change in this voltage with temperature is much less than for other diodes, ranging from about $-1{\cdot}25$mV/degC at V_{fp} (forward voltage at current equal to peak current I_p) down to $-1{\cdot}1$mV/degC at currents of $2I_p$. This compares with drifts of approximately -2mV/degC for silicon diodes of normal construction.

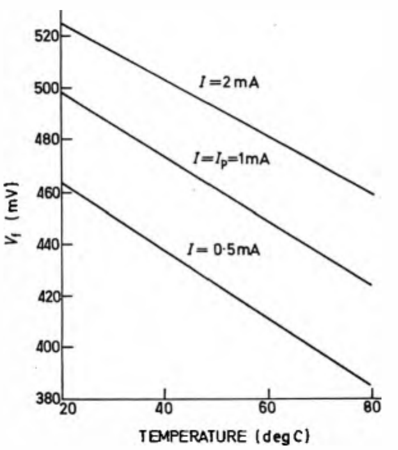

Fig. 1 Graph of temperature variation of voltage drop across germanium tunnel diode in forward conduction for various currents (diode type GE IN3712)

Thus operating the tunnel diode from a source that provides sufficient current to trigger it gives a voltage source of about ½V with moderately low slope resistance and a temperature drift of $-0{\cdot}2$% per degC. The falling cost of germanium tunnel diodes means that they can be considered even for such unorthodox uses. A further improvement follows from using two such diodes in series to bias the base of an emitter follower (either silicon or germanium). The diode and transistor V_{be} drifts are comparable at about -2mV/degC, leaving the emitter load with a voltage which might be held to $\pm 0{\cdot}01$% per degC with careful selection. Alternatively, one might make use of the resulting constancy of collector current, since this is only slightly less than the stabilized emitter current; i.e. a low-voltage constant-current source.

P. WILLIAMS
W. P. APPLETON
Paisley College of Technology
Paisley, Renfrewshire

Negative-resistance transistorized oscillator

SIR,—The three essential parts of any oscillator circuit are a power source, a means of storing energy and an amplifier or a dynamic negative-resistance element. If the means of storing energy is an *LC* circuit, it is not difficult to determine how these three parts function in producing oscillations. The *LC* circuit has a natural oscillation frequency given by the relation $f_n = 1/2\pi\sqrt{(LC)}$, at which the energy stored in the circuit is transferred back and forth between L and C. However, resistive losses in the circuit absorb some of this circulating energy, and the oscillations of current and voltage in the *LC* circuit are damped out. The role of the amplifier or the dynamic negative-resistance element is therefore to release energy from the power source to the *LC* network, to make up for these energy losses. The mechanism by which energy is generally released to the *LC* tank circuit of an oscillator is through a periodic supply of current in the correct phase to make up for the energy losses during each cycle. In another case (Fig. 2) a network comprising active elements provides the dynamic negative resistance or conductance across the pair of terminals *AB*, across which an *LC* tank circuit, if connected, produces oscillations under proper conditions.

A bistable switching circuit exhibits an unstable negative-resistance region between the two stable states[1,2]. As a 2-terminal negative-resistance element, this circuit is convenient and quite suitable for constructing an oscillator on the above principle. The circuit diagram of the oscillator is shown in Fig. 3. A typical composite curve of this bistable circuit is also shown (Fig. 4). It has three distinct regions: region 1, where the transistor VT_1 is cut off and VT_2 is active; region 2, where both VT_1 and VT_2 are active, i.e. the transition period; and region 3, where VT_1 is active and VT_2 is cut off. As the transistors VT_1 and VT_2 switch alternately from conduction to nonconduction and *vice versa*, they operate through the negative-resistance region, i.e. region 2, twice in each cycle. During this period, energy is released to the *LC* tank circuit from the power source, to compensate for the inherent resistive losses. A circuit of this type has been constructed to produce pure sinusoidal waves. The frequency of this type of oscillator is very nearly given by the classical formula mentioned above, and the distortion and frequency drift have been found to be negligible. The amplitude of the output can be varied by the adjustment of R_4.

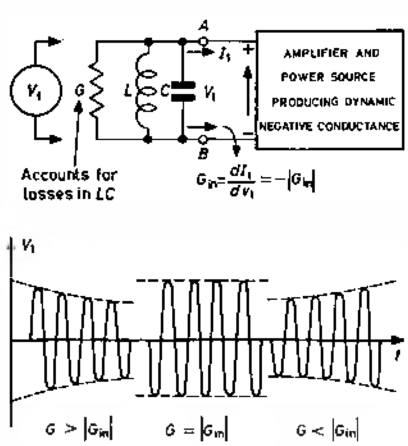

Fig. 2 Use of negative dynamic conductance to account for circuit losses

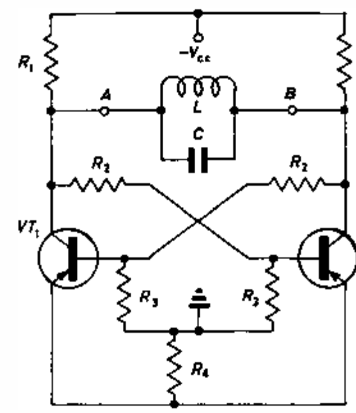

Fig. 3 Circuit of the oscillator

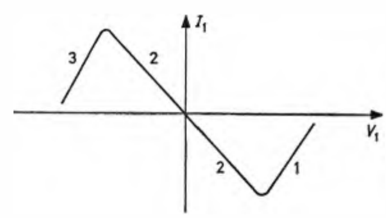

Fig. 4 Characteristic between terminals *A* and *B*

P. E. SANKARANARAYANAN
National Aeronautical Laboratory
Bangalore, India

REFERENCES

1 HULL, J. E.: *A flip-flop circuit using saturated transistors.* Texas Instruments Application Report (Dec. 1958)

2 GODDEN, A. K., and COOKES, T.: A negative-resistance computing element, *Electronic Engng.*, *35*, 751 (1963)

Binary-to-decimal converter

Sir,—My article on this subject (October 1966) appears to have aroused a certain amount of comment (March, July and October 1967) and I would like to reply to some of the points which have been mentioned. Most of the interest seems to have centred on the addition of the filler 3 immediately before a shift. This is largely a function of the particular code in which the *bcd* number is obtained. It is just as easy to devise a converter which operates in any one of a number of other codes, particularly if only one of the code weightings is odd. For example, 2421 *BCD* can be obtained from binary code as shown below.

states before shifting $Q\ R\ S\ T$	states after shifting $P\ Q\ R\ S$	change function
0 0 0 0	0 0 0 0	0
0 0 0 1	0 0 0 1	0
0 0 1 0	0 0 1 0	0
0 0 1 1	0 0 1 1	0
0 1 0 0	0 1 1 1	+3
0 1 0 1	1 0 0 0	+3
0 1 1 0	1 0 0 1	+3
0 1 1 1	1 0 1 0	+3
1 1 1 0	1 0 1 1	−1
1 1 1 1	1 1 1 1	0

The states 1000-1101 do not occur. The following example, in which binary 98 is converted into 2421 *BCD*, illustrates the method.

```
    P Q R S T
              1 1 0 0 0 1 0
            1 1 0 0 0 1 0
          1 1 0 0 0 1 0
        1 1 0 0 0 1 0
    1 0 0 1 0 0 1 0
  1 0 0 1 0 0 1 0
1 0 0 1 1 1 1 0
1 1 1 1 1 1 0
 (9)     (8)
```

It was suggested by Mr. Raven that this principle had been described by Couler. Couler's converter certainly had some points of similarity, but he used logical networks to inhibit selectively the clock pulses to the flipflops, rather than to gate the J and K inputs of JK flipflops operated from a common clock line. Further, he did not state that the method could be used for division by any other radix than 10, nor for any other code than 8421 *BCD*. I would like to take this opportunity of thanking my several correspondants.

K. J. Dean
The College of Technology
Letchworth, Hertfordshire

Binary-quinary decade counter

Sir,—In several published papers[1,2,3] there are attempts to make cost comparisons between various decade counters. While one of these[3] takes into account the costs of transistors, diodes (including the differences in price of counting, decoding and reset diodes), resistors and capacitors, the others count only the active devices. The first way is very exact, but it is very difficult and time-consuming, especially if one has to compare many different decades. The other way, which only counts the number of active devices, may give very wrong comparisons, as diodes are not considered, and some designs using a small number of active devices need many diodes, obviously increasing the cost of the decade (ring counters or decoding matrix).

TABLE 1

Device	T.E. Number	Symbol
Transistor	1·00	T
Diode	0·25	D
Neon bulb	0·50	N
Photoresistor	1·25	P
Tunnel diode	3·00	E
Thyristor	1·50	SCR
S.C.S.	2·50	SCS

TABLE 2
Counting-decade comparison by t.e.

Counting Decade	Used Devices	T.E.
Binary	$18T+52D$	31·00
Decimal	$30T+\ 1D$	30·25
Bi-quinary	$24T+\ 6D$	25·50

It seems that the method proposed here may be used for easy cost comparisons of the counting decades. For this, a t.e. (transistor equivalent) number is proposed for every semiconductor device (including diodes and neon bulbs). The t.e. number represents the relative costs of components and assembly of the circuit, including all resistors and capacitors; the reference is a circuit with one transistor, for which t.e. = 1. For other semiconductor devices, t.e. numbers may be assumed as given in Table 1.

Using these t.e. numbers, Table 2 gives the cost comparison by t.e. numbers for binary, decimal and bi-quinary decades, which includes counting, decoding and indicating (tube-driving) stages. These decades are described in a recent paper[1]. As seen from Table 2, and from the mentioned papers[1,3], the bi-quinary decade should be more economical than other decades. But the counting decades used in electronic counters and similar instruments (digital frequency meters, digital voltmeters etc.) include, apart from counter, decoder and indicating (tube driving) stages, two more stages: memory and gate circuits (for transfer from the counter to storage stage). In these cases, the t.e. numbers for decades including storage, will be as given in Table 3. For example, a binary decade has $8T + 13D$ in the counter stage, $8D$ in the gates, $8T$ in the memory, $30D$ in the decoder and $10T$ in the indicating stage. From this, it is evident that the through bi-quinary decade is not the most economical decade, when the decade includes memory.

TABLE 3
Counting-decades (including memory) compared by t.e.

Counting Decade	Used Devices	T.E.
Binary	$26T+51D$	38·75
Decimal	$50T+21D$	55·25
Bi-quinary	$36T+28D$	43·00

Present-day counting decades with memories use many ways of minimizing the t.e. number:

- Circuits with various components other than diodes and transistors
- Different codes in some stages (for example binary code in the counter, and bi-quinary in the indicating stage)
- Different arrangement of successive stages (a commonly used arrangement is in the order: counter, gates, memory, decoder, indicating stage, tube; but other arrangements are also possible, for example: counter, decoder, gates, memory, indicating stage, tube).

By such ways, some present-day counting decades with memory have the t.e. numbers given in Table 4, which are lower than in Table 3.

TABLE 4 **T.E. numbers for counting decades with memory in some counters**

Manufacturer	Type	Devices Used	TE
Hewlett-Packard	5245L	$8T+13D+8N+18P$	37·75
Marconi	TF2401	$34T+19D$	38·75
Beckman	6144	$22T+13D+15N+7P$	41·50
Beckman	6020	$21T+21D$	26·25
Systron Donner	1037	$12T+20D+5SCS$	29·50
CMC	600A	$15T+34D+10N$	28·50
CMC	603A	$12T+30D+5SCS$	32·00

By combining various methods of minimization of t.e. numbers, even smaller t.e. numbers can be obtained. Such a counting decade with storage, which has t.e. = 22·75, will be the subject of a future paper.

Dragan Pantic
Electronic Industry Nis
M. Bondzulica br.1
Belgrade, Yugoslavia

REFERENCES

1 Ridler, P.: Binary-quinary decade counter (letters to the Editor), *Electronic Engng.*, 39, 517 (Aug. 1967)
2 Parshad, R., and Suri, S. P.: A binary-quinary decade counter using resistance logic, *Electronic Engng.*, 38, 800 (Dec. 1966)
3 Shepherd, B.: Economy and reliability in nucleonic instrument design, *Electronic Engng.*, 39, 100 (Feb. 1967)

NEW BOOKS

Communication system engineering handbook

Edited by D. H. Hamsher. pp. 972. McGraw-Hill. 1967. Price £11 8s.

Here is a *magnus opus* of 972 pages, compliled by no less than 34 contributors and apparently containing everything on the subject including the proverbial kitchen sink. The material ranges from speech characteristics, communication theory and telephone-switching methods, to wire and cable installation practices, administration for communication systems and cost-study methods, to name but a few of the 25 chapters. Some of the illustrations are hardly necessary: for example, the photograph of a 1927 telephone or the diagram of a telephone plug and cord. As the title suggests, this is a handbook for the benefit of systems engineers or graduate students already acquainted with the basic principles of communications. Apart from the chapter on communication theory, the book is virtually devoid of mathematics: for example, fundamental equations on propagation, aerials and modulation methods are quoted without derivation, though adequate references are supplied for the reader who wishes to check their validity.

It is to be expected that the quality of the material will vary considerably in a book written by so many contributors, but, fortunately, the sections of low standard are in the minority; therefore it is, perhaps, more constructive to detail some of the chapters of particularly high standard: namely, address-communication systems, power-line-carrier systems and radiofrequency allocation and assignment, the latter providing a wealth of information in a readable form. In spite of the vastness of the subject matter, there are some serious omissions, such as p.c.m. systems (there is only a brief 3-page description of the principle of modulation), satellite systems (although there is a comprehensive section on ground-to-ground radio-relay communication), and frequency synthesis. In short, the book provides a competent account of well established techniques, and, with this qualification in mind, the chapters on telegraph and telephone switching methods are also to be recommended. In conclusion, it can be said that any systems engineer will undoubtedly find some illuminating and interesting facts in this handbook, but it is unlikely to provide him with much information on the design of future communication systems.

J. A. BETTS

Advances in microwaves: Vol. 2

Edited by L. Young. pp. 418. Academic Press Inc. 1967. Price £6 16s.

This serial publication contains critical reviews covering a wide range of topics of interest to the microwave engineer and physicist. The contributions reflect the most significant contemporary progress in microwaves and are written by experts who have played a major role in the development of the specific subject being covered. Volume 2, with 259 illustrations and 329 references, contains six chapters, of which four are concerned with recent developments in microwave solid-state devices and circuits. There has been much activity in this area in recent years, and these chapters are particularly timely. They give comprehensive descriptions of tunnel-diode parameters, oscillators, amplifiers and frequency converters (by F. Sterzer, RCA), microwave solid-state sources, including transistors, harmonic generators and tunnel, avalanche-transit-time and Gunn diodes (by B. C. De Loach, Bell Telephone Laboratories) and cooled-varactor parametric amplifiers (by M. Uenohara, Bell Telephone Laboratories), and discuss the principles of design and analysis of varactor harmonic generators (by J. O. Scanlan, University of Leeds). The last two chapters are concerned with diplexers and multipliers (by G. L. Matthaei and E. G. Cristal, Stanford Research Institute) and with the numerical solution of TEM-mode transmission-line problems (H. E. Green, Weapons Research Establishment, Salisbury, Australia) both of which are important not only for microwave solid-state circuits but for many other microwave applications as well. Articles already planned for future volumes include those on high-power millimetre-wave sources, the Gunn effect, millimetre-wave astronomy, crossed-field amplifiers, precision coaxial connectors and a variety of topics concerned with aerials, transmission lines and microwave components. New microwave techniques and devices are being developed at such a rate that it is hard to keep up with so much knowledge. It is hoped that Advances in Microwaves will document at least the most important advances and will keep the reader abreast of new developments by means of these comprehensive and authoritative articles. The series is invaluable to all scientists and engineers working directly with microwaves as well as to those in related fields who require a good general review of the particular topic described.

F. A. BENSON

The electrical properties and applications of thin films

Edited by R. A. Coombe. pp. 154. Pitman. 1967. Price £1 5s.

This book is largely based on the proceedings of a symposium held at the Woolwich Polytechnic, and purports to provide for the nonspecialist engineer a useful introduction to the scope and potentialities of thin-film devices. The book is divided into seven quite distinct chapters by seven authors drawn from industry, government establishments and educational institutes. After an introductory chapter which briefly reviews the basic features of thin films, preparation techniques etc., we move straight into the realm of ferromagnetic thin films—a rather specialised subject clearly and concisely treated. This is followed by a chapter on superconducting thin films—a subject of comparatively restricted interest, nonetheless treated authoritatively. The fourth chapter reviews the now familiar resistive thin film and quotes numerous charts and tables from previously published material concerning the various parameters of these films. Dielectric thin films are then treated rather briefly in chap. 5; and chap. 6 moves into the forward-looking field of semiconducting thin films. After an initial discussion of the physical properties of semiconducting thin films, the author examines the thin film transistor, but this is deflected into a discussion of m.o.s. devices which, although relying on a thin dielectric film for the gate action, are made by the normal planar processes used throughout the semiconductor industry and cannot be considered true thin-film devices in the accepted sense of the word. Finally, this chapter examines other semiconductor properties of thin films such as the Hall effect and photoemission. The final chapter describes in some detail the design and manufacture of thin-film circuits and is liberally illustrated. It is difficult to resist comparing this book with a previous volume, also by several authors, covering very similar ground, which went into considerably greater depth than the present volume. This book appears on the whole to be rather superficial, and as acknowledged by the authors, draws very liberally on previously published material. Intended, as it is claimed, for electronic engineers rather than solid-state physicists, it would appear to be attempting to cover too many separate areas of activities, and will not adequately satisfy an inquisitive mind, although ample references are, in fact, given for further reading.

S. FORTE

Gas lasers

By C. G. B. Garrett. pp. 144. McGraw-Hill. 1967. Price £4 8s. 6d.

This book is a good, though naturally somewhat specialized, introduction to the important topic of gas lasers. It not only deals with the physical aspects of the problem, but also discusses at some length the technology and design of gas lasers. Since the author is employed by Bell Telephone Laboratories, it is not surprising that the information provided is both accurate and up to date. After a brief section dealing with the history of the subject, he opens, appropriately enough, with a description of various systems of spectroscopic notation (Paschen, Russell-Saunders, Racah), a topic which is important, though tedious, from the point of view of an engineer. This is followed by discussion of such topics as the optical properties of various media, optical cavities and the associated mode distributions, means for establishing an inverted population in gases and a brief description of specific systems in the categories of noble gas, ion and molecular gas lasers. There is then a discussion of the right choice of materials and various other problems associated with the design of mirrors, cavities, external excitation sources and other accessories. Interesting features of the laser output, including amplitude and frequency stability, noise, mode competition and Q-switching are discussed in the last chapter. It is only right to say that the reader is expected to have acquired familiarity with the problems of physical optics. This is not surprising, since the book forms a new and useful contribution to the Advanced Physics Monograph series. It is somewhat odd that the author uses a nonrationalized system of units, possibly in an effort to placate the odd devotee of c.g.s., but fortunately this has little effect on the text.

P. A. LINDSAY

Music, physics and engineering

By H. F. Olson. pp. 460. Constable and Co. Ltd. Price £1 2s.

This book is a condensation of Dr. Olson's previous publications, plus additional material on recent developments. It appears in paperback form, a new departure which now has an extensive following in the United States for popular technical works. The object is to keep the price down, which it certainly does. The principal difficulty with encyclopaedic works is to find the type of reader at whom they are directed. As must follow, some of the subject matter is too condensed to inform the tiro, and insufficient for the knowledgable; perhaps the publishers' category 'enthusiasts in general' is the most suitable. Although a good deal of the text concerns music, it is clear that the author himself is not a musician, and not all will agree with some of his definitions and positive statements about subjective matters. For instance, few musicians would take kindly to the claim that the text 'helps conductors to position their orchestras'. However, despite the foregoing and a good deal of repetition, the book is extremely interesting and brings together most of Dr. Olson's long experience in electroacoustics together with extracts from the work of the principal American investigators into sound and hearing, and, of course, Rayleigh. In particular, the sections on musical scales, resonators, radiators and characteristics of musical instruments are excellent. Since RCA is one of the leading recording companies, the sections on stereophony and reproduction in general, which include the acoustics of rooms and studios, are very well presented. The section on electronic music is restricted and none of the work of the continental investigators is mentioned. This book is excellent value and a fascinating addition to the bookshelf; it is not a textbook but a resumé of current practice, to be read again and again, and in factual matters it bears the stamp of Dr. Olson's acknowledged authority.

A. DOUGLAS

Der Einfluss von Hochfrequenzüberlagerungen bei Stossspannungen auf das Durchschlagverhalten von Luft unter Atmosphärendruck bei verschiedenen Elektrodenanordnungen

By G. Sonnenschein. pp. 35. Westdeutscher Verlag GmbH. 1967. Price DM22

For many years, the breakdown behaviour of air between spark gaps with an applied direct, impulse, or alternating high voltage has been well known. The electrical stability is modified if a high-frequency voltage is superimposed on the impulse voltage, and the behaviour under these conditions has not received so much attention. In this monograph, an account is given of experiments to investigate this effect. The production and measurement of the impulse voltage with a superimposed high-frequency component are described. Breakdown is considered in air at atmospheric pressure; the electrode configurations examined are two spheres, two points, and a sphere and a point. Results are given for electrode separations up to 14cm, and for voltages up to about 100kV. The frequency range of the superimposed high-frequency component is about 0·3-1·5MHz.

G. D. BERGMAN

Electronic inverters

By F. G. Spreadbury. pp. 201. Constable and Co. Ltd. 1967. Price £2 10s.

The author of the book has used the title in its widest sense, and, although any device converting d.c. to a.c. might technically be called an inverter, it generally has a more restricted meaning. The book deals with transistor and valve sinewave oscillators as well as thyratron and mercury-arc d.c.-to-a.c. inverters. A chapter (24pp.) is devoted to low-voltage inversion; this deals with mechanical synchronous choppers, transistor choppers and tunnel-diode inverters. The final chapter (33pp.) appears to have little relevance to the title: it is called 'Inverter applications and energy sources.' This is concerned with such matters as discharge lamps, d.c. transmission, regeneration and braking, fuel cells, thermionic, diode, magnetohydrodynamic and thermocouple generators and solar cells. The first chapter is concerned with principles and characteristics of inverter elements, but it is difficult to deal adequately with such a wide range of devices (e.g. transmitting valves, high-voltage mercury-pool converters, transformers) in 40 pages. The book is useful, as it collects all d.c.-to-a.c. converters together in one book. A number of mathematical expressions are worked out, but one wonders whether many are of value, e.g. critical mutual inductance for a valve oscillator. In some cases, expressions are used without full explanation, and some statements tend to be confusing. One is surprised to see c.g.s. units used and no captions provided to the figures. Some useful references are included.

G. N. PATCHETT

Low-noise electronics

By W. P. Jolly. pp. 149. English Universities Press. Price £1 5s.

This book is intended to give a first- or second-year university student a quick and simple introduction to the whole subject, and in this it succeeds admirably. Starting from a very elementary level, virtually all the important devices, classical and quantum-mechanical, are discussed. The Bohr atomic model is used and parametric systems are introduced by using a quantum-mechanical treatment. Realistic assessments are given of device possibilities, and, in some very useful examples, the noise contributions from the different portions of existing systems are quoted. A useful selection of references from books and journals is included. In a book of this nature, many features will be incomplete, and the clarity of the writing may lead students to overlook some of them. Thus the *p-n* junction is discussed without reference to the Fermi level. The appendix on electron-beam amplifiers gives the impression that they require the presence of positive ions to function. Other appendixes use some jargon which will not be familiar to many students.

I. A. SNOWDON

High-frequency communications

By J. A. Betts. pp. 98. English Universities Press. 1967. Price 25s.

Written for those with the general background of the second-year university student, this book is one of the 'Introductory Science Texts' under the general editorship of Prof. W. P. Jolly. It is concisely written and, as well as chapters on transmitter and receiver technique at h.f., there are sections on error detection and correction, ionospheric forecasting and frequency prediction and a short and valuable chapter on the historical development of h.f. communication. References to the literature are included as footnotes throughout the text.

Basic television : Part I

By H. A. Cole, in conjunction with the publisher's editorial staff. pp. 138. Technical Press. 1967. Price 21s.

Here is the first part of a 2-volume book aimed at a simple qualitative account of monochrome television. It covers basic principles, scanning, the television signal, the transmitter and the studio. A final chapter describes bandwidth as derived from the aspect ratio and picture elements. The book is illustrated with many diagrams. It is suitable for elementary technician training and is part of a series of 20 manuals on subjects connected with electricity and electronics.

Basic electrical engineering : Circuits, electronics, machines, control

By A. E. Fitzgerald, D. E. Higginbotham and A. Grabel. pp 746. 1967. 3rd edition. McGraw-Hill. Price 96s.

The subtitle to the book indicates the contents in brief. Circuit analysis is handled first with simple differential equations, followed by a consideration of experimental force-functions and s-plane diagrams. Harmonic force-functions are then described, leading to vector diagrams and their application. The frequency response of networks is briefly covered and Nyquist diagrams and Bode plots receive some consideration. The fundamental physics of electronics is qualitatively treated; electronic active circuits, both linear and non-linear are discussed in three chapters, where the emphasis is on semiconductors. Following a presentation of the principles of magnetic circuits and transformers, three chapters describe electromechanical conversion, a.c. and d.c. machines and angular-control devices. Finally, feedback control systems are briefly introduced and a short description is given of their transfer functions and frequency response. The aim of the book is to give, in one volume, the basis of electrical engineering students who will eventually specialize. The approach is a generalized one but the problems at the end of each chapter are oriented practically.

A comparative study of programming languages

By B. Higman. pp. 164. Macdonald. 1967. Price 45s.

The author is a reader in computer science at the University of London, and the book is primarily for postgraduate students in computing science, although it will be useful for programmers etc. and to those interested in language generally. The opening chapters discuss the nature of language and some of the special processes, such as redivision, applicable generally to any program language. The transition from machine codes to autocodes is explained and subsequently particular autocodes are described in some detail, for example, Cobol, Fortran, etc., leading to the newer CPL and PL/1 systems. The problem of the interface between programming language and data language is introduced and specific examples of such interfaces are described. A bibliography is appended.

Circuit design for audio, a.m./f.m. and t.v.

Prepared by the engineering staff of Texas Instruments Inc. and edited by W. A. Stover. pp. 352. McGraw-Hill. 1967. Price £5 17s.

Originally published as two separate books ('Audio and a.m./f.m. circuit design handbook' and 'Television circuit design handbook'), the book is intended as a practical circuit guide for the designer. It is the fifth in the well known Texas Instruments electronics series, and has chapters on audio design, a.m./f.m. design, and television design. After theoretical principles of each system have been explained, practical semiconductor circuits are given. The television section is, of course, concerned with American standards, both at v.h.f. and u.h.f., in monochrome circuits. It is, nevertheless of general interest to television-circuit designers.

Generalized electric machines

By A. J. Ellison. pp. 146. George G. Harrap. 1967. Price 20s.

The book is the sixth in the 'Engineering Science Monographs' under the general editorship of Prof. M. W. Humphrey Davies and Dr. H. Tropper. It is complementary to a previous book by the same author ('Electromechanical energy conversion') in that it suggests a laboratory course where the emphasis is on fundamental operating principles rather than their characteristics. The generalized electric machines which the author describes are therefore teaching instruments. Five appendixes lay down the details of five such machines made by four firms. Each section of the book, after a general discussion, gives instructions in practical work followed by questions and discussion.

Publications of the National Bureau of Standards : published by N.B.S. July 1960 through June 1966; published by others 1960 through 1965

By Betty L. Oberholtzer. pp. 740. 1967 National Bureau of Standards. Obtainable from Superintendent of Documents. US Government Printing Office, Washington, DC, USA. Price $4.00

A catalogue of all documents published by the Bureau and of documents whose authors are on the staff of N.B.S. The arrangement is that of the form of the publication, i.e. whether it is a purchase procedure, published in the N.B.S. Journal of Research etc. All documents published by the N.B.S. have a short abstract; those published elsewhere are listed; author and subject indexes are included.

Handbook of electronic instruments and measurement techniques

By H. E. Thomas and C. A. Clarke. pp. 398. 1967. Prentice-Hall. Price 96s.

The material presented here is intended for the engineer operating electronic equipment and for the technician. It embraces a wide range of instruments, and the 14 chapters are organized in three groups: chapters 1-7 detail the tools and instruments, e.g. meters, bridges, oscilloscopes etc.; chapters 8-11 are concerned with technique and components, i.e. transducers, voltmeters, d.c. instruments and instrumentation for valves; chapters 12-14 demonstrate how receivers, transmitters and microwave equipment are tested. The book is illustrated throughout and contains 22 appendixes of general data concerned with testing and electronics.

Publications received

RCA transistor manual
pp. 544. Crown 8vo. RCA, Harrison, NJ, USA. 1967. Price $2.00

RCA silicon power circuits manual
pp. 416. Crown 8vo. RCA, Harrison, NJ, USA. 1967. Price $2.00

Radioisotope-measurement applications in engineering
By R. P. Gardner and R. L. Ely, Jr. pp 483. Med. 8vo. Reinhold Publishing Corporation, London. 1967. Price £6 10s.

Making electric things happen (the career of a chartered electrical engineer)
By P. L. Taylor. pp. 127. Demy 8vo. Educational Explorers Ltd, Berkshire. 1967. Price 21s.

Economic computation and economic cybernetics studies and research
pp. 151. Med. 8vo. Centre of Economic Computation and Economic Cybernetics, Bucharest, Rumania. 1966.

A manual of Kaldas programming
By J. L. Dineley and C. Preece. pp. 36. Med. 8vo. Oriel Press Ltd, Newcastle upon Tyne 1. 1967. Price 12s. 6d.

Rezonanta paramagnetica electronica
By B. Nicolau. pp. 391. Demy 8vo. Editura Technica, Bucharest, Rumania. (in Rumanian)

Structure of the atomic nucleus
By J. Kvasmica. pp. 121. Crown 8vo. Iliffe. 1967. Price 15s.

Packaging directory: 18th edition
pp. 366. Demy 4to. Tudor Press Ltd. 1967. Price 63s.

BEAMA 1967/68 directory
pp. 556. Post 4to. Pergamon Press. 1967. Price 60s.

An 880kbit/s data-transmission system for computer-to-computer communication
By J. S. Austin, R. C. M. Barnes and P. J. B. Fergus. pp. 11. Atomic Energy Research Establishment 1967. Price 2s. 6d. (from HMSO)

Computer-aided production control: a brief survey of practical experience in the UK
pp. 50. Demy 8vo. The National Computing Centre, Manchester 3. 1967. Price 10s. 6d.

Recent research on studio sound problems
By D. K. Jones and H. D. Harwood. pp. 23. Demy 4to. British Broadcasting Corporation. 1967. Price 5s.

Productivity, prices and incomes: a general review, 1966
pp. 42. Crown 4to. National Economic Development Council. 1967. Price 4s. 6d. (from MHSO)

A report to industry
By J. Delin. pp. 66. Loughborough University of Technology. 1967.

Calculation of noise/signal ratio of a nuclear pulse amplifier employing gated active integration
By M. O. Deighton. pp. 55. Atomic Energy Research Establishment. 1967. Price 8s. (from HMSO)

Basic Algol
By W. R. Broderick and P. J. Barker. pp. 121. Iliffe. 1967. Price 15s.

SHORT NEWS ITEMS

Survey of professional engineers

A report jointly initiated by the Ministry of Technology and the Council of Engineering Institutions on a survey of professional engineers was published on the 27th September. Entitled 'Survey of Professional Engineers 1966' (published by HMSO at 8s. 6d.), it is a detailed survey of professional engineers, by background, present activities and income, and is the most comprehensive yet undertaken of a profession in Britain. Questionnaires were sent to 25 000 professional engineers, representing a cross-section of the 14 engineering institutions of the CEI. In its introduction, the report mentions the academic qualifications needed for future chartered engineers, with the emphasis on a university degree. At present, about half of new engineers have university degrees, but in the 1970s it is expected that nearly all new chartered engineers will be graduates. The section on age distribution indicates that engineering is a young and thriving profession; two-thirds of the members of the professional institutions are under 45 (there has been an increase of nearly 50% in annual output of new engineers in the past ten years). The section on employment shows that private industry and commerce take 53% of the total stock of engineers; design, research and development account for 31%, and over half the sample questioned stated that they held administrative or managerial positions. The section on incomes gives the first detailed figures of where engineers rank in the professional incomes ladder; the figures represent gross earned for the tax year 1965/66. Median income for engineers aged 40-45 was over £2200, with the top 10% in that group earning over £3500. Nearly one in four of graduates earned over £3000; 2% of engineers in the sample earned £6000 and more, ranging to £17 400, the great majority of this group being self-employed or in industry. The rise in median incomes over the six years 1959-1965 was 7·2% per annum for electrical engineers.

Thorn Bendix

Thorn Electrical Industries Ltd and the Bendix Corporation of the USA have completed their negotiations for merging certain of their interests, and an agreement for the formation of a new company, Thorn Bendix Ltd, was signed last week. The Chairman of the new company will be Mr. A. Deutsch, the Technical Director of Thorn Electrical Industries Ltd; the Managing Director will be Mr. P. Brennan, formerly Managing Director of Bendix Electronics Ltd. As previously announced, the new company, which will have a share capital of £750 000, will merge the current activities of Thorn Electronics Ltd, Thorn Special Products Ltd, Thorn Electrical Laboratories Ltd, Bendix Electronics Ltd and M.P.J. Gauge & Tool Co. Ltd. Initial activities of Thorn Bendix Ltd will be mainly in the fields of aircraft electrical connectors, aircraft components, avionics, defence and industrial electronics, equipment-process-control instrumentation, scientific instrumentation, electronic and pneumatic gauging and measuring equipment. Expansion into other specialized fields such as fluidics, fibre optics, electro-optics and industrial oceanography is envisaged.

Use of nuclear medicine in Britain

The first International Nuclear Medicine Symposium to be held in Britain, entitled 'Radioactive isotopes in the localisation of tumours', was held at Imperial College in September. One of the main aims of the project, which was organised by the Institute of Cancer Research: Royal Cancer Hospital, was to propagate the varying applications of nuclear medicine in cancer diagnosis. Although Britain is among the largest producers and exporters of radiochemicals in the world, as far as the use of these materials is concerned, British hospitals lag behind those of other countries, including America, where it has become a normal part of clinical practice. At the symposium, about 70 papers were presented by experts from Britain, America and the Continent. They discussed established and new techniques for localising tumours using scanners, gamma cameras and other devices. Throughout the three days of the symposium a technical exhibition showed a comprehensive range of equipment used in nuclear medicine. At the present time, some 20 different radioactive preparations are being used in scanning, and the technique can be applied for both locating tumours and determining the shape of particular organs. The method is now in routine use for clinical investigations of the thyroid, liver, spleen, kidneys, lungs, bone and brain; the necessary equipment is commercially available.

Symposium on microwave power

The 1968 Symposium on Microwave Power, sponsored by the International Microwave Power Institute, will be held at the Statler Hilton Hotel in Boston, Mass., USA, on the 21st, 22nd and 23rd March 1968. The symposium will be concerned with the application of microwave power to processes within the food, agricultural forest product, textile, chemical and other industries and to advanced concepts in scientific apparatus and power-transmission systems. Papers are being solicited; to be considered, abstracts should be submitted not later than the 1st January, 1968. Abstracts should be approximately 250 words long and should be mailed to: 1968 Symposium on Microwave Power, Box 342, Weston, Mass. 02193, USA.

Harbour-radar orders

Decca Radar Ltd has recently received four important orders for the installation of harbour-radar systems in Montreal, Brisbane, Rostock and Wallasey (near Birkenhead). The Canadian contract is worth over $250 000 (£82 000), and includes berthing displays and auxiliary items such as buildings and towers, as well as basic radar equipment valued at $190 000 (£67 850). The berthing system comprises an elaborate console for controlling ship movements in the harbour, particularly the actual berthing movements. The harbour radar to be installed at Brisbane will be a dual radar system having 9ft aerials and 12in displays, which have been specified by the harbour authorities; the order is worth £5000. The installation at Rostock (East Germany) will be used by the port authority to control the movements and berthing of shipping in this rapidly expanding German port; valued at £35 000, it comprises a 2-channel radar with two 16in displays and a large aerial to provide the exceptionally narrow bandwidth specified by the Port of Rostock. Equipment worth £6000 is to be installed at the Wallasey operations centre for the direction of the Seacombe ferries operating across the Mersey. Short-based control radar has been used at Wallasey longer than anywhere in Britain, the original installation having been made in 1945.

Elliott-Automation expansion in Fife

Elliott-Automation is planning to expand its Hill End, Fife, factory by a further 40 000ft^2; a request to more than double the size of the existing factory there has been made to Fife County Council. The additional space is required for the manufacture of digital trainers and simulators and other advanced electronic equipment. Hill End is the third Elliott factory in Fife and the fourth in Scotland. The others are the Satchwell factory at East Kilbride, which is in excess of 150 000ft^2, a 120 000ft^2 computer and automatic-control-valve factory at Cowdenbeath, and the company's microelectronics plant at Glenrothes, with 35 000ft² of production space, in addition to a large new research and development laboratory which was opened there last year. These four factories make some of the most sophisticated products in the Elliott range; they have established in Scotland a number of self-contained businesses, each with its own sales, design, research, engineering and production teams.

Radio & Space Research at RSGB Exhibition

Equipment used in studies of the atmosphere in relation to radiocommunication was shown by the Science Research Council Radio & Space Research Station exhibit at the International Radio Engineering and Communications Exhibition held in the New Horticultural Hall, London, in September. The exhibition, sponsored by the Radio Society of Great Britain, was opened by the Director of the Radio & Space Research Station, Dr. J. A. Saxton. The exhibit demonstrated three types of research being carried out to find out more about the effects of the lower and higher atmospheres on radiowaves—in particular on frequencies down to 3cm wavelengths, which include those used for colour television and communication satellites. Studies of the structure of the lower atmosphere are important, because variations in the refractive index affect many aspects of radiowave transmissions—broadcasting, television, radiocommunications and radar. Microwave refractometers used at RSRS for measuring humidity and temperature changes in the refractive index were demonstrated. Studies of the outer atmosphere by topside sounder satellites were also featured. The behaviour of the of the ionosphere has an important influence on the propagation of radiowaves used in long-distance h.f. radiocommunications. Predictions of radiowave conditions are worked out from information supplied by a world network of ground-based ionospheric-sounder stations. These stations, however, are not evenly distributed over the earth and cannot supply information about the major portions of the ionosphere above the maximum ionization height. The launch of *Alouette*, in 1962, first of a long series of 'topside sounders', started a new era of ionospheric studies. Topside-sounder satellites, with a global view of the ionosphere, can provide comprehensive pictures of the earth's permanently ionized environment.

Reversing the brain drain

A new MSL (Management Selection Ltd) information and recruitment centre which opened in Park Avenue, New York, recently, will provide help and information for engineers, technologists, scientists and managers at present in the USA who would like to work in Britain. This marks an important event in Mintech's programme to go out and get the American and British graduates from the USA who are needed to man Britain's expanding production industries. The centre will provide a 2-way service of information, both to prospective staff in America and to potential employers in Britain, advising on salaries, responsibilities, career prospects and vacancies, matching applications to companies and arranging interviews. Later on, permanent offices will be set up in San Francisco and Toronto. An announcement that Mintech was going to sponsor a sustained drive to reverse the brain drain was made in May. Since the signing of the contract, MSL has undertaken a preliminary tour of many of Britain's top companies to assess recruitment needs and to explain the operation of the new centre.

Britain adopts the Mallard

Britain has joined with the USA, Australia and Canada in a collaborative research and development project which has the object of developing a tactical trunk-communication system for the field armies of these nations and their associated navies and air forces. The project, known as Mallard, will cost the four governments some £45 million in research and development and will take about eight years to complete. The Mallard system will provide secure fully automatic switched communications in the battlefield area from army headquarters down to battalions. There will be facilities for the transmission and reception of voice, telegraph, data and facsimile. Initially, work on the Mallard project was carried out during one year of meetings between the four countries. In an agreed report, the operational and technical requirements were defined and a research and development plan proposed. In the initial development phase of the Mallard program, competitive system-design studies will be carried out by the American and British electronics industries. Supporting technique efforts are being conducted by US, Australian and Canadian concerns, and British industry will undertake a share of this work, which will be phased in with the work being carried out in the other participating countries. The Mallard system uses the building-block or modular principle of equipment construction to ensure flexible interoperation between the field armies of the four countries.

Battlefield-surveillance equipment for the army

The first man-portable radar to be widely adopted by any army will shortly be coming into use in British field regiments for battlefield surveillance. One man will be able to keep watch over a large sector of front in virtually any conditions of weather and visibility, both by day and by night, locating and identifying the movement of men and vehicles. The radar, GS-14-MK1, developed by Elliott-Automation (as the ZB 298), can be carried by two men and brought into action in 2min. It is extremely easy to handle and operate and, by the use of solid-state technology, has been given the standard of ruggedness and reliability required to allow it to stand up to military use under battle conditions. This has made it possible to dispense with any additional protection, such as special carrying cases. The equipment also has a wide range of potential civilian applications in internal security and in such things as coastguard operations. The radar has already aroused great interest in many countries overseas, where it has been demonstrated by joint teams from the Ministry of Defence and Elliotts under all sorts of conditions.

Orders for p.c.m. equipment

Further orders for £4million-worth of p.c.m. equipment have been placed recently by the Post Office with five British manufacturers. These orders follow others valued at £1million placed last year. The plant will be installed by Post Office engineers on junction telephone cables in many districts in Britain, and will provide additional capacity more economically and in some cases earlier than would be possible by laying additional cables. P.C.M., which has been developed for the Post Office initially for use on junction cables between 12 and 20 miles in length, makes it possible to carry 24 conversations over only two pairs of wires, using existing cables. It is the system's high resistance to cross-talk and noise disturbances which makes it possible to increase the traffic-carrying capacity of standard audio cables.

Solartron enter scientific digital-computer field

The Solartron Electronic Group has announced its entry into the scientific digital-computer market with an order approaching £200 000 for an AS6040 computer for British Petroleum. The system will be installed at Britannic House, London, during January 1968. BP will use the computer to process selected seismic-exploration records. The advanced seismic programs provided will be extended to recover additional data from low-quality exploration records. A digital-computer department has been formed by Solartron at its Farnborough (Hampshire) headquarters, which will provide not only hardware but also maintenance and strong software support for systems incorporating the computers. The computers are at present manufactured by a sister company within the parent Schlumberger Group, Electro-Mechanical Research. The computers are manufactured from monolithic integrated circuits, and they are among the first commercially available scientific machines to make use of multi-layer-board construction techniques.

International conference on microwave and optical generation and amplification 'MOGA 68'

The 7th international conference on

microwave and optical generation and amplification 'MOGA 68' will be held from the 16th to 20th September, 1968, in Hamburg. The conference will be sponsored by the Nachrichtentechnische Gesellschaft im VDE (NTG) in co-operation with the Verband Deutscher Elektrotechniker (VDE), Hamburg section, and the German Section of the IEEE. The scientific program of the conference will be co-ordinated by a committee under the chairmanship of Professor Dr.-Ing. F. W. Gundlach. The object of the conference will be to report and discuss further scientific knowledge achieved in this particular field, thus continuing the tradition established by previous international conferences on microwave tubes in Paris (1956 and 1964), London (1958), Munich (1960), The Hague (1962) and Cambridge (1966). Since 1966, the original scope of the conference has been extended by the discussion of the application of solid-state devices, plasmas and other systems to the generation and amplification of oscillations in the optical and microwave ranges. The Hamburg section of the VDE will be responsible for the organisation of the conference. In January 1968, the sponsors intend to contact previous participants and those who have shown interest by writing to the conference office [Address: Tagungsbüro (Conference Office) MOGA 68, c/o VALVO GmbH, Burchardstrasse 19, D-2 Hamburg 1, F.R. Germany]. At the same time the program committee will commence calling for papers.

BEAMA analysis of British exports and imports of electrical products

The outstanding achievement in 1966 of the British electrical trade was the increase in exports to North America. Total despatches to Canada rose from £16·8M to £20·3M and those to the USA from £13·9M to £22·3M. These figures are given in the latest comprehensive guide to the British Electrical and Allied Manufacturers' Association. The publication, which is divided into sections covering imports and exports, gives a detailed breakdown of figures for all types of electrical equipment and apparatus. The export statistics show that, of the additional £26·6M electrical exports last year, £12·5M came from increases in radio and electronic equipment exported, £4·1M from insulated wires and cables, and £1·4M from telegraph and telephone apparatus.

Process for thin-film and printed circuits

A process for the wiring-in of patterns on a thin-film substrate that will directly produce interconnexions and resistors has been developed by Standard Telecommunication Laboratories, Harlow. The process is being evaluated for production at the STC Film Circuit Unit at Paignton in connexion with their new fast-turnround prototype facility. The new technique completely eliminates all the photolithography normally associated with printed wiring and thin-film circuits, and allows a typical circuit to be written on a substrate in a matter of minutes by unskilled personnel. The new process uses a specially developed stylus and etch-resistant inks, with a micro-positioning table. The table moves under the stationary stylus according to co-ordinate instructions from a punched paper tape which can be prepared using a computer fed with basic design information. For film circuits, the starting material is typically a $1\times\frac{1}{2}$in glass substrate having a deposited layer of, for example, nickel-chromium alloy under a similar layer of gold. In the first writing-in process, the interconnexion pattern is traced out in etch-resistant ink on the upper layer of gold. The ink is hardened and then etched selectively to remove the gold not coated with resist, but leaving the underlying alloy unaffected. The resist is then removed leaving the gold interconnexion pattern. A second writing operation next places etch-resistant ink on the exposed alloy in stripes which, when selectively etched to remove alloy only (leaving the gold connector pattern unaffected), are converted into resistors. Line widths down to 0·003in have been produced. A tolerance of $\pm 5\%$ is typical for the major range of resistor values. For printed-circuit wiring, the starting material is a normal copperclad plastic laminate, and in this case all the copper is etched away except for that lying under the written-in circuit pattern; line widths up to 0·15in can be produced.

Radio- and television-receiver disposals

Following a slight uplift in the June figures for radio and television receivers, home disposals for July have dropped, following the seasonal pattern, according to the Economic and Statistical Division of the British Radio Equipment Manufacturers' Association. Television receivers, at 85 000, show a drop of 6000 compared with June, but are 39 000 lower than July 1966—a decrease of 31%; July last year, however, showed an unusual increase in home disposals in anticipation of the tougher credit restrictions imposed later that month. Radio receivers for July 1967 were higher, at 122 000, by 16 000 compared with the same month of 1966, but showed a decline from the June 1967 total by 18 000. Radiogram deliveries remained steady at 13 000, the same as for June this year, showing an increase of 3000 over July 1966 and 1000 more than the same month of 1965.

Canada-Bermuda submarine telephone cable

Submarine Cables Ltd, an AEI company, has been awarded contracts totalling some £3½M for a deep-sea submarine telephone-cable system, to provide 640 circuits between Canada and Bermuda; the system will be installed in 1969. The orders include about 800 nautical miles of 1·47in coaxial submarine telephone cable, 81 submersible repeaters and five submersible equalizers. All this equipment is to be manufactured by Submarine Cables Ltd. The special terminal-station transmission and power-feed equipment will be supplied by the AEI Telecommunications Group. The contracts were placed by Cables and Wireless Ltd on its own behalf and as agents for the Canadian Overseas Telecommunication Corporation. Materials used in cable manufacture will include supplies from Canadian sources.

GPO man heads world radio conference

The 1967 World Administrative Radio Conference, convened in Geneva by the International Telecommunications Union (ITU), elected, as its Chairman, R. M. Billington, T.D., D.L., Head of Wireless Telegraphy, Radio Services Department, GPO. The world administrative conference is the first of its kind devoted exclusively to problems of the maritime mobile service, i.e. radiocommunication between ships or between coast stations and ships. The meetings, which have been taking place from the 18th September to the 4th November are being attended by some 250 delegates from 50 countries. Mr. Billington is head of the British delegation.

Equipment for giant US aircraft

The first Elliott-Automation modular air-data computer for the US Air Force C-5A Galaxy, the world's largest aircraft, has been delivered on schedule to the Lockheed Georgia company's factory at Marietta, USA. The C-5A air-data computer is one of five orders for aviation equipment, together worth millions of pounds, placed with Elliott-Automation by US manufacturers, both military and civil. The first digital head-up display for the US Navy integrated light-attack avionics system (ILAAS) was delivered by Elliotts early in August. Approaching first deliveries are the energy-management analogue computer and the undercarriage-alignment control, both also for the lockheed C-5A. More recently, Boeing has selected the Elliott true-mass fuel flow-meter for its 747 super jet. The C-5A Galaxy is being developed for the USAF Systems Command and 58 have been ordered so far. The first flight is scheduled for June next year. The air-data computer supplies indicated and true airspeeds, Mach number, altitude, differential pressure and temperature, to 57 points in the giant military transport aircraft. The unit just delivered is the first of a production run of well over 100 units ordered by Lockheed last September. The production line now set up at Elliott's Rochester factory will produce at least ten further air data systems for the C-5A by the end of this year.

ERRATUM

The author's name for the article on p. 578 of the September issue was given without the first initial; it should have been L. J. Ricardi.

NEW EQUIPMENT

A description, compiled from information supplied by the manufacturers, of new components, accessories and test instruments.

MINIATURE TRIMMERS

Reliance Controls Ltd,
Drakes Way, Swindon, Wiltshire

Reliance Controls offer from stock a range of miniature rectangular trimmers ideally suited as discrete components in conjunction with integrated circuits or where space-saving is at a premium. Dimensioned 0·75in long × 0·165in wide × 0·28in high, the CW50 has been designed for printed-circuit application, with pins on the standard 0·1in matrix, thus giving complete interchangeability.

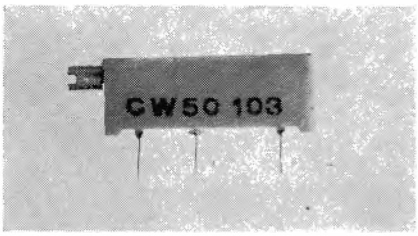

The relatively high operating torque of 3oz-in ensures stability of setting. Resistance range: 100Ω to 20kΩ; temperature range: −65 to +125°C; rating: 1W at 40°C; life under full loads: 1000h at 40°C.

For more information circle **No. 271**

STEP-RECOVERY VARACTOR

Motorola Semiconductor Products Inc.,
York House, Empire Way, Wembley, Middlesex

The Motorola IN5157 is a step-recovery varactor with an output power of 1W at 10GHz. The latest high-power microwave varactor diode, it offers a minimum efficiency of 38·5% when doubling from 5 to 50GHz. This device can be used in the radar band of 8·5 to 9·6GHz, as a driver for high-power valves or as a multiplier for solid-state local oscillators. It can also be used in microwave-link communication equipment for both transmitter and local-oscillator signal sources and in other equipment as a single source up to 13GHz with over 100mW output power. The IN5157 thermal resistance from junction to case, θ_{JC}, is 38·5degC/W maximum and the reverse breakdown voltage is a minimum of 10Vd.c. These two characteristics are largely responsible for the power-handling capability of the IN5157. The *Q*-factor is 3600 at 50MHz and 6V d.c. reverse bias, and the diode capacitance is 0·6 to 1·0pF at 1MHz and 6Vd.c. reverse bias. The unit is housed in the standard pill-type package with two prongs, also designated as case number 46.

For more information circle **No. 272**

PLASTIC-OVERLAY TRANSISTOR

RCA (Great Britain) Ltd,
Sunbury-on-Thames, Middlesex

A package utilizing a 'terminal-block' structure has recently been introduced by RCA (Great Britain) into its overlay-transistor range. The package (2N5017) is an epitaxial silicon *n-p-n* planar transistor, and its terminal-block structure allows a choice of stripline, printed-circuit or lumped-circuit mounting. The performance, ruggedness and versatility of the 2N5017 make it ideally suited for class-B and class-C r.f. amplifiers in military and industrial u.h.f. communication equipment; while its broadband radiofrequency capability provides r.f. power outputs of 23W (typical) at 225MHz and 15W (minimum) at 400MHz, operating from a 28V power source. Amplifier measurements made on u.h.f. transistors in various package configurations indicate that lead length greatly affects performance, with emitter-lead inductance the most important factor. A reduction in lead length has been achieved in the package by bringing the leads directly out of the top of the case, permitting circuit components to be placed as close to the chip as possible. Also, small pins have been placed in the electrodes to provide mechanical support to the attached components. Performance is improved by low emitter and base inductances, which optimize power and gain, while the low base-lead inductance is of particular importance in wideband-equipment applications. The use of an isolated-package technique also eliminates circuit restrictions normally associated with grounded-emitter designs.

Maximum ratings:
Collector-emitter voltage = 65V (with $V_{BE} = -1{\cdot}5V$) and 40V (with $R_{BE} = 30\Omega$)
Emitter-base voltage = 4V
Collector current = 4·5A
Transistor dissipation at case temperatures up to 50°C = 30W
Temperature range, storage and operating (junction) = −65 to 200°C
Case temperature (during soldering) for 10s maximum = 230°C

For more information circle **No. 273**

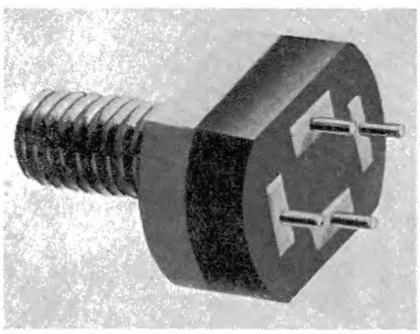

SILICON RECTIFIERS

Mullard Ltd, Torrington Place, London WC1

The Mullard range of low-cost plastic-encapsulated 1A silicon rectifiers, type-BYX36, have been uprated to give repetitive reverse maximum voltages of 150, 300 and 600V. These voltages are included as suffixes to the type number in accordance with the pro-electron scheme used throughout Europe. 'Whiskerless' construction is used for items in the BYX36 family, to give a high surge-current capability with extremely rugged characteristics. Their DO-7 construction allows high packing densities to be achieved, while the hard thermosetting plastic used for encapsulation has been specially chosen for normal soldering techniques: the BYZ36 will tolerate 245°C for up to 5s without damage.

For more information circle **No. 274**

MINIATURE P.T.F.E. TUBULAR CAPACITOR

Oxley Developments Co. Ltd, Ulverston, Lancashire

Two versions of a tubular capacitor, one for mounting on a printed-circuit board (illustrated) and the other for chassis mounting, are being offered by Oxley Developments. These components use p.t.f.e. as the dielectric medium and display a high stability under adverse

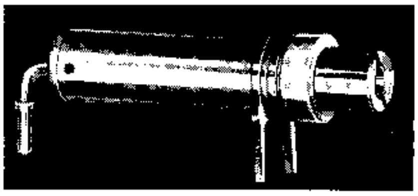

conditions. The insulation is greater than 10^6MΩ and the capacitance is in the order of 30pF. The power factor is less than 0·0005 at 10kHz. This component will withstand a test voltage of 10000V.

For more information circle **No. 275**

POLYESTER-FILM CAPACITORS

G. A. Stanley Palmer Ltd, Island Farm Avenue, West Moseley Trading Estate, Surrey

Polyester-film capacitors, made by the German firm of Ernst Roedenstein, are now available from G. A. Stanley Palmer Ltd. These capacitors, which use aluminium foil as one element, are of flat construction, and have leads made from flat tinned-copper wire, metallically connected to the aluminium foil to provide a perfect contact. One lead takes the form of a 'snap-in' connection. H.V. capacitors are available in values ranging from 1000mmF to 0·33mF with working voltages of 160 or 400Vd.c.; equivalent-a.c. 50Hz figures are 100 and 150V. Normal capacitance tolerance is ±10%, but ±5% is available if and when required. Insulation resistance for capacitors smaller than 0·1mF is more than 100^9Ω, and each capacitor meets the relevant clauses of DIN 40 040. Sizes range from 4 × 10 × 13mm to 9 × 26 × 18mm.

For more information circle **No. 276**

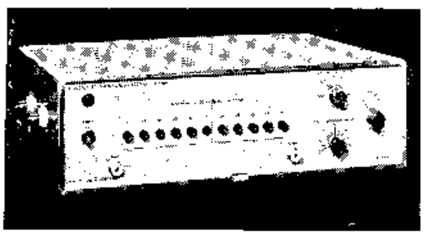

ZENER DIODES

Motorola Semiconductor Products Inc., York House, Empire Way, Wembley, Middlesex

A series of ¼W Surmetic-20 Zener diodes is available from Motorola. The IN5221-81 devices cover a Zener-voltage span of 2·4 to 200V and, although rated at ¼W with normal mounting conditions, they have good failure resistance when overstressed in 1W, 1000h testing. All units are 100% oscilloscope tested and characterized at six critical points, including temperature coefficient, and have a 10W surge rating. All devices above 14V have a leakage current typically less than 100nA. High-temperature and high-humidity operation is possible as a result of flame- and distortion-resistant plastic DO-7 packaging. The 200°C operating temperature and the results of repeated 50-day moisture-resistance tests give design confidence for several environments. The leads are readily soldered or welded. All special requirements, such as nonstandard voltages, matched sets, double anode clippers and tight-tolerance types can be supplied.

For more information circle **No. 277**

MINIATURE MONOLITHIC CERAMIC CAPACITORS

ERG Industrial Corporation Ltd, Luton Road, Dunstable, Bedfordshire

Erg Industrial announce a range of miniature monolithic ceramic capacitors which includes two sizes of moulded axial-lead types covering the range 10 to 27000pF. The standard tolerance is ±10%, and closer or broader tolerances are available. The standard temperature coefficient conforms to MIL-C-11015C characteristic BX, which ensures that the value observed at 25°C is maintained within ±15% over the range −55 to +125°C. Working voltages are from 50 to 200Vd.c. and these capacitors can withstand a direct potential of 400% of rated voltage applied at 25°C for 5s with the current limited to 50mA maximum. The dissipation factor after 1000h at twice the rated voltage in an ambient of 125°C is less than 2·5%. Standard leads are tinned copper and dual-purpose weld/solder leads of gold-flashed Dumet are readily available.

For more information circle **No. 278**

BROADCAST RECEIVER

Eddystone Radio Ltd, Eddystone Works, Alvechurch Road, Birmingham 31

The Eddystone broadcast receiver, model-EB36, is fully transistorized and

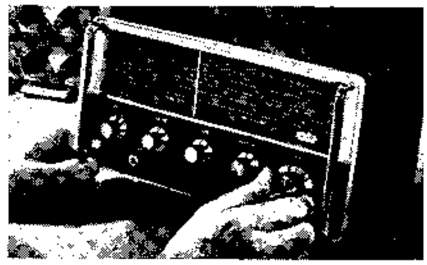

covers long- and medium-wave broadcast bands throughout and provides continuous coverage of the short-wave bands down to below the popular 16m band. Battery power supplies are provided within the receiver unit, to make the complete receiver independent of any external supply. A mains power unit is also available to replace the battery carrier in the receiver and provide a suitable power supply from any standard mains alternating voltage. The EB36 incorporates the Eddystone tuning control, with a high tuning ratio allowing precise frequency settings to be obtained. The tuning control is loaded with a heavy flywheel, which makes it possible to spin the dial to cover large changes in frequency very rapidly; five frequency scales are provided, covering long-wave, medium-wave and three short-wave bands. An additional scale, calibrated in arbitrary units, can be used in conjunction with a small vernier dial to provide a very precise definition of points on any of the five frequency scales. Frequency coverage: 8·5 to 22MHz, 3·5 to 8·5MHz, 1·5 to 3·5MHz, 550 to 1500kHz, and 150 to 350kHz. For a 15dB signal/noise ratio, sensitivity is better than 5µV on ranges 1 to 3, and better than 15µV on ranges 4 and 5. The bandwidth is 5kHz at the 6dB points and 25kHz at the 40dB points. The image rejection is approximately 50dB at 2MHz and 15dB at 18MHz. Breakthrough at the i.f. of 465kHz is at least 85dB down on ranges 1 to 3 and greater than 65dB down on ranges 4 and 5. Audio output is up to 750mW.

For more information circle **No. 279**

PRECISION SERVOPOTENTIOMETER

Brookes and Green Ltd, Gomshall, Guilford, Surrey

The Maurey potentiometer type-50-M208 maintains close electrical tolerances in a ½m-diameter (size-05) servo size. The unit is a product of the *Sidewinder* missile program. The resistance range is 50Ω to 50kΩ, and it has linearity to

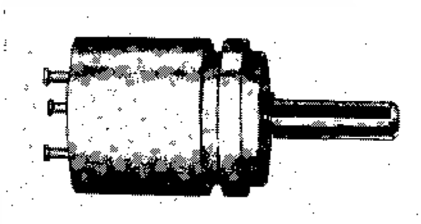

±0·3%. This model is available with bronze or stainless-steel ballbearings; it has an anodized aluminium housing and a stainles-steel shaft. The electrical functional angle is 354° standard; however, it is available to any specified angle or for continuous rotation. It is for use where good accuracy and reliability are required but where space is limited.

For more information circle **No. 280**

POWER RECTIFIERS

Solitron Devices Inc.,
256 Oak Tree Road, Tappan, NY 10983, USA

A series of Hi-pac power rectifiers has been added to Solitron's line of modular assemblies. The rectifier units available are: centre tap, doubler and single-phase and 3-phase halfwave or full-wave bridges; all junctions are passivated. They are mounted on an insulated aluminium heat sink made using the Solitron Hi-pac process. This method of mounting overcomes insulation problems, and the rigid metal substrate provides a low-thermal-resistance path to the heat sink. Where miniaturization is

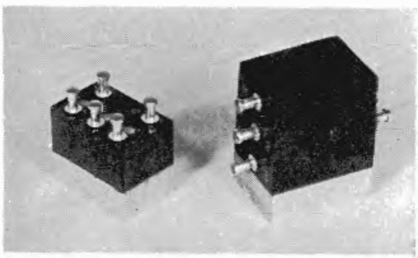

essential, as in the aerospace field, the new series of devices is valuable, as no hardware is needed, assembly costs are reduced, and, at the same time, micro-capability is greatly increased. Standard units (G600-series) are: single-phase bridge rated at 8A d.c. at voltages up to 800V; two series of 3-phase full-wave bridges, designated F-967 and F-928, rated at 6A d.c. at voltages up to 1000V p.i. and at 8A d.c. at voltages up to 1000V p.i. (both units are rated at a base temperature of 70°C).

For more information circle **No. 281**

COAXIAL BANDPASS FILTER

Microlab/FXR, Livingston, New Jersey, USA

An interdigital 18-section coaxial bandpass filter offering a high rejection band has been released by Microlab/FXR. Designed originally for use in a submarine-deception-buoy system developed

by General Instrument Corporation, the new filter (model-BL-A31) offers a rejection factor of 60dB at 1·7 and 4·4GHz, with a passband of 2 to 4GHz; insertion loss is 1·5dB. The intrinsic economies of the interdigital-construction techniques allow the sharp stop-band skirts, coupled with excellent passband response. As a result, more expensive and less reliable techniques previously used are no longer required.

For more information circle **No. 282**

FREQUENCY DOUBLER/PHASE SHIFTER

Brookdeal Electronics Ltd,
Myron Place, London SE13

Brookdeal Electronics are introducing the frequency doubler/phase shifter DP325. This is believed to be the first sinusoidal aperiodic frequency doubler to be produced. It is very simple to operate: switch on the instrument, set the input attenuator, connect a sinewave to the input and a sinewave of double frequency can be obtained from the output socket. The output level can be monitored on the output meter, and inputs between 10mV and 100V full-scale can be accepted. There are facilities for shifting the phase of the output waveform, with or without frequency doubling, and for using the DP325 as a flat amplifier giving up to 50dB gain. It was particularly designed for use in the reference channel of a phase-detection small-signal-recovery system, where the information frequency is twice that of the excitation or modulating waveform. The wideband design allows swept-frequency measurements to be made where hitherto only tedious point-by-point plotting has been possible.

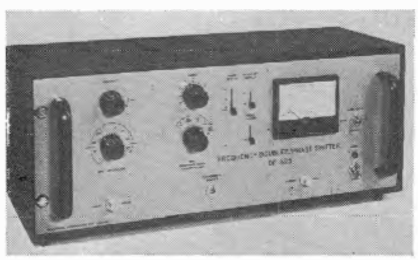

Typical applications of the doubler include: n.m.r. and e.s.r. (second derivative), and measurement of contact potential, second sound and electro-optical effects. The circuit is stabilized by a high degree of d.c. and signal-frequency feedback, and silicon planar transistors are used throughout the design. Facilities are incorporated to compensate for input sinewaves of poor waveshape. Frequency range: 3Hz-300kHz; input level: 10 to 100mV for f.s.d.; input attenuator: 10dB steps; input variable gain: 15dB; input impedance: 100kΩ; output level (f.s.d.): 3V r.m.s.; output impedance: 600Ω; non-linearity 0·1% (excluding doubler), 1% (doubling circuit) total harmonic distortion; phase-shift control: greater than 180° control plus switched 180° increment; output meter: 0-3V mean sensing.

For more information circle **No. 283**

SELF-ADJUSTING WIRE STRIPPER

A.B. Engineering Co.,
Apem Works, St. Albans Road, Watford, Hertfordshire

A wire-stripping hand tool has been produced by A.B. Engineering which is fully self-adjusting within the range of all standard conductors from 0·015 to 0·15in. A dial adjustor is provided to extend the range downwards to 0·003in,

to accommodate nonstandard cables and co-axials. The wire stripper will strip the insulation from a very wide range of cables without damaging the wire, regardless of core diameter. Co-axial cables are dealt with by stripping the outer and inner sheaths separately.

For more information circle **No. 284**

MODULAR CONTROL PACKAGE

Shirehall Electronics Ltd,
Station Yard, Borough Green, Sevenoaks, Kent

The Shirehall Duabox provides an attractive and practical housing for the new Dualine system of mounting plug-in circuit cards. Constructed in light-weight anodized aluminium, the Duabox comprises a basic pack framework (with perforated trays, snap-in card guides and connectors) complete with a base-plate and removable cover. The user may either build up his own circuits on blank Dualine cards (with a 0·1in hole matrix and copper strips leading to a 22-way connector), or use Dualine standard circuit cards for appropriate parts of his instrument or control system. Basic ±12V power packs ($1\frac{1}{2}$, 3 or 6A ratings) are available in unstabilized or stabilized versions as an integral part of the Duabox; so that very compact self-contained units may be constructed. A major feature of the system is that the positioning and wiring of cards and connectors is completely flexible, and may be modified after the equipment has been assembled. This feature is particularly useful for the newly designed equipment or develop-

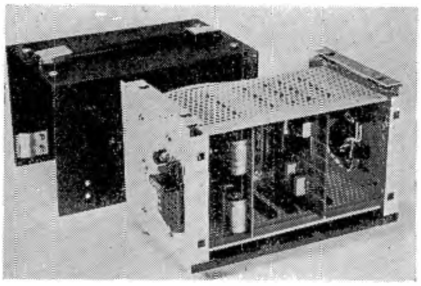

ment prototypes, where modifications are likely to be needed at a later date. The Duabox may be used for portable instruments or may be panel-mounted by fixing mounting brackets to the appropriate side. The cover is designed to slide over any side of the square end frames, and its removal by four quick-release fasteners gives complete access to the circuit boards and wiring. The equipment is designed for rapid assembly and wiring and uses snap-in components wherever possible. Jumper leads fitted with plug-in jack pins reduce connector wiring time to a minimum. The Duabox is now available in four standard lengths: 6, 8, 12, and 16in (152, 203, 305 and 406mm), and is obtainable in kit form or fully assembled.

For more information circle **No. 285**

BOARD-TO-BOARD CONNECTORS

Varelco Ltd, Newmarket, Suffolk

A range of precision board-to-board connectors, designed for reliable and economical printed-circuit-board packaging, is being manufactured and marketed by Varelco Ltd. Three difference arrangements are available, to meet all printed-circuit-board design applications; boards can be connected in the same plane, at right angles to each other or in parallel with each other, thus giving design engineers complete freedom from standard sizes of connectors. It is necessary only to use the exact number of contacts required on

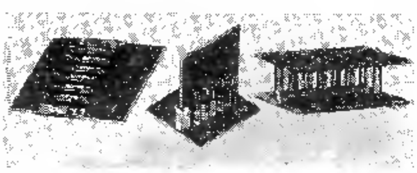

each board, immediately reducing the overall cost of each connector. With the use of Varelco production equipment, contacts can be staked quickly and efficiently to the printed-circuit boards, and, unlike plated-on edge connectors, Varelco connectors are not affected by variations in the thickness tolerances of printed-circuit boards. This ensures that proper mating of connectors is achieved every time and the contact resistance is kept to a minimum. Contacts are made from phosphorbronze and are nickel-plated with a gold finish; contact-pitch range: 0·100, 0·125, 0·150 and 0·200in; contact rating: 5A (minature contacts 3A): contact resistance: 0·006Ω (maximum); standard board thicknesses: 1/16, 3/32 and 1/8in.

For more information circle **No. 286**

GOLD-INLAID BERYLLIUM COPPER

Johnson Matthey Metals Ltd, 78 Hatton Garden, London EC1

Johnson Matthey Metals announce the introduction of gold-inlaid beryllium-copper, which will be of great interest to manufacturers of plug-and-socket components, particularly of those used for printed-circuit boards. Until now, it has been the practice to electroplate the contact surfaces of such components; but, owing to their irregular shape and to the difficulty of masking, it has often been necessary to gold-plate the entire contact assembly. The use of beryllium-copper strip with a gold inlay can therefore result in considerable saving, as the gold alloy is confined to those areas where it is required. The inlay of gold-inlaid beryllium-copper strip is of 5% nickel-gold, the minimum dimensions of the inlay being 0·25in wide by 0·0002in thick. The thickness of the inlay, must, however, always exceed 3% of the total thickness of the strip. The overall dimensions of the strip are subject to the same limitations as apply to Mallory-73 beryllium-copper. The material can be supplied in various grades of hardness to suit individual requirements. A simple heat treatment can be used to develop a hardness in excess of 330HV.

For more information circle **No. 287**

TRANSMISSION TEST EQUIPMENT

Hatfield Instruments Ltd, Borrington Way, Plymouth, Devon

The standard milliwatt sender type-IE730 and the milliwatt test set type-LE738 are recent additions to the range of transmission equipment manufactured by Hatfield Instruments Ltd. The milliwatt sender produces a distortion-free, sinusoidal output with an exceptionally high order of stability. The output is balanced and floating, the impedance level being 600Ω ±1%. The output frequency as normally supplied is 820Hz. This frequency is close to the C.C.I.T.T.-weighting-curve centre frequency but avoids harmonics

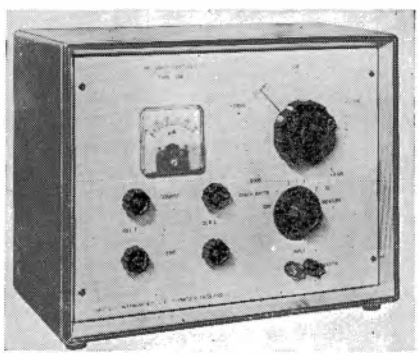

of 50 and 60Hz. Alternative frequencies can be specified in the range 800 to 1200Hz. The total harmonic distortion is typically 0·12% and is composed predominantly of odd harmonics. The unit is small and compact, measuring only $11\frac{1}{4} \times 8\ 5/16 \times 6$in, and is battery-operated. The milliwatt test set (illustrated) is designed primarily as a calibration standard for use with the standard milliwatt sender. However, it may be used wherever it is desired to set or check a level in the range 0 ±0·1dB relative to 1mW in 600Ω, subject to the restriction that the input to the test set is terminated unbalanced. The accuracy of the instrument is ±0·01dB and the frequency range covered is 20Hz to 20kHz. The instrument is powered by internal dry batteries.

For more information circle **No. 288**

SOLID-STATE CHARGE AMPLIFIERS

Environmental Equipments Ltd, Denton Road, Wokingham, Berkshire

Environmental Equipments announces three new amplifiers for applications in a variety of environments ranging across the whole spectrum of shock- and vibration-measuring problems. All the amplifiers use the same circuit and exhibit the same electrical performance. Different forms of packaging are used for various environmental conditions. A charge calibrator is built into the rack- or bench-mounting (illustrated) type which accommodates 14 channels in a standard $19 \times 5\frac{1}{4} \times 6$in assembly. The calibrator is available as a separate item for calibrating 4-, 8-, or 12-channel packages constructed to withstand a more severe environment or for a single-channel package designed for the most severe environment. Even the rack- or bench-mounting amplifier is tested on a bump-testing machine, to provide a very high degree of reliability under rough-usage conditions. Other versions are shock, vibration, temperature and humidity tested. The amplifiers have only 1% output-voltage variation for 9000pF input-capacitance change, which represents 300ft of low-noise cable at 30pF/ft; frequency response: 2·5Hz to 25kHz ±5%; 1Hz to 100kHz, −1·5dB; output: 5V, 0·3mA maximum; gain: 0-20 continuous; noise: 6mV at maximum gain; input: 3000pC maximum. The rack- or bench-mounting version can be supplied with 7 channels, each including ±2·5V, ±50mA, output for driving galvanometers.

For more information circle **No. 289**

VARIABLE-CAPACITOR BOXES

J. J. Lloyd Instruments Ltd, Brook Avenue, Warsash, Southampton, Hampshire

J. J. Lloyd Instruments are now manufacturing two new variable-capacitor boxes designed primarily for the electronics-research laboratory and in educational establishments where there is a need for a moderately priced infinitely variable capacitance box with a very low minimum setting, calibrated to an accuracy of 1% and suitable for use over a very wide frequency range. Two models are available: types-VC1 and VC2. Type-VC1 consists of a calibrated twin-ganged air-spaced capacitor; both gangs are brought out to separate low-loss terminals, so that, by connecting the gangs in parallel, the capacitance indicated on the dial may be doubled. The gangs may also be series-connected for very small capacitance readings, which are indicated on a separate scale. Type-VC2 is a similar instrument, but it incorporates a single air-spaced capacitor used in conjunction with a single decade or close-tolerance silvered mica capacitors to give a wider capacitance range. The instruments are normally calibrated with the terminals fully floating, but each instrument is individually marked with the additional capacitance that must be added when one of the terminals is linked to the screened case. Both instruments are directly calibrated in picofarads and no allowance has to be made for inherent stray capacitance within the instruments themselves. The operating shaft of the airspaced capacitor is also insulated to reduce the effects of hand capacitance to a minimum. The specifications are as follows: Model-VC1: 10 to 65pF (range 1), 20 to 130pF (range 2), 40 to 260pF (range 3); model-VC2: 20 to 1130pF; tolerances at 20°C: ±1% or ±1pF, whichever is greater; maximum d.c. working voltage: 500V.

For more information circle **No. 290**

COUNTER CONVERTERS

Marconi Instruments Ltd, St Albans, Hertfordshire

The top frequency-measurement limit for the Marconi TF-2401A counter has been increased to 2·5GHz by the introduction of two new plug-in heterodyne converter units. The TM8334 covers the frequency range 50 to 610MHz in 10MHz steps in its heterodyne mode; in addition, it permits direct measurement of frequency up to 50 or 110MHz, depending on the range unit in use. The TM8094/1 is a higher-frequency unit with a heterodyne range of 0·3 to 2·5GHz. It is normally intended for use in conjunction with the 50MHz-range unit, and the heterodyne range is therefore covered in 50MHz steps. However, the 110MHz-range unit can also be employed with this converter, if desired. Provision is made for direct measurement of frequency up to the range unit maximum.

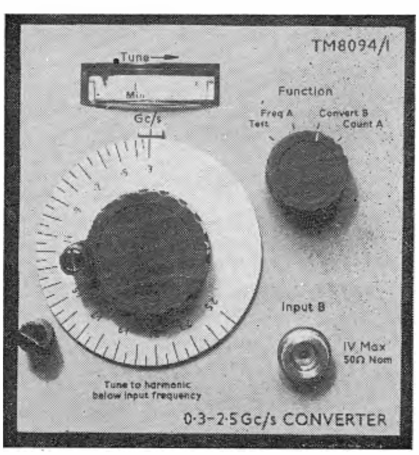

For more information circle **No. 291**

MICROWAVE PEAK-POWER METER

Aveley Electric Ltd, South Ockendon, Essex

Microwave peak-power measurements over the range of 3 to 300mW can now be made directly with ease and accuracy. Peak power in kilowatt and megawatt ranges can be measured with calibrated directional couplers and attenuators. The Narda microline 66A3A peak-power meter requires no special skill or additional equipment other than a bolometer mount with a calibrated barretter. Completely portable operation and small size and weight permit simple field measurements. Overall measurement accuracy using the 66A3A is within 8% total r.m.s. error, excluding the directional coupler. Readings may be taken continuously and instantly. This may be compared with average power techniques which involve approximately 10% r.m.s. error and require up to 60min for a single reading. Errors in the average power measurement result from inaccuracies in average-power measurement, determination of effective pulsewidth and shape, and measurement of pulse-repetition rate. The average-power method is extremely difficult to apply to multipulse systems or those with irregular pulse rates. Operation of the Narda microline 66A3A is based on the barretter-integration-differentiation technique.

For more information circle **No. 292**

F.E.T.-INPUT OPERATIONAL AMPLIFIER

Advance Electronics Ltd, Roebuck Road, Hainault, Ilford, Essex

Advance Electronics now offer a range of f.e.t.-input operational amplifiers in a miniature module package. The series offers an extremely high input impedance (10^5MΩ) and low offset current (20pA). The amplifiers are suitable for accurate integration, sample-hold, buffering or any application requiring high input impedance and low offset current. Typical drift rate for the series is 5μV/degC. Other characteristics are output voltages of ±10V and ±20V, together with output currents up to 20mA. In common with other operational amplifiers in the range, the f.e.t. series features high slew rate (7V/μs) and bandwidth (4·5MHz). The f.e.t.-series units are packaged in a module 1·5 × 1·5 × 0·4in and can be mounted directly onto a printed-circuit board or the appropriate socket.

For more information circle **No. 293**

PLASTIC-FILM ELEMENTS FOR PRECISION POTENTIOMETERS

Bourns (Trimpot) Ltd, Hodford House, 17/27 High Street, Hounslow, Middlesex

A film element for precision potentiometers, developed by Bourns Inc., California, is claimed to produce essentially infinite resolution and provide a longer life than its equivalent wirewound unit. The first models introduced, incorporating Bourns Infinitrom™ conductive plastic elements are the ⅞in-diameter 10-turn bushing-mount model-3501 and servomount model-3551. The noise specification of 100Ω or 1% is comparable with wirewound types. Maximum resistance change in any environment is only 5% throughout a life of 4 million shaft revolutions for the model-3501, and 10 million revolutions for the model-3551. Resistance range: 1 to 500kΩ; resistance tolerance: ±5%; independent linearity: ±0·5%; power rating: 2W at 70°C; temperature coefficient: ±300 parts/10^6 per degC; shock: 100*g*; vibration: 20*g*.

For more information circle **No. 294**

TEMPERATURE-COMPENSATED CRYSTAL OSCILLATOR

Wessex Electronics Ltd, Royal London Buildings, Baldwin Street, Bristol 1

The model-6202 temperature-compensated crystal oscillator from Varo Inc., USA, was designed for application where no warm-up time is permitted, no oven power is available and size is important. The unit may be mounted on a printed card and the 0·5in maximum profile allows standard card-rack spacing. Thermistor-varactor compensation networks and silicon i.c. active devices provide optimum performance in a small package. Long-term stability results from use of a glass-enclosed quartz crystal. Input voltage: 12 to 20V d.c. nominal (or specified); regulation: 1%; input current: 5 to 30mA; output frequency range: 10kHz to 10MHz; output voltage: 1·0V r.m.s. minimum; calibration: $\pm 1 \times 10^{-6}$; load: 1000Ω minimum; waveshape: sine or square; frequency stability: −40 to +70°C $\pm 10^{-6}$, 0 to +50°C, $\pm 10^{-7}$.

For more information circle **No. 295**

PLUG-IN R.F. POWERMETER

Dymar Electronics Ltd, Rembrandt House, Whippendell Road, Watford, Hertfordshire

The increasing use of personal radio-communication sets in the v.h.f. and

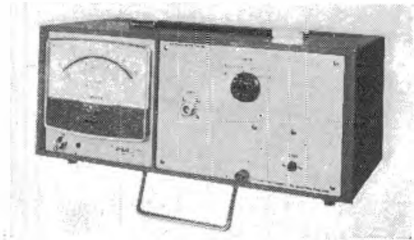

u.h.f. bands has created a need for r.f. powermeters with power-range spans from milliwatts to a few watts. The Dymar r.f. powermeter type-781 satisfies this requirement, having four ranges from 300mV full-scale deflection to 10W. True power is measured by means of a thermocouple and the slab-line load gives a good v.s.w.r. up to 500MHz. Provision of a 5in mirror-backed linear scale ensures good reading accuracy and enables measurements of a few milliwatts to be made. The instrument is available as standard with either 50 or 75Ω load impedance.

For more information circle **No. 296**

Ku-BAND PULSE MAGNETRON

Varian Bomac Division,
Salem Road, Beverly, Mass., USA

Designed for use in ground-radar systems and beacons, the BLM-143A pulsed magnetron delivers a peak output of at least 1kW over the frequency range 16·0 to 16·5GHz. Special design features provide a very low frequency/temperature coefficient. The tube is extremely reliable and frequency-stable, even under severe environmental conditions. Sturdy cathode construction resists damage from excessive anode voltage and load mismatch. The BLM-143A weighs only 23oz, including its integral permanent magnet. Either conduction or forced-air cooling may be used. Overall dimensions are 2·625 × 2·375 × 3·422in.

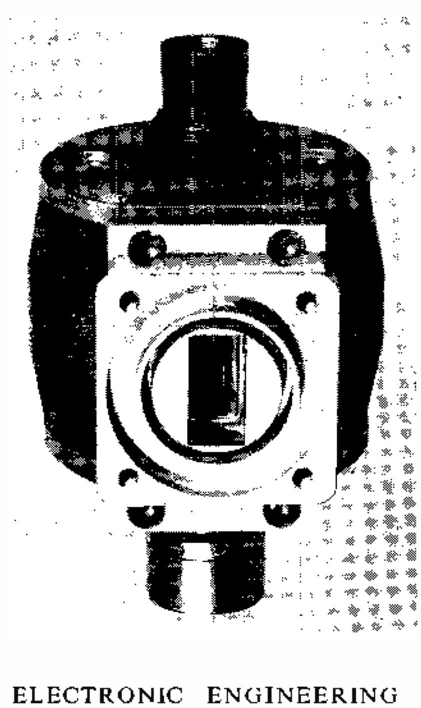

The output connector mates with a UG-419/U standard flange. Typical characteristics: anode voltage peak = 3·0kV; anode current peak = 1·6A; input-power average, including heater = 8·0W; duty cycle = 0·001; pulse duration = 0·25μs; pulse-repetition rate = 4000 pulse/s; voltage risetime = 0·08μs; load v.s.w.r. = 1·3 : 1; envelope-temperature maximum = 150°C.

For more information circle **No. 297**

TELEVISION MEASURING INSTRUMENTS

Marconi Instruments Ltd,
St. Albans, Hertfordshire

Marconi Instruments announces a new and comprehensive range of television-transmission measuring equipment, with units suitable for all colour and monochrome systems and which conform with the recommendations of the main authorities. The range takes the form of instruments suitable for bench or rack mounting. New instruments in the range include: sine-squared-pulse-and-bar generators for monochrome and colour, a test set for luminance/chrominance gain and delay equality measurements on colour-television links (illustrated), blanking and sync. mixers allowing sweep or video test waveforms to be superimposed on studio blanking and sync. pulses. These are complemented by existing equipments, including the television transmitter sideband analyser, and the 20MHz sweep generator.

For more information circle **No. 293**

DOUBLE-BALANCED MIXERS

Hewlett Packard Ltd,
224 Bath Road, Slough, Buckinghamshire

TWO broadband double-balanced mixers from Hewlett Packard are housed in a compact package (1·63×0·70×0·43in) for mounting directly on printed-circuit boards or in stripline circuits. The advantages of the mixer family may thus be obtained in compact printed circuits (illustrated). A third new mixer is in a metal case with BNC connectors. One of the new p.c.-mounting mixers (model-10514B) retains all of the characteristics of the model-10514A but it is in a more compact package and is offered at a lower price. The frequency range of the 10514B is 0·2 to 500MHz at the local oscillator and signal ports, the third port is d.c.-coupled. The frequency range of the model-10534A, with BNC connectors, and the companion printed-circuit-mounting model 10534B, is 50kHz to 150MHz. These broadband untuned mixers are useful as pulse modulators, capable of high carrier suppression between pulses, as current-controlled attenuators and as a.m. modulators, and also as spectrum or comb generators. Of particular importance, the i.f. noise specified for all the

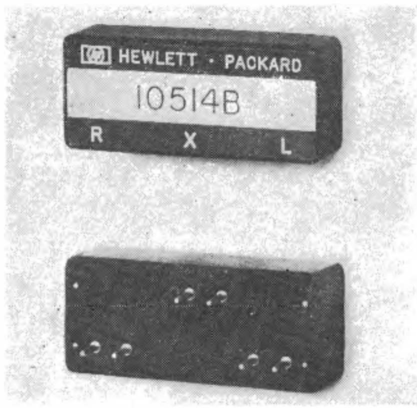

mixers is less than 0·1μV per root cycle at an output frequency of 10Hz. Mixer conversion loss (single sideband) of the 0·2-500MHz model-10514B is less than 9dB over the full input-frequency range, and less than 7dB (typically 6dB) in a frequency range of 0·5 to 50MHz. Mixer conversion loss of the 0·05-150MHz models-10534A and 10534B is less than 6·5dB, between 0·2 and 35MHz, and less than 8dB throughout the rest of the range. Other performance data and comprehensive specifications for these mixers are given over a wide environmental range. Because of their balance, the result of using selected hot-carrier diodes in the diode-bridge modulator circuit, these double-balanced mixers have high carrier suppression. Intermodulation products are low also.

For more information circle **No. 299**

WIRE DELAY LINE

The M.E.L. Equipment Co., Ltd,
Manor Royal, Crawley, Sussex

Requirements for higher-speed working and increased data storage are met with a new wire delay line announced by M.E.L. The line (type-YL2161) works at a speed of 500kHz and can be supplied with a delay between 0·1 and

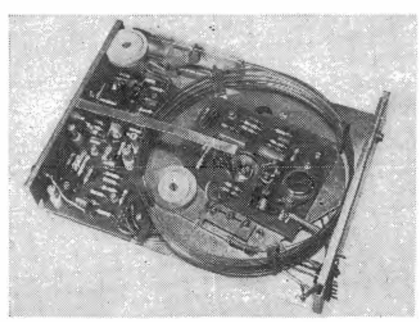

3·2ms, giving storage capacity of up to 1600 bits. The line can be used with both *n-p-n* and *p-n-p* logic circuits and its 500kHz working speed makes it suitable for use with modern high-speed circuit modules. It has the same appearance as the widely used YL2108 line and is housed in a steel case measuring 9¼ × 6¾ × 1½in.

For more information circle **No. 300**

FUNCTION GENERATORS

General Test Instruments Ltd, Gloucester Trading Estate, Hucclecote, Gloucestershire

Trigger, phase-lock and tone-burst capabilities are now available in two new portable function generators by Wavetek. The model-115 offers triggered or gated operation as well as phase-lock capability. In the trigger mode, a manual or external voltage of ±0·5V will generate one cycle. In the gated mode, a discrete number of cycles can be generated by applying a +0·5V gate. The unit will frequency-lock to any input within 10:1 of dial frequency and will phase-lock to the fundamental of the dial frequency within a spcified accuracy. The model-116 has all the capabilities of the model-115 with the addition of tone-burst operation, which may be generated automatically in the trigger mode. Selectable from a front-panel control, the 116 will generate from 1 to 256 discrete cycles. Both models will also generate sine, square, triangle, ramp and sync.-pulse waveforms. Nine simultaneous outputs are available over a frequency range of 0·0015Hz to 1MHz. Additionally, both units are voltage-controlled, allowing a 20:1 frequency sweep over the full dial spread. Basic specifications for the two

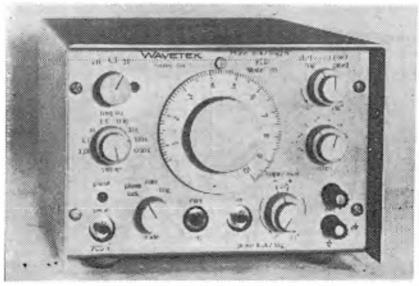

portable instruments are common: dial accuracy: 0·5% of reading; frequency response: amplitude change with frequency less than 0·1dB; amplitude stability: 0·1% of maximum peak-to-peak values for 30min short term; d.c. offset stability: 0·1% of maximum peak-to-peak values for 30min short term; sinewave distortion: less than 0·5%; triangle and ramp linearity: greater than 99% to 100kHz; square wave rise and fall time: less than 5ns; operating temperature: 25°C ±5°C; size = 7¾ × 5¼ × 11½in; weight: 10lb net. Both models use all silicon semiconductors throughout and have individually calibrated dials; each is available both a.c. and battery-operated.

For more information circle **No. 301**

CAPACITORS FOR PRINTED-CIRCUIT BOARDS

Mullard Ltd, Torrington Place, London WC1

New-style capacitors designed to plug into printed-circuit boards are now available from Mullard under type number 344. Post Office approval under specification D2283 type-8019A has been received for the 0·9μF capacitor, which is widely used in the telephone industry. Instead of radial or axial leads, these capacitors have short, accurately-spaced pins that match the 0·01in grid on printed-circuit boards. Because they have a regular rectangular outline, a high packing density can be achieved. Stand-off lugs prevent moisture from being trapped between the capacitors and the board, and raised markings on the top surface ensure immediate and easy identification. Metallized polyester foil completely encapsulated in moisture-proof resin is used in the construction of the capacitors. The range extends from 0·01 to 2·2μF; values up to 0·22μF have a 20% tolerance, and values of 0·33μF and above have a tolerance of 10%. The capacitors have a direct-voltage rating of 250V, and operating-temperature limits are −55 to +85°C with an IEC climatic category 55/085/56.

For more information circle **No. 302**

Data Sheets and Catalogues

Selenium-rectifier data summary

Standard Telephones and Cables Ltd, Rectifier Division, Edinburgh Way, Harlow, Essex

This summary gives a selection of the wide range of STC stack assemblies available. They are split into five groups: radio and television, h.t. and e.h.t., medium and high power, low power and special assemblies.

For more information circle **No. 303**

Microwave anechoic chambers

Emerson & Cuming Inc., Canton, Mass. 02021, USA

This 4-page leaflet describes recent advances in the design and construction of microwave anechoic chambers. Photographs show nine recently built chambers, each illustrating an advance in the state of the art.

For more information circle **No. 304**

Microwave and electronics engineers' wall chart

Polarad Electronic Instruments, 34-02 Queens Boulevard, Long Island City, NY 11101, USA

Polarad is offering a 30 × 40in 3-colour wall chart of engineering reference information for engineering departments, test laboratories and drafting rooms of communication and radar-equipment manufacturers and microwave-systems prime contractors. It covers oft-used spectrum-analysis data, signal and transmission data, and receiver and r.i./f.i. information.

For more information circle **No. 305**

Integrated power supplies

Solitron Devices Inc., Tappan, New York 10983, USA

This 12-page brochure covers the features of the Solitron HI-PAC(R) power supplies, gives technical information and illustrates product applications.

For more information circle **No. 306**

Photomultiplier tubes

EMI Electronics Ltd, Valve Division, Hayes, Middlesex

This 63-page book commences with a valuable and very interesting introduction to the photomultiplier, which is followed by detailed descriptions and characteristics of all the different types available from EMI.

For more information circle **No. 307**

Stabilized d.c. power supplies

A.P.T. Electronic Industries Ltd, Chertsey Road, Byfleet, Surrey

This 6-page publication, with photographs and diagrams, contains details of the APT series-30 range of modular mains-operated d.c. power units with output voltages from 0 to 500V. Features include 'all-silicon, fully protected, tropical rating, robust with high-efficiency transformers'.

For more information circle **No. 308**

Environmental-test laboratories

Ether Engineering Ltd, Dalton Gardens, Stanmore, Middlesex

Ether Engineering offers a wide range of facilities for testing components and assemblies at their environmental-test house at Stanmore. These facilities are described briefly in this 15-page brochure.

For more information circle **No. 309**

Image orthicons

English Electric Valve Co. Ltd, Chelmsford, Essex

This booklet details 3in and 4½in image orthicon tubes for both colour and monochrome pick-up; sufficient details are given for selection to be made and an equivalents index is given.

For more information circle **No. 310**

Power triacs

International Rectifier, Hurst Green, Oxted, Surrey

A 6-page data sheet outlines the principles, characteristics and construction of the new IR high-power bidirectional triode thyristor, commonly called the triac, rated at 200A.

For more information circle **No. 311**

Calcium aluminate glasses

Barr and Stroud Ltd, Armiesland, Glasgow W3, Scotland

Because of their outstanding optical and mechanical properties, calcium aluminate glasses are superior for many infrared applications. They feature useful transmission in the 0·3-0·6μm range, complete freedom from 3μm water absorption, transparency to visible light, and mechanical strength. A 7-page booklet from Barr and Stroud describes their products in detail.

For more information circle **No. 312**

R.F.-circuit-design library
Motorola Semiconductor Products Inc., York House, Empire Way, Wembley, Middlesex
Motorola has compiled a comprehensive r.f.-circuit design booklet containing circuit-design and testing information. The 150-page volume contains ten application notes describing the use of basic techniques in r.f. design. Besides application information, the booklet also contains highlight specifications for Motorola r.f.-amplifier transistors to assist the design engineer in device selection.

For more information circle **No. 313**

DIARY OF THE MONTH

1 Television-sound techniques by Glyn Alkin. Royal Television Society. At Westward Television Studios, Plymouth, 7.30 p.m.

1 Integrated-circuit applications by J. A. Cayzer. I.E.R.E. At Department of Electrical Engineering lecture theatre, Leeds University, 7 p.m.

1 Battery television and electronic devices by R. Simmons and L. Newton. Society of Electronic and Radio Technicians. At Washington Suite, Five Bridges Hotel, Gateshead, 7 p.m.

1 Deflexion circuits for colour and monochrome t.v. receivers by K. E. Martin and B. E. Attwood. I.E.R.E. At London School of Hygiene and Tropical Medicine, Keppel Street, Gower Street, London WC1, 6 p.m.

1–3 Circuits and systems. I.E.E.E. and Santa Clara University. At Pacific Grove, California.

2 Radio telemetry by P. R. Barkway. I.E.R.E. At Farnborough Technical College, 7 p.m.

6 Thyristor control by F. F. Mazda. I.E.E. At Savoy Place, London WC2, 6.30 p.m.

7 Piezoelectric properties of thin films by Dr. M. G. Cornwall. I.E.R.E. At College of Technology, Brighton, 6.30 p.m.

7 Colour in general and the PAL system in particular by I. Nicholson. Royal Television Society. At Co-op Educational Centre, Broad Street, Nottingham, 7.45 p.m.

7 Microwave radio-relay systems; noise and its bearing on planning by C. Johnston. Institution of Post Office Electrical Engineers. At Savoy Place, London WC2, 5 p.m.

8 A forum on colour servicing. Royal Television Society. At the Vaughan College, St. Nicholas Street, Leicester, 7.15 p.m.

8 Close-range radar by M. J. Withers. Society of Electronic and Radio Technicians. At University of Birmingham, Electrical Engineering Department, Selly Oak, Birmingham, 7 p.m.

8 Microelectronics by Dr. S. Forte. I.E.R.E./I.E.E. At The College, Swindon, 6.15 p.m.

8 Multistandard colour television by B. Marsden. Royal Television Society. At Angel Hotel, Cardiff, 7.30 p.m.

8–10 M.F., l.f. and v.l.f. propagation. I.E.E./I.E.R.E. colloquium. At Savoy Place, London WC2.

9 The engineering principles and applications of microwave filters by G. Craven. I.E.E./I.E.R.E. At University Engineering Laboratories, Trumpington Street, Cambridge, 8 p.m.

9–10 Broadcasting conference. I.E.E.E. At Ambassador Hotel, Los Angeles, California.

10 Technical training for the electronic industry by G. M. Rendall. Society of Electronic and Radio Technicians. At Y.M.C.A., 100 Bothwell Street, Glasgow C2, 7.30 p.m.

13 Storage systems for telephone switching by J. R. Pollard. I.E.R.E./I.E.E./I.P.O.E.E.. At G.P.O. Central Training School, Yarnfield, nr. Stone, 7 p.m.

13, 20 27 Modern developments in stage and studio lighting and control. Course. At Borough Polytechnic, Borough Road, London SE1, 1.30 p.m.

14 Military mobile communications equipment by Maj. Meadows. Society of Electronic and Radio Technicians. At East Berks College, Boyn Hill Avenue, Maidenhead, 7 p.m.

14 Translating and transcoding colour t.v. system common scanning standards by S. M. Edwardson. I.E.R.E. At Plymouth College of Technology, 7 p.m.

14 Going metric by Dr. W. S. Hollis. Institution of Production Engineers. At Doncaster Technical College, Waterdale, Doncaster, 7.15 p.m.

14 Satellite communications by D. Wilkinson. I.E.E. At Woolwich Polytechnic, Wellington Street, London SE18, 6.30 p.m.

14–16 R.F. measurements and standards. I.E.R.E./I.E.E. conference. At National Physical Laboratory, Teddington, Middlesex.

15 Symposium on thick-film technology. BTU Engineering Corp. At the Richmond Room, Royal Lancaster Hotel, London W2.

15 Colour television: a practical approach by B. Rogers. Royal Television Society. At Queens University Lecture Hall, Belfast, 7 p.m.

16 Gas lasers by H. Foster. I.E.R.E. At Renold Building, Manchester College of Science and Technology, Altrincham Street, Manchester, 7.15 p.m.

16 Are component specifications being improved? I.E.E. discussion meeting opened by R. H. W. Burkett, J. D. Hinchcliff and D. S. Girling. At Savoy Place, London WC2, 5.30 p.m.

17 Electronics in photography by by C. W. Hooper. Society of Electronic and Radio Technicians. At Llandaff Technical College, Western Avenue, Cardiff, 7.30 p.m.

22 The strange journey from retina to brain by Dr. R. W. G. Hunt. Royal Television Society. At Birmingham Medical Institute, Harborne Road, Edgbaston, 7 p.m.

22 PAL delay lines by R. W. Gibson. Society of Electronic and Radio Technicians. At London School of Hygiene and Tropical Medicine, Keppel Street, Gower Street, London WC1, 7 p.m.

22 M.O.S. transistors by G. G. Bloodworth. I.E.R.E./I.E.E. At Bristol University, 7 p.m.

22–24 Automation in information service. Czechoslovak Committee for Scientific Management conference. At Prague.

23 Radio astronomy by Prof. J. G. Davies. I.E.E. At Savoy Place, London WC2, 6.30 p.m.

28 The Anglo-European 480-circuit submarine cable systems by R. Bayfield. Institution of Post Office Electrical Engineers. At the Conference Room, Fleet Building, 70 Farringdon Street, London EC4, 5 p.m.

29 Generation, propagation and applications of microwave acoustics by Prof. K. W. H. Stevens. I.E.R.E. At 8/9 Bedford Square, London WC1, 6 p.m.

Résumés des principaux articles

Étude d'une synthèse de circuit appliqué par R. H. Dadd

Résumé de l'article aux pages 668 à 670

L'auteur indique quelques méthodes simples au moyen desquelles on peut réduire le format d'un amplificateur afin de répondre aux prescriptions d'une spécification donnée. Il fait mention, à cet égard, des méthodes habituelles pour réaliser la synthèse nécessaire du réseau de réaction et montre, par un exemple précis, l'utilisation de cette méthode.

Multivibrateur à rapport très réduit de repère/espace par S. Tesic

Résumé de l'article aux pages 671 à 673

L'auteur décrit un multivibrateur non-asservi produisant des formes d'ondes très asymétriques. La durée des deux états quasi-stables peut être contrôlée séparément, autorisant ainsi un rapport repère/espace très réduit, de l'ordre de 10^{-4} et 15^{-5}. Dans ce mode de fonctionnement, le circuit, basé sur l'emploi de transistors supplémentaires, assure une consommation électrique totale très économique.

Thermomètre sensible à thermistor par J. C. S. Richards

Résumé de l'article aux pages 674 à 676

Un thermomètre à spécification très précise a été utilisé dans un circuit en pont à courant alternatif pour la réalisation d'un thermomètre à lecture directe et à échelle quasilinéaire. Sans étalonnage, les erreurs caractéristiques sont inférieures à $\pm 0,5°C$ dans une gamme de 20°C. Un signal de sortie de $\pm 2,5V$ en continu peut être obtenu pour une changement de température de $\pm 0,05°C$.

Référence de basse tension par P. Williams

Résumé de l'article aux pages 676 à 679

Le circuit décrit dans cet article a fait l'objet d'une précédente étude sur ses propriétés en tant que source à la foir de courant constant et de tension constante. Dans une nouvelle application de ce circuit, on a pu obtenir une stabilité comparable à celle des circuits de référence conventionnels mais exigeant, une tension d'alimentation inférieure à celle de la diode Zener à la tension la plus faible.

Paramètres de transistors et leur influence sur les temps de montée d'amplificateurs par D. Ivekovic

Résumé de l'article aux pages 680 à 682

L'auteur analyse l'influence du gain de courant β_0 à fréquence réduite, de la fréquence de coupure f_1, de la capacité du collecteur à la base et de la résistance d'étalement à la base r_b sur le temps de montée du transistor à émetteur commun. Il établit une comparaison de ces paramètres pour plusieurs types de transistors américains et européens. Il indique, en outre, les limites de validité de circuit simplifié à transistor équivalent pour déterminer une fonction de transfert de gain unipolaire sans tenir compte du collecteur-émetteur.

Générateur en escalier linéaire par M. Cadwallader

Résumé de l'article aux pages 682 à 685

Le circuit à générateur en escalier dont il est question dans cet article est du type à résistance chargée binaire à commutation, fréquemment utilisé pour la conversion numérique-analogique. Une nouvelle méthode de réalisation pour les circuits à transistors de commutation donne une erreur de linéarité de $\pm 0,025\%$ seulement, avec une tension d'alimentation par transistor normale. Un amplificateur d'un type nouveau contribue à la bonne linéarité et au coefficient de température de 0,01 par degré centigrade.

Étude des moyennes de réponse de pulsations de coeur de rats à la suite d'une stimulation électrique du cerveau par W. J. Mundl

Résumé de l'article aux pages 686 à 690

Cet article décrit un système qui donne une courbe de sortie représentant les réponses moyennes des pulsations du coeur d'un rat à des stimulations répétées. On a mis au point des instruments à l'aide desquels on peut régler les intervalles de temps entre les pulsations successives suivant une tension permettant le traitement des données obtenues à l'aide d'une calculatrice.

Caractéristiques des systèmes asynchrones et bipolaires de modulation de longueur d'impulsion par P. D. Sharma

Résumé de l'article aux pages 691 à 695

Deux nouvelles approximations, basées sur des segments linéaires à pente de ± 1 ou de $\pm 1/0$, ont pu être obtenues par l'emploi de circuits non-linéaires simples. Une simple différenciation de ces approximations à segment linéaire produit des impulsions de ± 1 ou $\pm 1/0$ dont les largeurs et les temps de répétition sont modulées suivant la pente de la forme d'onde du signal d'approximation, ce qui donne lieu à des systèmes de modulation de longueur d'impulsion asynchrone et de modulation de longueur d'impulsion bipolaire asynchrone.

Calcul à limites ouvertes par C. G. Mayo et J. W. Head

Résumé de l'article aux pages 696 à 699

Si deux ou plusieurs processus ou quantités obtenus en fermant les limites se produisent simultanément dans un calcul, il est parfois d'une importance critique de savoir laquelle de ces limites est fermée la première. Si les limites sont fermées dans l'ordre voulu, il ne se produira aucune difficulté et, grâce à l'intégrale de Fourier, aucune technique spéciale n'est nécessaire. Toute l'attention nécessaire a été accordée à cet égard à la possibilité qu'un problème puisse être formulé de telle manière qu'une limite d'une importance critique ait été fermée prématurément par inadvertance.

Convertisseur précis de triangles symétriques en ondes sinusoidales par G. Klein et H. Hagenbeuk

Résumé de l'article aux pages 700 à 704

On obtient une conversion précise et instantanée d'angles symétriques en ondes sinusoidales pour des fréquences allant jusqu'à 1MHz à l'aide d'un circuit hybride intégré de résistances au nickel-chrome à film mince et de réseaux à diodes monolithiques. On peut, ainsi, obtenir une onde sinusoidale d'un triangle symétrique avec une distorsion inférieure à 0,1%.

Environnements à température contrôlée avec précision pour les lignes à retard à quartz à fusible à ultra-sons par D. Howorth, C. R. Caine et L. T. E. Ward

Résumé de l'article aux pages 706 à 710

Cet article décrit la conception et la construction d'un environnement pour une ligne à retard à ultra-sons de 2,5ms dont la température est contrôlée avec précision. Il traite également de la réalisation en général de ces environnements.

Zusammenfassung der wichtigsten Beiträge

Angewandte Schaltungssynthese von R. H. Dadd

Zusammenfassung des Beitrages auf Seite 668-670

Der Beitrag beschreibt einfache Methoden, mit deren Hilfe beim Entwurf eines Verstärkers Erreichung einer gewünschten Spezifikation erzwungen werden kann. Routinemethoden für die Synthese der Rückkopplungsnetzwerke und ein Beispiel für die Anwendung der Methode werden gegeben.

Multivibrator mit sehr niedrigem Tastverhältnis von S. Tesic

Zusammenfassung des Beitrages auf Seite 671-673

Ein frei laufender Multivibrator, der für die Erzeugung sehr unsymmetrischer Wellenformen geeignet ist, wird beschrieben. Die Dauer der beiden quasistabilen Zustände wird getrennt gesteuert, wodurch sehr niedrige Tastverhältnisse in der Grössenordnung von 10^{-4} und 10^{-5}—erreicht werden. In dieser Arbeitsweise hat die auf komplementären Transistoren beruhende Schaltung eine sehr niedrige Gesamtstromaufnahme.

Empfindliches Thermistor-Thermometer von J. C. S. Richards

Zusammenfassung des Beitrages auf Seite 674-676

Verwendung eines genau spezifizierten Thermistors in einer Wechselstrom-Brückenschaltung gestattet Konstruktion eines direktanzeigenden Thermometers mit fast linearer Skala. Ohne Eichung sind typische Fehler über einen Bereich von 20°C niedriger als $\pm 0,5$°C. Eine Temperaturänderung von $\pm 0,05$°C erzeugt ein Ausgangssignal von $\pm 2,5$ V.

Zweiteiliges Niederspannungs-Ringnormal von P. Williams

Zusammenfassung des Beitrages auf Seite 676-679

Eine Schaltung, die vor kurzem sowohl als Konstantstrom- wie Konstantspannungsquelle besprochen wurde, wird beschrieben. In einer neuartigen Anwendung wird eine mit herkömmlichen Bezugsschaltungen vergleichbare Konstanz erreicht, wobei jedoch eine Speisespannung erforderlich ist, die unter der niedrigsten Spannung der Zenerdiode liegt.

Transistorparameter und ihr Einfluss auf die Verstärkeranstiegszeit von D. Ivekovic

Zusammenfassung des Beitrages auf Seite 680-682

Der Einfluss der niederfrequenten Stromverstärkung β_0, Grenzfrequenz f_t, Kollektor/Basis-Kapazität C_c und des Basis-Innenwiderstands r_b auf die Anstiegszeit der Emitter-Transistorschaltung wird behandelt. Diese Parameter verschiedener amerikanischer und europäischer Transistortypen werden verglichen. Die Gültigkeitsgrenzen für die Bestimmung einer Übertragungsfunktion für Einpolverstärkung mit der vereinfachten Transistor-Ersatzschaltung bei Vernachlässigung der Kollektor/Emitter-Kapazität werden gegeben.

Ein linearer Treppengenerator von M. Cadwallader

Zusammenfassung des Beitrages auf Seite 682-685

Die beschriebene Treppengeneratorschaltung arbeitet nach dem Prinzip des geschalteten, binärbewerteten Widerstandes, das oft für Digital-Analogwandlung Anwendung findet. Eine neue Entwurfsmethode für Schalttransistor-Schaltungen ergibt bei normaler Transistor-Speisespannung einen Linearitätsfehler von nur $\pm 0,035$%. Ein neuartiger Summierverstärker trägt zur guten Linearität und dem Temperaturkoeffizienten von 0,01 per °C bei.

Mittelwertbildung der Herzschlagreaktionen von Ratten nach elektrischer Gehirnreizung von W. J. Mundl

Zusammenfassung des Beitrages auf Seite 686-690

Ein beschriebenes System erzeugt eine Ausgangskurve, die gemittelte Herzschlagreaktionen unbehinderter Ratten nach wiederholter Reizung darstellt. Entwickelte Spezialgeräte gestatten Umsetzung des Zeitintervalls zwischen aufeinander folgenden Herzschlägen in eine für Computerverarbeitung geeignete Spannung.

Eigenschaften asynchroner und bipolarer Pulsbreitenmodulationssysteme von P. D. Sharma

Zusammenfassung des Beitrages auf Seite 691-695

Mit Hilfe einfacher nichtlinearer Schaltungen werden zwei neue Annäherungen, die auf linearen Abschnitten der ± 1- oder $\pm 1/0$-Steilheit beruhen, entwickelt. Einfache Differenzierung dieser Linearabschnitt-Annäherungen ergibt Impulse, deren Breite und Folgeperioden entsprechend der Steilheit der Eingangswellenform moduliert werden. Es entstehen daher asynchrone Pulsbreitenmodulationssysteme und asynchrone bipolare Pulsbreitenmodulationssysteme.

Unbestimmte Integrationsrechnung von C. G. Mayo und J. W. Head

Zusammenfassung des Beitrages auf Seite 696-699

Wenn zwei oder mehr Rechnungsarten oder Quantitäten in einer Rechnung durch gleichzeitige Begrenzung abgeleitet werden, ist es manchmal von kritischer Bedeutung, welche Grenze zuerst eingeführt wird. Es treten keine Schwierigkeiten auf, wenn die Begrenzung in der richtigen Reihenfolge vorgenommen wird, und für das Fouriersche Integral sind keine Sonderverfahren notwendig. Besondere Aufmerksamkeit wird der Möglichkeit gewidmet, dass ein Problem so formuliert werden kann, dass versehentlich eine kritisch bedeutende Grenze zur vorzeitigen Bestimmung führt.

Genauer Dreieck-Sinuswellen-Umsetzer von G. Klein und H. Hagenbeuk

Zusammenfassung des Beitrages auf Seite 700-704

Eine genaue, momentane Umsetzung von Dreieckwellenformen in Sinuswellenformen für Frequenzen bis zu 1 MHz wird mit Hilfe einer integrierten Hybridschaltung aus Dünnfilm-Chromnickelwiderständen und monolithischen Diodenfeldern erreicht. Von symmetrischen Dreiecken kann man Sinuswellen mit Verzerrungen unter 0,1% erreichen.

Präzisionstemperaturregelung der Umgebung für Ultraschall-Verzögerungsleitungen aus geschmolzenem Quarz von D. Howorth, C. R. Caine und L. T. E. Ward

Zusammenfassung des Beitrages auf Seite 706-710

Der Beitrag beschreibt Entwurf und Konstruktion einer für 2,5-ms-Ultraschallverzögerungsleitungen geeigneten Umgebung, deren Temperatur genau geregelt werden kann. Ausserdem wird der Entwurf solcher Umgebungen im allgemeinen besprochen.